BRANCHED AMPHIPHILIC PEPTIDES: AN ALTERNATE NON-VIRAL GENE DELIVERY SYSTEM

by

LUZ ADRIANA AVILA FLORES

B.S., Universidad Autónoma de Madrid, Spain, 2007

M.S., Universidad del Pais Vasco, Spain, 2008

AN ABSTRACT OF A DISSERTATION

submitted in partial fulfillment of the
requirements for the degree

DOCTOR OF PHILOSOPHY

Department of Biochemistry and Molecular Biophysics
College of Arts and Sciences

KANSAS STATE UNIVERSITY
Manhattan, Kansas

2014

Abstract

Success for gene therapy clinical protocols depends on the design of safe and efficient gene carriers. Nature had already designed efficient DNA or RNA delivery devices, namely virus particles. However, the risk of insertional mutagenesis has limited their clinical use. Alternatively, safer approaches involving non-viral carriers have been and continue to be developed. While they have been reported to be less efficient than viral vectors, adding genome editing elements to pDNA makes the integration of corrective sequence site specific moving non-viral gene delivery systems closer to clinical applications. Over the last decade, peptides have emerged as a new family of potential carriers in gene therapy. Peptides are easy to synthesize, quite stable and expected to produce minimally immunogenic and inflammatory responses. We recently reported on a new class of Branched Amphiphilic Peptides Capsules (BAPCs) that self-assemble into extremely stable nano-spheres. BAPCs display a uniform size of $\sim$20 nm if they are incubated at 4°C and they retain their size at elevated temperatures. In the presence of DNA, they can act as cationic nucleation centers around which DNA winds generating peptide-DNA complexes with a size ranging from 50nm to 100nm. However, if BACPs are not incubated at 4°C, the pattern of interaction with DNA differs. Depending of the peptide/DNA ratios, the peptides either coat the plasmid surface forming nano-fibers (0.5-1 μM in length) or condense the plasmid into nano-sized structures (100-400nm). Different gene delivery efficiencies are observed for the three types of assemblies. The structure where the DNA wraps around BAPCs display much higher transfection efficiencies in HeLa cells in comparison to the other two morphologies and the commercial lipid reagent Lipofectin®. As a proof of concept, pDNA was delivered *in vivo*, as a vaccine DNA encoding E7 oncoprotein of HPV-16. It elicited an immune response activating $CD8^+$ T cells and provided anti-tumor protection in a murine model.

BRANCHED AMPHIPHILIC PEPTIDES: AN ALTERNATE NON-VIRAL GENE DELIVERY SYSTEM

by

LUZ ADRIANA AVILA FLORES

B.S., Universidad Autónoma de Madrid, Spain, 2007

M.S., Universidad del Pais Vasco, Spain, 2008

A DISSERTATION

submitted in partial fulfillment of the
requirements for the degree

DOCTOR OF PHILOSOPHY

Department of Biochemistry and Molecular Biophysics
College of Arts and Sciences

KANSAS STATE UNIVERSITY
Manhattan, Kansas

2014

Approved by:

Major Professor
John M. Tomich

Copyright

Abstract

Success for gene therapy clinical protocols depends on the design of safe and efficient gene carriers. Nature had already designed efficient DNA or RNA delivery devices, namely virus particles. However, the risk of insertional mutagenesis has limited their clinical use. Alternatively, safer approaches involving non-viral carriers have been and continue to be developed. While they have been reported to be less efficient than viral vectors, adding genome editing elements to pDNA makes the integration of corrective sequence site specific moving non-viral gene delivery systems closer to clinical applications. Over the last decade, peptides have emerged as a new family of potential carriers in gene therapy. Peptides are easy to synthesize, quite stable and expected to produce minimally immunogenic and inflammatory responses. We recently reported on a new class of Branched Amphiphilic Peptides Capsules (BAPCs) that self-assemble into extremely stable nano-spheres. BAPCs display a uniform size of $\sim$20 nm if they are incubated at 4°C and they retain their size at elevated temperatures. In the presence of DNA, they can act as cationic nucleation centers around which DNA winds generating peptide-DNA complexes with a size ranging from 50nm to 100nm. However, if BACPs are not incubated at 4°C, the pattern of interaction with DNA differs. Depending of the peptide/DNA ratios, the peptides either coat the plasmid surface forming nano-fibers (0.5-1 μM in length) or condense the plasmid into nano-sized structures (100-400nm). Different gene delivery efficiencies are observed for the three types of assemblies. The structure where the DNA wraps around BAPCs display much higher transfection efficiencies in HeLa cells in comparison to the other two morphologies and the commercial lipid reagent Lipofectin®. As a proof of concept, pDNA was delivered *in vivo*, as a vaccine DNA encoding E7 oncoprotein of HPV-16. It elicited an immune response activating $CD8^+$ T cells and provided anti-tumor protection in a murine model.

Table of Contents

List of Figures

List of Tables

Acknowledgments

The results presented in this dissertation are not exclusively the result of my effort, but also of various collaborations and partnerships.

I would like to thank my advisor Dr. John Tomich, for whom I have a deep admiration and respect, both as a person and as a scientist. He trained me to be an independent researcher and taught me that taking risks in my research is sometimes the way to accomplish great and original results. I appreciate the freedom he gave me to pursue various projects without objection.

I thank my committee members: Dr. Stella Lee who is my primary resource for getting answers and scientific advice in regard to cell biology and cell culturing; Dr. Michael Zolkiewski for providing advice many times during my graduate school career and for many insightful discussions and suggestions that in addition to saving me time, provided rigor to my work; Dr. Phillip Klebba for their helpful career advice and suggestions in general; Dr. Jianhan Chen for his useful ideas regarding molecular modeling; and Dr. Meena Kumari, the chairperson of the examining committee.

I would like to thank the people who contributed to generate the microscopy images, Dr. Robert Szoszkiewicz and Nicoleta Ploscariu for the AFM analysis, Dr. Yoonseong Park and Dr. Ladislav Simo for the great confocal pictures and Dr. Prem thapa, from KU who helped me with the TEM studies.

I am very grateful to our collaborators at the São Paulo University, Dr. Luís C.S. Ferreira and Luana Aps for the *in vivo* vaccination assays carried out in their laboratory and also for allowing me to realize that I understand Portuguese!

I thank my lab members, Dr. Pinakin Sukthankar, Ben Katz, Jammie Laymann, Susan Whitaker and other past members, Dr. Yasuaki Hiromasa, Dr. Sushanth Gudlur , Rachael

Ott and the new arrivals, Patricia Games who created a friendly atmosphere that made me feel at home.

I also thank my friends Nicole Green, Jordan Woehl and Chester McDowell for the occasionally Bloody Marys that made life easier when results didn't come out as expected. I also thank friends from other labs, Sara Duhachek Muggy, Prashant Wani, Rohit Kamat, Lorne Jordan, Yan Shipelskiy and Stacy Littlechild for entertaining discussions about life and experiments.

I especially thank my family, my Dad who unfortunately is not here to share this moment with me but who seeded in me the scientific curiosity since I was a child and my Mom who sacrificed her life for my education. I thank my brothers, Adolfo Avila, César Avila and my oldest brother Germán Avila who I will always miss. I thank particularly my sister, Silvia Avila, a busy entrepreneur and Mom who always find time to help me if I am in trouble, who is my best friend and who always encourage me to pursue my professional and personal dreams.

I thank my in-laws, nephews and nieces for the affection provided along these years. I thank particularly my brother in law, Jose Luis Castrillo who has been very supportive during my career and to my little and wonderful niece, Leire Castrillo who brought happiness and funny moments to my life.

There is a very important person in my life to who I owe special thanks, my fiancée Guillaume Laurent, an excellent physicist and great person who has been my partner and best friend for several years and with who I share a philosophy about how to life live. Thanks for the unconditional support, patience and love during these four years of graduate school. I appreciated your cheer and practical advice during the bad and frustrating moments. Also, thanks for teaching me computer programs that made my life easier and for your help in editing this manuscript.

Dedication

To my parents (Pedro Avila and Ma. Luisa Flores) to my sister (Silvia Avila) and my fiancée (Guillaume Laurent), for their patience and the moral and financial support to pursue this dream.

Preface

"And Jesus said to him, If you can! All things are possible to him who believes" Mark 9:23

Chapter 1

Synthetic *in vitro* Delivery Systems For Plasmid DNA in Eukaryotes

This chapter has been reproduced in its current format with permission from L. Adriana Avila, Stella Y.Lee and John M. Tomich, *Journal of Nanopharmaceutics and Drug Delivery*, 2:1-19, 2014.

1.1 Introduction

Not until the early 1960s was foreign DNA introduced as-permanent, stable, functional, and hereditable elements into mammalian cells[1]. With this achievement new approaches for treating human diseases became imaginable. Theoretically, the insertion of DNA to correct genes that are either absent or miscoded could ameliorate many genetic disorders. Since then, an increasing number of methods have been and are currently being developed for delivering DNA into cells.

Besides plasmid DNA (pDNA), various types of RNA molecules have been introduced into cells. In contrast to pDNA, which is used to introduce a new or corrected copy of the defective gene, RNA is used to inhibit translation of mRNAs,[2] in a transient fashion[3,4].

Plasmid DNA can also be used as genetic vaccines leading to activation of specific immune responses either preventing or treating infectious or degenerative diseases[5,6,7].

The delivery of foreign genetic material involves overcoming several extracellular and cellular barriers. For *in vitro* delivery, nucleic acids must cross the cell membrane, then avoid lysosomal degradation and then traverse the nuclear membrane, and achieve therapeutic levels of expression without disrupting other genes[8]. For *in vivo* delivery additional challenges must be overcome. The added genetic material has to be protected from circulating nucleases present in the organism, phagocyte degradation, aggregation with serum proteins and finally target specific tissues[4]. Furthermore, when used to target central nervous tissues, the genetic material must efficiently cross the blood-brain barrier to reach the targeted cells[9].

In vivo, cells can take up naked DNA however the mechanism is not fully understood. Injections of naked DNA into skeletal muscle may result in the expression of the proteins coded by the added DNA however at low and extremely variable levels[10]. For this reason the development and use of molecular carriers that both coat and shield the nucleic acids from hydrolysis by nucleases and target the negatively charged DNA to specific tissues is vital. Nature had already designed efficient DNA or RNA delivery devices, namely virus particles. Viruses effectively package, protect and deliver genetic material. Researchers seized on this approach and began working with certain viruses for use as human gene delivery systems. Adenovirus and retrovirus were the first carriers used to delivery therapeutic genes. At present, they remain the vectors of choice, showing the highest efficiency[11]. One of the advantages of viral gene delivery system is that a gene can be integrated into the host's genome. However, the death of a patient receiving an adenoviral vector triggered safety objections and questioned the further use of viral vectors[12]. Also, other issues including the potential risk of insertional mutagenesis, previously established immunity to the virus vector, and the size limitation on the DNA that can be packaged have limited clinical applications[13]. Despite these risks, researchers continue working to improve the efficacy and safety of these

vectors. In recent years, research has focused on the use of lentivectors, which, like their retrovirus counterparts, are devoid of viral proteins, not replication competent, and able to transduce non-dividing cells[14]. Currently, these lentivectors are being used in about 3.3% (n = 67) of clinical trials (http://www.wiley.co.uk/genmed/clinical/ [July 2013])[15]. Alternatively, non-viral biological methods are being investigated for DNA delivery as safer systems[16]. While somewhat less efficient than their viral counterparts, significant progress has led to improved transfection efficiencies and made them feasible alternatives. With the newly developed genome editing, such as CRISPR/Cas9 and zinc-finger nuclease (ZFN) systems, integration of the corrected gene into the genome can be site specific[17,18]. When incorporating genome editing elements to pDNA, non-viral gene delivery can provide a significant refinement for gene therapy.

Non-viral synthetic systems employ biocompatible molecules that facilitate the uptake of nucleic acids into cells. Synthetic carrier methods first require the complexation of cationic amphiphilic molecules with anionic nucleic acids followed by cellular uptake through a facilitated membrane translocation. The application of these newer methods ranges from preclinical studies to human trials. Lipid base vectors now account for the 5.5% (n=112) of gene therapy clinical trials (http://www.wiley.co.uk/genmed/clinical/ [July 2013]). The biggest challenge for non-viral gene therapy will be translation from bench to clinical applications[19]. This review focuses on the most recent (2010-present) non-viral pDNA delivery systems *in vitro* and compares their transfection efficiencies and potential.

1.2 Synthetic nonviral DNA carriers

Synthetic non-viral DNA carriers are cationic molecules that bind to DNA, predominantly through electrostatics. Cationic lipids, polysaccharides, peptides, synthetic polymers, and metals are examples of molecules that are currently used as chemical DNA carriers (Figure 1.1). The electrostatic interactions between the chemical vectors and pDNA generate com-

plexes with different topologies; either spherical vesicles, rod-like or ordered multi-laminar structures[20].

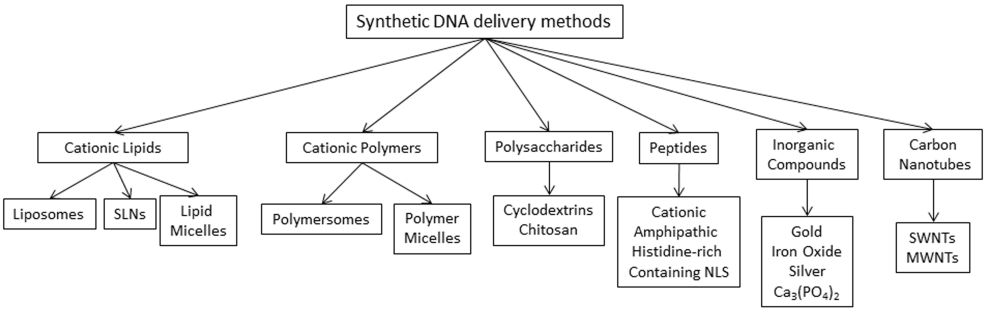

Figure 1.1: *Current synthetic DNA delivery vectors.*

These complexes even with incorporated DNA retain their net positive charges, facilitating interactions with negatively cell membrane surfaces[21,22] Natural Glycosaminoglycan chains such the sulfated forms of heparin, dermatan and chondroitin, are responsible for the eukaryotic cell membrane's negative potential[23]. Once bound, endocytosis serves as the principle route of uptake of the polycation/DNA complexes[24,25,21]. Endocytosis in itself is a broad term that encompasses specific pathways. They can be broadly classified in four types: phagocytosis, clathrin-mediated endocytosis (CME), caveolae-mediated endocytosis (CvME) and macropinocytosis[26]. According to several reports there is no evidence linking the mode of entry to transfection efficiency[27,24]. It is generally assumed that low to moderate gene expression is due mostly to the trapping and degradation of the pDNA within intracellular vesicles and limited translocation to the nucleus[28,16].

Due to their cationic nature, non-viral nanocarriers can be toxic[29] The integrity of organelle membranes can be compromised and undesirable interactions with other negatively charge compounds such nucleic acids and proteins could affect the protein expression and other natural cellular process[30]. Factors that have a direct impact in cytotoxicity are: charge density, molecular weight, presence of free carrier and degree of biodegradability[31]. Currently, research on how to improve the transfection efficiency without compromising cell

viability remains the largest obstacle for non-viral DNA/RNA delivery *in vitro*.

1.3 Cationic Lipids

Cationic lipids are the most commonly used synthetic gene delivery molecules due to their high transfection efficiency. The most common systems for gene delivery using lipids are: liposomes, solid lipid nano particles and micelles[32]. Cationic lipids used for DNA delivery generally contain four functional domains: a hydrophilic head-group, a linker, a backbone domain, and a hydrophobic domain[33] (Figure 1.2). The most commonly hydrophilic head groups are primary-, secondary-, tertiary-amines, or quaternary ammonium salts. However, guanidino, imidazole, pyridinium, can be present[34,35]. The hydrophobic tails are usually made of two types of hydrophobic moieties, aliphatic chains or steroids. The most common linkages between the hydrophilic head and hydrophobic moieties are ethers, esters, carbamates, or amides[36]. The structure of cationic lipids is a major factor for their transfection activity and toxicity[36]. Masotti et al.[37] have compared different parameters of some commercially available cationic lipids influencing toxicity and transfection efficiency on Rat Glioma Cell Line (C6) (Table 1.1).

A pioneering design by Felgner et al.[38] was the glycerol backbone-based cationic transfection lipid-DOTMA (N-[1-(2,3-dioleyloxy)propyl]-N, N, N-trimethylammonium chloride). Since then a number of compounds have been developed and display considerable diversity in structure, number of aliphatic chains, asymmetry, chain length and degrees of unsaturation. Often they are combined with neutral helper lipids such dioleoyl phosphatidylethanolamine (DOPE) and 1, 2-dioleoyl-sn-glycero-3-phosphocholine (DOPC) to yield higher transfection efficiencies in many cell types.

Mevel et al.[40] reported on the synthesis of a novel cationic lipid: N', N'-dioctadecyl-N-4, 8-diaza-10-aminodecanoylglycine amide (DODAG). This cationic lipid contains two chains in the hydrophobic domain and a guanidinium functional group. Using DODAG in

		Transfection efficiency (RLU/per 96-well)	Lipid/DNA charge ratios	Incubation time	Serum	Ref.
Rat Glioma (C6)	DOTAP/DOPE	5×10^5	1:1	4h	+	[37]
	DC-Chol/DOPE	4×10^5	5:1	4h	-	[37]
	DDAB/DOPE	1×10^5	2.5:1	4h	+	[37]
	FUGENE^{++}	4×10^6	-	4h	+	[37]
	DMRIE/Chol	8×10^4	2.5:1	4h	-	[37]
	LIPOFECTIN	4×10^5	5:1	4h	-	[37]
	LIPOFECTAMIN 2000	1.1×10^5	4:1	4h	-	[37]
	CELLEFECTIN	6×10^4	2.5:1	4h	-	[37]
CHO	DOTAP/DOPE	1.1×10^5	5:1	4h	-	[39]
	OLON/DOPE	2×10^6	5:1	4h	-	[39]
	LHON/DOPE	2.5×10^6	3:1*	4h	-	[39]
	CTAB/DOPE	5×10^4	2:7*	4h	-	[39]
	DOGSH/DOPE	4×10^5	3:1	4h	-	[39]

Table 1.1: *Luciferase expression in various mammalian cell lines transfected with cationic lipids commonly used for gene transfer. Transfection efficiency is expressed in Relative Light Units (RLU). The comparison was done at the optimal charge/ratio (that one that shows be more efficient) of each liposome formulation after 24h of transfection. *Represents the w/w ratio. $^{++}$Fugene has a protected formulation. Abbreviations: DC-Chol: cholesteryl-3b-N-(dimethyl-aminoethyl)carbamate hydrochloride DDAB: dimethyldioctadecylammonium bromide. DMRIE: 1,2-dimyristyloxypropyl-3-dimethyl-hydroxyethyl ammonium bromide. CELLEFECTIN: 1:1.5 molar mixture of the cationic lipid N, N, N, N -tetramethyltetrapalmityl-spermine (TM-TPS) and DOPE. DOGSH: 19,29-dioleyl-sn-glycero-39-succinyl-1, 6-hexanediol CHO: Chinese Hamster Ovary.*

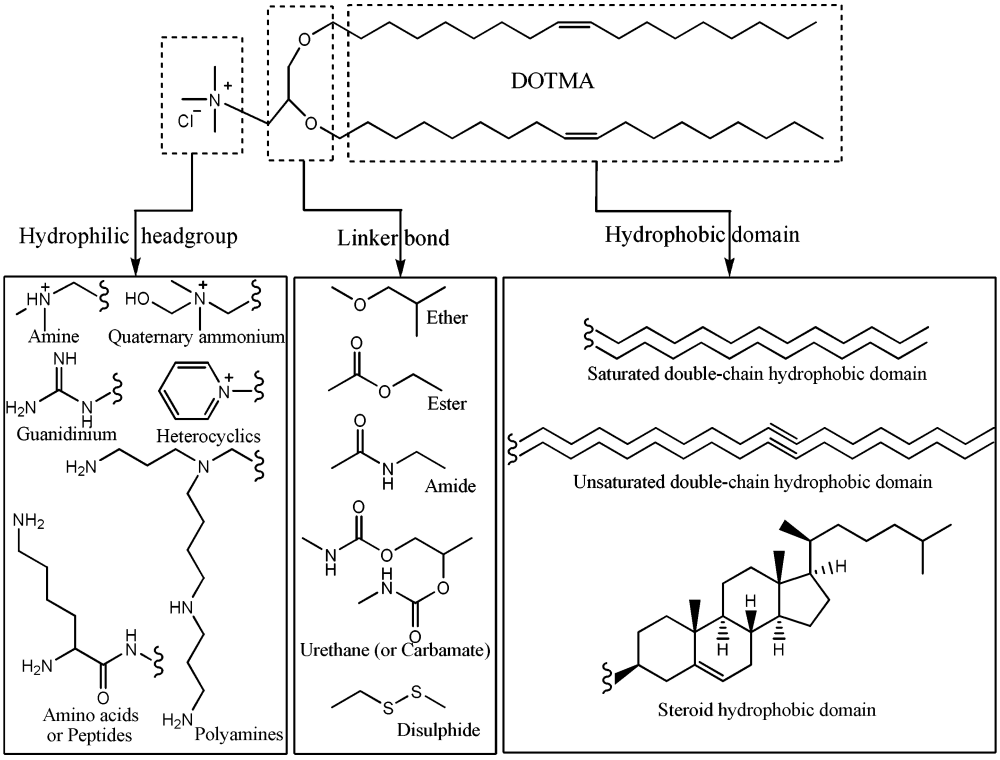

Figure 1.2: *Different structural components of cationic lipids: hydrophilic headgroup, linker bond, and hydrophobic domain. Reprinted with permission from ref. 33, D. Zhi, S. Zhang, S. Cui, Y. Zhao, Y. Wang, D. Zhao, The Headgroup Evolution of Cationic Lipids for Gene Delivery, Bioconjugate Chem, 24, 487519 (2013). Copyright® 2013, American Chemical Society.*

combination with the helper lipid DOPE three cell lines were transfected obtaining high levels of luciferase expression compared to Lipofectamine 2000 (Table 1.2). They reported as well moderate cytotoxicity; only around 5% of LDH release was found using immortalized adherent cell lines. For the same type of cell line, around 20% lactate dehydrogenase (LDH) release (equivalent to cell death) has been reported for Lipofectamine 2000. Safinya and co-workers[41] have designed a cationic lipid (CMVL5) that contains a disulfide bond spacer between the headgroup and the hydrophobic tails. The objective of this modification was to facilitate the degradation in the reductive environment of the cytoplasm and with this decrease the cytotoxicity. Although, the transfection efficiency was similar than Lipofectamine 2000, cell viability was 10% more than what was reported for the commercial

reagent. Zhi et al.[33] have reported similar results in terms of transfection and cytotoxicity but using carbamate linkages between the ammonium heads and the hydrocarbon chains. Medvedeva et al.,[42] synthesized a biodegradable cholesterol-based (CcHPB), obtaining 22% GFP expression on HEK 293 (Human Embryonic Kidney 293) cells. While significant transfection efficiencies have also been reported for single-tailed cationic lipids, for to most part single-tailed and three-tailed cationic lipids appear to be more toxic and less efficient than their double-tailed counterparts[38]. Examples of single-tailed cationic lipids include: cetyl trimethylammonium bromide (CTAB), oleoyl ornithinate (OLON), and 6-lauroxyhexyl ornithinate (LHON)[39] (Table 1.1).

Comparison of transfection efficiencies of lipophophoramidates[43] and Biotinylated[44] cationic lipids formulations are show in Table 1.2.

1.3.1 Liposomes

Liposomes are lipid vesicles that are usually formed through the self-assembly of cationic di-acyl phospholipids which are amphiphilic in nature. The first lipid vesicle reported was formed by the dispersion of phospholipids in water by Bangham and coworkers[45]. Since then, a number of structurally diverse lipid vesicles have been developed. Unlike polypeptides, polysaccharides and polynucleotides, lipids are not polymers, by definition, however they are rarely found as monomers[46]. They prefer to assemble into macromolecular assemblies, such micelles and vesicles to escape exposure of the hydrophobic segments to water. Lipid vesicles will have different sizes depending on the method of preparation. Vesicle sizes fall into the nanometer to micrometer range[47]. Liposomes have found uses in many biological and pharmaceutical applications including diagnostic agents and drug delivery vehicles.

A major limitation for liposomes, *in vivo*, is the short circulating half-life[48]. Systemic elimination of cationic lipids takes place upon formation of larger aggregates via their interactions with the negatively charged serum molecules or cellular components (primarily erythrocytes and platelets). Surface shielding through the use of hydrophilic and charge

		Transfection efficiency (RLU/per mg/protein)	Lipid/DNA charge ratios	Incubation time	Serum	Ref.
HeLa	LIPOFECTIN	3.3×10^5	5:1	4h	-	[40]
	LIPOFECTAMINE	4.8×10^7	2.5:1*	4h	+	[40]
	DODAG/DOPE	1.3×10^8	4:1*	4h	+	[40]
	CDAN/DOPE	5×10^7	8:1*	4h	+	[40]
	CAPG/DOPE	2×10^7	2:1*	4h	+	[40]
	KLN47	1×10^7	2:1	4h	-	[43]
	BSV10	1×10^6	2:1	4h	-	[43]
	BSV36	1×10^7	2:1	4h	-	[43]
	DDCTMA	3.2×10^5	2:1	N/A	N/A	[43]
SWB-95	DOTAP/Chol	8×10^6	1:1	1h	+	[35]
	2Oc	1×10^7	1:1	1h	-	[35]
HEK-293	Lipofectamine	1×10^{11}	N/A	4h	+	[44]
	5c	1×10^9	8:1	4h	+	[44]

Table 1.2: *Luciferase expression in various mammalian cell lines transfected with cationic lipids commonly used for gene transfer. Transfection efficiency is expressed in Relative Light Units (RLU). The comparison was done at the optimal charge/ratio (that one that shows be more efficient) of each liposome formulation after 24h of transfection. *Represents the w/w ratio. Abbreviations: CDAN: N1-cholesteryloxycarbonyl-3,7-diazanonane-1,9-diamine. CAPG: N1-cholesteryloxycarbonyl-3-aza-pent-1-amino-5-guanidiniumchloride. DDCTMA: N-[1-(2,3-didodecylcarbamoyloxy)propyl]-N,N,N-trimethylammonium iodide. 2Oc: 1-(2,3-dioleoyloxy-propyl)-2,4,6-trimethylpyridinium. KLN47: trimethylarsonium Lipophosphoramidate polar head. BSV36: trimethylammonium polar head. BSV10: guanidinum polar head. DDCTMA: N-[1-(2,3-didodecyl carbamoyloxy)propyl]-N-ethyl-N,N-dimethylammonium iodide. SWB-95: Brain Glioma. HEK-293: Human Embryonic Kidney 293.*

neutral polymers such as polyethylene glycol (PEG) to reduce excessive chargecharge interaction appears very effective in prolonging the circulation half-life of lipoplexes[49]. However, some reduction in the overall transfection efficiency has been reported[49].

DNA complexation, cellular uptake and DNA release

Cationic liposomes when mixed with pDNA, in aqueous solutions, are capable of self-assembly into different liquid crystalline structures. These structures are called "lipoplexes" and the morphology of the phase depends on the packing parameter of the lipid molecules. Two phases appear to be more efficient for mammalian cell transfection: lamellar (L_α) phase with alternating lipid bilayer and DNA monolayers and inverted hexagonal (H_{II}) phase consisting of DNA coated with a lipid monolayer in a hexagonal lattice. It has been argued that the H_{II} phase complexes have a much higher transfection rates than do the L_α phase ones[50]. One explanation could be that this phase promotes the lipoplex fusion with cellular membranes facilitating the cellular uptake and the endosomal release[51].

A number of recent publications indicate that the usual endocytic routes of uptake for lipoplexes are: clathrin- and caveolae-mediated endocytosis and/or macropinocytosis[21,25,24]. It appears that lipoplexes are not limited to a single uptake pathway; rather they can utilize several of these pathways. It was observed that the inhibition of one pathway produced an increase in uptake though the other one (compensatory effect). Also, modifications in particle size, shape and exposed ligands on the lipoplexes can alter the route of uptake[52]. Nevertheless, the method of entry of these structures does not appear to contribute to transfection efficiency, no direct relationship has been observed[53,54]. For instance, for two lipoplex formulations, i.e., DOTAP/DOPC and DCChol/DOPE the same endocytic route (macropinocytosis) was observed in CHO cells, however the sub-cellular co-localization and the transfection efficiency was remarkable different. One explanation is that DCChol/DOPE lipoplexes or their cargos were capable of escaping the endosomes while the DOTAP formulation appeared to accumulate within these sub-cellular compartments[55]. These results

suggest that transfection efficiency correlates more directly with the ability of a lipoplex to escape the lysosome than its method of cellular uptake[56].

It has been proposed that for lipid-base systems escape from the endosomal/phagosomal vesicles is facilitated by membrane fusion and formation of transient pores in the organelles with the concomitant release of nucleic acids into the cytosol[52]. The presence of the helper lipid DOPE in some formulations promotes the transition from lamellar (L_α) phase to hexagonal (H_{II}) phase thus helping the insertion of lipoplexes into endosomal membranes[48]. This mechanism has been explained by the phenomenon called "ion paring". In this scenario the cationic and anionic phospholipid head groups neutralized each other thereby favoring the transition to the hexagonal (H_{II}) phase. Upon neutralization, dissociation of the DNA from the complex occurs[57]. The results suggest that strong lipid-DNA binding will interfere with the dissociation process and decrease transfection efficiencies. The incorporation of some modifications to the cationic lipids such pH sensitive linkers between the head group and the acyl portion of the molecules can promote enhanced DNA release[58]. Others have proposed that shorter hydrocarbon chains in the lipoplexes will increase the fluidity of the bilayer and favor higher rates of inter-membrane delivery and lipid membrane mixing, resulting in the increased disruption of the endosomal membrane and DNA escape[48].

Cytotoxicity of Lipoplexes

An important issue to address when considering *in vivo* studies is the toxicity of a specific nano carrier. Various cellular and tissue responses could lead to altered signaling or physiology, cell death and induced immune responses[59]. One cause of lipid cytotoxicity is the interaction of the tertiary or quaternary nitrogen functional groups that bind to and inhibit enzymes such as PKC[60]. In addition, cationic liposomes are known to affect the function of membrane proteins involved in signal cascades implicated in immune responses[29]. It was shown that some liposomes will induce immune response in the absence of antigens such as DOTAP liposomes which can induce expression of monocyte chemo-attractant protein-1

(MCP-1), macrophage inflammatory protein-1 alpha (MIP-1a) and macrophage inflammatory protein-1 beta (MIP-1b) together with transcription of a dendritic cell maturation marker, CD11c[61]. Nevertheless, a novel strategy has been proposed to take advantage of this specific immune-stimulating (adjuvant) feature to enhance the development of an anticancer vaccine using the peptide antigen derived from E7 oncoprotein of human papillomavirus (HPV) type 16 mixed with the cationic lipid DOTAP[62]. While several reports have described this phenomenon these effects have not been studied in great detail. Also, cationic lipids have been reported to activate several kinases implicated in immune responses and regular cell signaling[63,64]. In addition, cationic lipids fusing with cell membranes could lead to the insertion of foreign lipids into the membrane[65]. Having foreign lipids in a membrane could alter the physio-chemical properties of the bilayer thereby affecting membrane protein structure, cell signaling and interactions between lipids and protein membranes. It has been reported that this process can cause non specific inflammatory responses[66].

1.4 Polymeric DNA carriers

Polymers used in gene delivery, like their lipid counterparts, are generally cationic in character. They are made up of a wide variety of polymerized monomers[67]. The most frequently used to deliver DNA include: Polyethylenimine (PEI)[68], poly(α-[4-aminobutyl]-l-glycolic acid (PAGA)[69], Poly(β-Amino Ester) (PBAE)[70], poly(amidoamine) (PAMAM), poly-propylenimine (PPI), Poly(2-(dimethylamino)ethyl methacrylate (DMAEMA)[71] and polyethylene glycol (PEG) (Figure 1.3). They are easy to synthesize, and some of them including PBAE and PAGA, contain biodegradable linkages designed to reduce cell toxicity. PEI, is one of the most widely studied non-viral vectors due to its high transfection efficiency. Its highly cationic surface strongly associates with and helps condense DNA efficiently, however it is one of the most toxic agents being investigated[72]. Dendrimers, such PAMAM and PPI are synthetic, hyper-branched spherical molecules that are capa-

ble of entrapping small molecules within their structures[73]. Their large size and multivalent surfaces provide an excellent platform for the attachment/associate of different drugs and therapeutic genes. DMAEMA is a cationic polymer offering the advantage of being a water-soluble cationic polymer[74]. PEG is commonly conjugated to some of the polymers mentioned above to prevent aggregated complexes and to increase stability and circulation half-life, *in vivo*[75]. Natural occurring polymers in complexion with other molecules, such as collagen with DMPC[76] and gelatin with PEI[77] have been tested also as pDNA delivery vehicles where they have shown promising results and having the advantage of good cytocompatibility. These properties have made these molecules popular choices in areas outside of gene delivery namely, tissue engineering scaffolding applications[78].

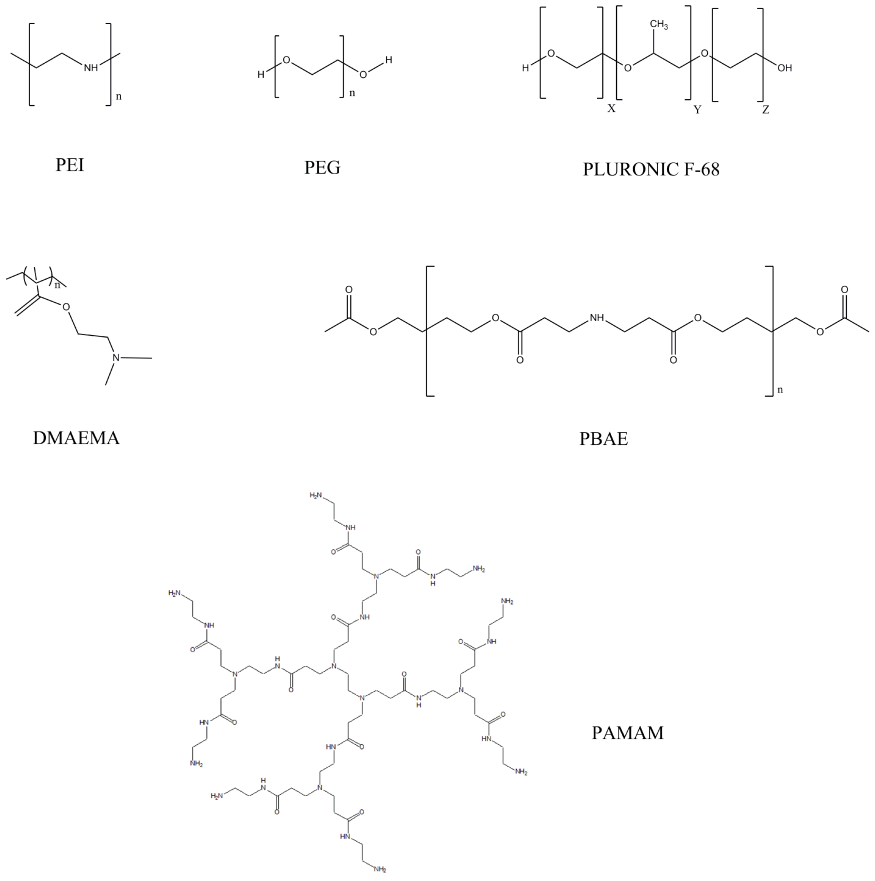

Figure 1.3: *Structures of the most common synthetic polymers used for gene delivery.*

Recently, Newland et al.,[79] reported on a new polymeric gene vector formed predominantly through internal cyclization reactions within the polymer instead the usual hyperbranching between polymer chains. Ethylene glycol dimethacrylate (EGDMA) was the cyclizing unit while 2-(Dimethylaminoethyl) methacrylate (DMAEMA) was the cationic unit. Despite the multi-step and synthesis of the polymer involving a dialysis process for several days, significant transfection efficiencies and moderate toxicity was observed when compared to commercial agents such as SuperFect® (partially degraded PAMAM) and PEI (Figure 1.4, Table 1.3 and 1.4). Zhou et al.,[80] synthesized a family of biodegradable poly(amine-co-esters) formed through enzymatic copolymerization of di-esters with amino-substituted diols. They reported very high transfection efficiencies and low toxicity in comparison to polyethylenimine and Lipofectamine 2000. However, the formation of the poliplexes has to be done under slightly acidic conditions and in the presence of DMSO. These conditions could be a drawback for some sensitive cell lines. Keeney et al.,[81] reported on a poly(β-amino ester) biodegradable system for the efficient delivery of Mini Circle MC-DNA that gave significant GFP expression (Table 1.4). MC-DNA is a small supercoiled DNA molecule where the bacteria cassette commonly used in plasmids has been removed. They created a small library of 18 poly(β-amino ester) polymers differing in the backbone structure and the end-group chemistry. Subsequently, these polymers were tested in embryonic kidney 293 cells and mouse embryonic fibroblasts obtaining excellent transfection rates in some of them. In this study they demonstrated that higher transfection efficiency can be achieved for HEK cells using the MC-DNA instead the conventional plasmid.

Different materials have been combined with polymers to form hybrid gene delivery nanoparticles in order to improve the stability, targeting and the circulating half-life in blood[82,83,84,85]. Majoros et al.,[86] reported folate-mediate targeting where the poly(amidoamine) (PAMAM) dendrimer was conjugated to folic acid. These folate residues bind to folate receptors that are overexpressed in some cancer cells[87]. Comparisons of some commercial available polymeric-base transfection reagents[88] are shown in Table 1.4.

		Transfection efficiency (RLU/per 96-well)	Lipid/DNA charge ratios	Incubation time	Serum	Ref.
HeLa	Arrest In	5.4×10^5	5:1	4h	+	[88]
	Express Fect	2.9×10^5	1:1	4h	+	[88]
	JetPEI	6.5×10^5	2:1	4h	+	[88]
	SuperFect	2.2×10^6	5:1	4h	+	[88]
	Dextran-Spermine	4×10^5	5:1	4h	-	[88]
	Collagen	1×10^5	4:1	4h	-	[88]
CHO	PEI 800 Da	4×10^6	18	4h	-	[89]
	PEI 25kDa	3×10^{10}	9	4h	-	[89]
	PEI-DSP	8×10^9	9	4h	-	[89]
	PEI-DTBP	3×10^8	9	4h	-	[89]

Table 1.3: *Luciferase expression in various mammalian cell lines transfected with the indicated cationic polymers commonly used for gene transfer. Transfection efficiency is expressed in Relative Light Units (RLU). The comparison was done at the optimal charge/ratio (that one that shows be more efficient) of each polyplex formulation after 48 h of transfection. Abbreviations: DSP: cross-linking reagent, di-thio-bis(succinimidylpropionate). DTBP: cross-linking reagent dimethyl 3,3'-dithiobispropionimidate 2HCl.*

		% Cells transfected	Polymer/DNA charge ratios	Incubation time	Serum	Ref.
1018	Chitosan/γ-PGA	54	10:1:14*	4h	-	[90]
	Lipofectamin 2000	33	N/A	4h	-	[90]
PMSCs	Fugene	15	N/A	4h	-	[91]
	PEI-β-CD	12	N/A	4h	-	[91]
	TAT-PEI-β-CD	16	N/A	4h	-	[91]
HEK-293	PEI 25KDa	10	15	4h	+	[92]
	PEI 1.8KDa	4	90	4h	+	[92]
	PAMAM G5	22	90	4h	+	[92]
	PAMAM G1	18	10	4h	+	[92]
	PAMAM G2	8	50	4h	+	[92]
	EA-G1	18	50	4h	+	[92]
	EA-G2	43	50	4h	+	[92]
	PEI-25KDa	12	15	4h	+	[92]
	Lipo-2k	23	6	4h	+	[92]
HeLa	PEI	30	5:1	2h	-	[93]
	CTS	18	7	2h	-	[93]
	NMCTS-graft-PAMAM	36	5:1	2h	-	[93]
	MWCNT-CS-FA-NPs	4.1	5:1	6h	-	[94]
	MC/PBAE-1445	82	10:1	4h	+	[81]
3T3†	PEI	3	N/A	4h	-	[79]
	dPAMAM	10	N/A	4h	-	[79]
	PD-E 8 PEG	13	3:1*	4h	-	[79]

Table 1.4: *Transfection efficiency using the reporter plasmid pEGFP (Enhanced Green Fluorescence Protein) in various mammalian cell lines transfected with cationic polymers commonly used for gene transfer. The comparison was done at the optimal charge/ratio (that one that shows be more efficient) of each lipoplex formulation. *This represent w/w ratio. Fugene has a protected formulation. †Normalized to total parent events. Abreviations: NMCTS-graft-PAMAM: N-maleyl chitosan-graft-polyamidoamine. CTS: Chitosan. MWCNT-CS-FA-NPs: Multi-Walled Carbon Nanotubes (MWCNTs) of different functionalized with chitosanfolic acid nanoparticles. MC: Minicircle DNA. G: Generation of dendrimer. EA-G2 (or EA-G1) was prepared by aminolysis of poly(ethylene glycol)-poly(L-benzyl glutamate) (PEG-PBLG) using PAMAM G2 (or G1). HT-1080: fibrosarcoma. PMSC's: Parthenogenetic Mesenchymal Stem Cell.*

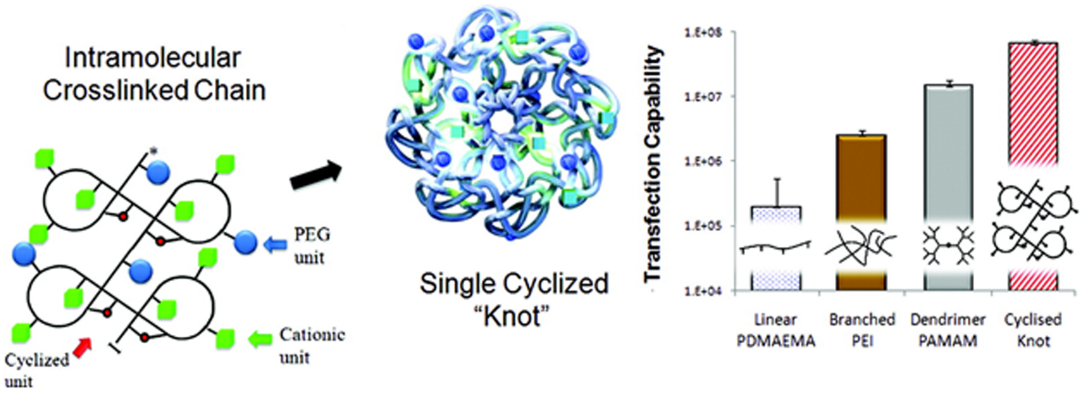

Figure 1.4: *The structure of the single cyclized polymer knot. This knotted polymer shows better transfection capability compared to linear, branched or dendritic polymers. Reprinted with permission from ref. 79, B. Newland, Y. Zheng, Y. Jin, M. Abu-Rub, H. Cao, W. Wang, A. Pandit, Single cyclized molecule versus single branched molecule: a simple and efficient 3D knot polymer structure for nonviral gene delivery. J Am Chem Soc USA, 134, 4782-4789 (2012). Copyright® 2012, American Chemical Society.*

Anderson and co-workers[95] reported a high-throughput method for assessing polymer-mediated transfection. Hundreds of polymers can be tested for gene delivery using 96-well plates in one day. One limitation of this high-throughput method is the small volumes that were used for the transfections where polymer-DNA complexation could not be guarantee. Nevertheless, this method has been already tested with some polymeric based transfection reagents. From these experiments there appear to be several parameters involved in the successful design and effectiveness of polymeric transfection reagents: cell type, carrier/DNA ratio, particle size, toxicity, solubility and stability in serum.

1.4.1 DNA complexation, cellular uptake and DNA release

Polymers due to their cationic nature are capable of interacting and condensing pDNA to generate nano-sized complexes called poliplexes[96]. Polymers bind DNA through electrostatic interactions between the phosphate groups present in the DNA and the cationic groups present in the polymer reagent[97] This is an entropic process, with counter ions be-

ing displaced from both, the DNA and the polymer. Surface charges and the "nitrogen to phosphate" (N:P) ratios are the primary factors controlling the size and morphology of the poliplexes[98]. They adopt structures that are typically blends of toroids and rods, with diameters ranging from 50-100 nm.

Regardless of the complex's topology, it is the net positive charge that facilitates the binding interactions with negatively charged cell surface. Subsequently, they are internalized, in most cases, through endocytosis[99]. It has been reported that internalization of poliplexes (<500 nm in diameter) occurs mostly through receptor-mediated endocytic routes such as clathrin-mediated endocytosis (CME) and caveolae-mediated endocytosis (CvME). Particles sizes > 500 nm are taken up by other internalization pathways[100]. Polymers can be internalized as well by non-endocytic pathways. Studies carried out by Hong et al.[101,102] demonstrated that PAMAM forms small holes in the cell membrane with its subsequently diffusion into the cell. However, modifications to this polymer such the conjugation to folic acid switches its enter route to receptor-mediated endocytosis. This indicates that the attachment of certain ligands can be used for targeting purposes to trigger a specific endocytic route and manipulate the intra-cellular localization of the poliplexes.

It is generally assumed that low to moderate gene expression is due to the trapping and degradation of the pDNA within intracellular vesicles and limited translocation to the nucleus[28,16]. For cationic polymers it is hypothesized that tertiary amine groups become protonated inside the endosome or (phagolysosome) due to normal acidification processes leading to an influx of Cl^- counter ions to restore charge neutrality. Subsequently, through osmosis excess water enters the endolysosomes causing membrane rupture[103]. This controversial process is referred to as proton "sponge escape"[104,105]. In order for this process to occur the pKa(s) of the *tert*-amines must be low enough such that they are unprotonated at physiological pH and only upon acidification acquire the quaternary form. Some reports using simulations or direct measurements suggest that more than 50% are already protonated under physiological conditions. In the original paper describing this phenomenon, all

of the structures that displayed this property were true imines containing a double bond at the bridging nitrogens[21]. Nearly all of the plasmid delivery structures produced through the polymerization of imines have been reduced to *tert*-amines at the bridging nitrogens, hence no double bonds. The most recent studies suggest that proton sponge escape is probably not the driving force for the rupture of the endosomes[106,107].The exact mechanism of endosomal escape is still open to debate.

Some studies suggest that poliplexes must escape the endosomes and release the DNA into the cytosol. The released DNA then makes its way to the nucleus for transcription[19]. However, the translocation of the DNA molecules through the nuclear pores is reported to be a relatively inefficient process with only 0.1% translocating into the nuclei. It has been proposed that the DNA is degraded in the cytoplasm and has difficulty traversing the small diameter of the nuclear pores[108]. Breuzard et al.[109] found using FRET and FRAP analyses that LPEI-DNA complexes are present in the nucleus. This has raised the question of how the poliplexes cross the nuclear membrane. The authors suggested that the poliplexes can undergo modifications in order to pass and fit through the nuclear pores. Also, they proposed that the plasmid is unpacked in the cytosol and repacked in the nuclei. In contrast to some polymers, lipids are never found in the nuclei suggesting that only the pDNA is translocate across nuclear pores[110].

While the mechanism of nuclear import of pDNA in poliplexes remains controversial, clearly the rate-limiting step, which determines transfection efficiency, lies between endosomal escape and translocation across the nuclear pore. Incorporation of nuclear localization signals and bimetallic nano rods made of Ni/Cu[111] that can associate with compacted DNA and target ligands simultaneously to the nucleus could be potential tools to enhance the DNA translocation step.

1.4.2 Cytotoxicity of polyplexes

Among all of the features of polymers, molecular weight and chain length have the most impact on transfection efficiency and toxicity. Generally, high-molecular weight polymers display better transfection rates yet are found to be more toxic for most of cell lines[54]. The inherent toxicity of some polymers is an issue that still needs to be addressed. Researchers are constantly developing novel cationic structures or optimizing existing ones with a variety of motifs hoping to reduce toxicity[80].

PEI, alone, can cause cell necrosis and apoptosis[112] and in some cases long-term expression is not achieved[59]. Hunter et al.[59] presented two phases of PEI cytotoxicity: Phase 1, cell membrane destabilization and trigger of apoptotic pathways and Phase 2, apoptosis and loss of Mitochondrial Membrane Potential (MMP), leading to drop the ATP production and loss of mitochondrial membrane integrity. It was found that N-acylation of a branched 25 kDa PEI can increase its gene delivery efficiency and at the same time reduce its cytotoxicity[113]. Conjugation of PEI with homo-bifunctional amine reactive reducible cross-linking reagents has improved the *in vitro* gene delivery efficiency in Chinese hamster ovary (CHO) cells, with a reduction in cytotoxicity[89] (Table 1.3). The incorporation of cyclodextrins and targeting peptides has also raised their transfection efficiency and decreased cytotoxicity[114].

Poly-amidoamine (PAMAM) and poly-propylenimine (PPI) are dendrimers that show high transfection efficiency[115]. However, the toxicity of dendrimers is the major concern limiting their medical use. Dendrimers interact nonspecifically with negatively charged biological membrane forming transient nano-holes leading to leakage of cytoplasmic elements and cell death[116]. Several approaches have been tried to reduce their toxicity including the design of more biodegradable and/or biocompatible dendrimers comprised of peptide and sugars. Surface modifications such the addition of PEG or Chitosan significantly reduces toxicity of these complexes[117]. Recently, Sarkar et al.[93], conjugated N-maleyl chitosan (NMCTS) by Michael type addition reaction to improve solubility, transfection efficiency and low the toxicity (Table 1.4). Pan et al.[92] reported as well high transfection activity with

moderate toxicity of a copolymer made of poly(ethylene glycol)-poly-(L-glutamine) mixed with high molecular weight PAMAMs (Table 1.4).

Outstanding issues regarding the bioactivity, metabolism and cytotoxicity of free polymers in the cytoplasm or in sub-cellular components needs to be fully characterized in order to design a less toxic poly-cations[65]. There are indications that these molecules could be used in medicine where cytotoxicity is desired such as cancer chemotherapy.

1.5 Polysaccharide-Based DNA Carriers

1.5.1 Cyclodextrins

Cyclodextrins (CDs) have been extensively studied as non-viral gene delivery vehicles due to their exceptional biocompatibility and high cation density[118]. Cyclodextrins by itself does not form stable complexes with pDNA and this has limited their application as a transfection system. For this reason they are being use mostly as enhancers with other cationic polymers or dendrimers due to their ability to make the cell membrane more permeable by depleting or affecting membrane cholesterol levels[91,119] (Table 1.4). However, CDs have shown potential for gene delivery due to their amphiphilic character, low immunogenicity and multiple reactive sites available for the attachment of target groups and cations. Cryan et al.[120] modified CDs with pyridylamino, alkylimidazole, methoxyethylamino or primary amine groups at the 6-position of the glucose and reported significant luciferase expression in COS-7 cells. Darcy and coworkers[121] converted the terminal hydroxyl groups of CDs into amino groups and obtained transfection efficient on COS-7 cells comparable to Lipofectamine 2000®.

1.5.2 Chitosan

Chitosan is a polysaccharide obtained through the chemical treatment of the naturally occurring cross-linked polymer- chitin, the primary constituent of crustacean exoskeletons[66]. Chitosan has been extensively studied for non-viral gene therapy due to its exceptional biocompatibility and high cation density[122]. Gene delivery efficiency of chitosan is affected by a number of factors, including molecular weight, counter ions, degree of deacetylation, and pH[12]. Even with optimized formulations, the application of chitosan-based gene delivery system is still limited by reduced water solubility, inefficient gene unpacking and low gene transfection efficiency. In recent years, various chitosan derivatives have been generated aiming to resolve these problems. The structural modification of these newer chitosan derivatives can be divided into hydrophilic and hydrophobic modifications[123]. Incorporation of negatively charged agents such as hyaluronic acid (HA) or poly (L-glutamic acid) (-PGA) with chitosan has increased its transfection efficiency significantly[90,124] (Table 1.4). Such improvements in the transfection ability of chitosan-based carriers has been attributed to the reduced charge density upon the addition of HA chains or the formation of -PGA/chitosan/DNA complexes that can dissociate into smaller sub-particles after cellular internalization, both of which could improve the release of bound DNA. It should be noted that the choice of the type and the amount of anionic polymer incorporated to chitosan/DNA complexes greatly influences the transfection ability through changes in cellular uptake, stability, the size of the nanoparticles, and condensing and dissociating ability of the DNA. Chitosan has also been conjugated to diverse molecules and polymers such: poly-L-lysine (PLL), arginine, guanido groups, PEG (Polyethylene glycol), histidine, cysteine, glutathione, glutamic acid, galactose, targeting peptides and proteins, biotinylated, chondroitin sulfate, chitosan nanobubbles, PEI (poly(ethylene-imine), lipid shells and spermine, with the purpose of lowering the cytotoxicity and increasing DNA delivery efficiency[75,125].

1.6 Peptide DNA carriers

The ability of some peptide sequences to translocate across cell membranes was discovered serendipitously through the observations of virologist working on the HIV-1 Tat transactivating factor and by neurobiologists working on the Drosophila Antennapedia transcription factor[126]. Short basic amino acid sequence segments, rich in arginine residues, were identified as the critical component responsible for membrane translocation. This region has ben given the term "peptide transduction domain" (PTD). After this discovery several variations of cell penetrating peptides (CPPs) have been reported in literature[127]. They vary significantly in their sequence, hydrophobicity, and polarity. However, common features are their amphipathic character and net positive charge. CPPs can be broadly classified into different structural categories: cationic peptides, amphipathic peptides, histidine-rich peptides and peptides containing nuclear localization signal (NLS)[128]. Older examples of cationic peptides (or peptides with low amphiphilic character) are poly-L-lysine (PLL)[129], polyarginines[130], penetrain[131] and TATp[132]. Examples of amphiphilic CPPs include MAP[133], transportan[134] and KALA[135]. Pep-1[136] it is a well know amphiphilic peptide but it is has been used mostly as a protein carrier rather than DNA carrier. Histidine containing peptides, due to the presence of the imidazole group, can produce membrane destabilization and promote endosomal release[68]. A nuclear localization signal sequence has been incorporated to some peptides (NLS)[137] in order to promote the nuclear localization of CPPs upon escaping the endosome. NLSs are characterized by short clusters of basic amino acids that are recognized and bind to cytoplasmic receptors knows as imporntins. The most well known NLS comes from the large tumor antigen of the simian virus 40 (S40) made of only 7 amino acids PKKKRKV.

The conjugation of proteins or peptides to cationic liposomes appears to be a promising method for improving pDNA delivery *in vitro*[32]. Several publications have reported significant advances in transfection efficiency using theses combined complexes[138,139,140]. While the liposomes can efficiently interact with pDNA and promote endosomal escape, peptides can aid in targeting the complex to a specific type of cell and even the nuclei. *In vivo* deliv-

ery still has drawbacks due to inactivation by serum components, renal excretion and rapid clearance by immune phagocytic cells if the size of the complexes is below or above 100 nm. Peptide adducts can affect the size and overall surface of the complexes making them more suitable for *in vivo* delivery. Sarker et al.[141] synthesized 100 nm arginine-based cationic lipid nanoparticles. They reported that these nanoparticles, when mixed with DNA, formed large aggregates in the absence of serum but in the presence of serum small vesicles were observed. Transfection of HeLa cells with these complexes showed higher efficiency and less toxicity when compare to Lipofectamine 2000.

To further enhance gene delivery peptides have been conjugated to several synthetic polymers as well. pTAT sequence has been couple to PAMAM, PEG and PEI[142]. Kwot et al.[143] explored peptide dendrimers as a new type of transfection reagent. They synthesized a collection of dendrimers conjugated to different cationic and hydrophobic peptides motifs in conjunction with the lipid DOTMA/DOPE (Table 1.4). The best results were observed for G1,2,3-KL ($(LysLeu)_8(LysLysLeu)_4(LysLysLeu)_2LysGlySerCys\text{-}NH_2$) with reported transfection efficiency up to 10-fold higher than commercial reagents.

Recently we developed a new type of cationic peptide particle that is comprised of two self-assembling branched amphiphilic peptides bis-(FLIVIGSII)-K-KKKK (h_9) and bis-(FLIVI)-K-KKKK (h_5)[144,145,146]. In water, a 1:1 mixture of these two peptides form water-filled bilayer delimited capsules. Solutes are encapsulated during the assembly process. When prepared at 25 °C and then cooled to 4 °C , extremely stable 20-30 nm capsules are formed that are resistant to temperature, chaotropes, proteases, detergents and the cells degradative machinery. Initial investigations involving the entrapment and delivery of pDNA failed as the peptides appear to coat the surface of the DNA and cause its linearization. Under these conditions the N:P ratio was 65.5. Very low transfection rates were observed using this method. Subsequent lowering the N:P ratio to near unity results in compaction of the DNA with the peptides acting like histones. This lower ratio gives much higher transfection rates (20% GFP). Recent refinements are pushing the transfection rates even

higher and with no measurable toxicity.

Peptide-based gene delivery systems have some advantages over other gene therapy strategies[147]. For instance, peptides are more stable, easier to synthesize on a large scale than lipids, less prone to oxidation, less toxic and are easy to covalently modify with cell specific recognition ligands[148]. These ligands include vitamins, cholesterol, metals and antibodies. These adducts can be added through the formation of amines, esters and disulfide linkages[149]. Nevertheless, the transfection efficiencies are low compared with the liposomes and some polymers. Endosomal entrapment and poor nuclear import have been suggested as the main causes for reduced transfection efficiencies for pure peptide systems[148].

1.6.1 DNA-Complexation, cellular uptake and DNA release

Cationic peptides can efficient packed DNA into nanoparticles and prevent their enzymatic degradation. Peptides containing lysine and arginine have been extensively used for gene delivery, however the mechanism of how they bind and condense DNA is poorly documented in comparison to lipoplexes and polyplexes. Mann et al.[150], in a recent publication studied the different patterns of DNA condensation between lysine and arginine based homopeptides and correlated these structures with gene delivery. By varying the charge ratio and the length of the homopeptides they characterized six different types of DNA-peptide structures ranging in a size between 30-350 nm using atomic force microscopy. Results showed that a lower peptide to DNA charge ratios the tendency is to form road-like structures. Whereas, at higher peptide to DNA charge ratios compact spheres were observed. The authors proposed two structures for the arg- and lys-containing complexes. A multi-molecular condensation pattern for arginine containing peptides, with multiple pDNA molecules associated with the peptide and a mono-molecular structure proposed with a single pDNA molecule for lysine containing peptides.

There are many factors that are involved in determining the peptide cellular uptake including: exposed ligands, particle size, particle shape, cell type, presence of cargo and

even culture conditions. Currently, it is accepted that peptides can be internalized by two pathways: non-endocytic and endocytic[151]. The non-endocytic pathway has three prominent modalities to explain peptide internalization: fusion, inverted micelle and formation of transient pores in the cell membrane. Some references propose that a tight ionic interaction between the basic groups of the peptide side chains and the negative charges of the phospholipid heads induce a local invagination of the plasma membrane[152]. The local reorganization of the phospholipid bilayer would then lead to the formation of inverted micelles with the peptide enclosed in the hydrophilic cavity and ultimately resulting in cytoplasmic release. There are few reliable methods available to definitively identify non-endocytic pathways. For the energy depend pathways, macropinocytosis seems to be the primary route responsible for CPP-mediated intracellular delivery of DNA[153]. However, as previously discussed nanoparticles can simultaneously enter cells through more than one pathway. Antp, nona-arginine, and the TAT peptide simultaneously used three endocytic pathways: macropinocytosis, clathrin-mediated endocytosis, and caveolae/lipid raft-mediated endocytosis[154].

For cationic peptides, the mode of escape from the lysosome is thought to occur through an endosomal lysis mechanism similar to that seen for lipoplexes[155]. Histidine-rich peptides contain ionizable imidazole groups that are partially unprotonated at physiological pH. Protonation through endosomal acidification could induce rupture of the endosomes as previously described. It has been suggested that TAT fusion proteins can enter the cell through endocytosis but escape the endosomal rout similarly thus evading the lysosomal degradation. Subsequently, they became localize near the perinuclear area[156]. The relatively low transfection level of PLL-DNA complexes is due possibly to the poor release of the complexes from endosomal compartments. Incorporation of histidine residues and lipids such myristic, palmitic and stearic acids have shown improved release into the cytoplasm with a concomitant increase in transfection efficiency.

1.6.2 Peptide Cytotoxicity

Peptides are made of natural occurring amino acids and display low toxicity at the concentrations typically employed. Very little has been reported in the literature associated peptide carriers with cell necrosis or apoptosis. This fact and the ability to easily penetrate cell membranes, could make them potentially the preferred carriers for gene delivery *in vitro* and *in vivo*. As far as we know, alterations in the cell physiology or immune responses have not been reported for pure peptide gene delivery systems. Hunter et al.[59] indicated that poly-lysines can induce mitochondrial-mediated apoptosis. Cardoso et al.[157] have reported that some amphiphilic peptides can produce membrane perturbations and induce transient influxes of calcium ions however the report indicates that cell membranes rapidly recovered and no permanent cell damage was observed.

1.7 Inorganic Nanoparticles

Inorganic nanoparticles are usually prepared from metals (e.g., iron, gold, silver), inorganic salts, or ceramics (e.g., phosphate or carbonate salts of calcium, magnesium, or silicon)[158]. The metal ion salts, in combination with DNA generate complexes with a typical size range of 10100 nm in diameter. The surfaces of these nanoparticles can be coated to facilitate DNA binding or target gene delivery. The small particle size offers several advantages including that they usually bypass most of the physiological and cellular barriers and produce higher gene expression. They can also be transported through the cellular membranes via specific membrane receptor or nucleolin, which delivers nanoparticles directly to the nucleus skipping the endosomallysosomal degradation. These nanoparticles have the ability to efficiently transfect post-mitotic cells *in vivo* and *in vitro*[159]. Additionally, they tend to show low toxicity and are immune silent. Supra-paramagnetic iron oxide-based nanoparticles display magnetic properties when placed in magnetic fields thereby allowing magnetic field guided delivery[160]. Progress in (*in vivo*) applications of inorganic nanoparticles has accelerated

recently. However, extensive studies are still required to assess the effect of their types, sizes, and shapes on transfection efficiency. It is certain that further studies focusing on long-term safety and surface functionalization will foster future clinical applications.

1.7.1 Gold Nanoparticles

The ability of gold nanoparticles (GNPs) to interact with and enter cells has prompted researchers to attach various compounds and biological macromolecules to gold in an effort to combine functionality with cellular uptake. The loading of gold nanoparticles with drugs or genes offers the prospect of greater control and increased therapeutic efficacy. In particular, the combination of gold nanoparticles and laser irradiation to control the release of drugs and genes has the potential to provide useful therapeutic benefits[161]. The attractive features of gold nanoparticles include their monitoring by surface plasmon resonance, the controlled manner in which they interact with thiol groups, and their low-toxicity. Gold nanoparticles were functionalized with cationic quaternary ammonium groups and then electrostatically bound to plasmid DNA. This composite particle could protect the DNA from enzymatic degradation and could regulate DNA transcription of T7 RNA polymerase[162]. In another report, cationic gold nanoparticles prepared by NaBH4 reduction in the presence of 2-aminoethanethiol formed a complex structure with plasmid DNA expressing a luciferase gene[163]. Figueroa et al.[164], conjugated gold nanoparticles (AuNP) to polyamidoamine (Figure 5). AuPAMAM conjugates have been synthesized by crosslinking PAMAM dendrimers to carboxylic-terminated AuNPs. This new hybrid system was capable of condensing and delivering pDNA in an efficient manner with low cytotoxicity.

1.7.2 Carbon Nanotubes

Carbon nanotubes (CNTs) consist of carbon atoms symmetrically arranged in sheets of graphene. Bianco et al.[165], were one of the earliest practitioners in the use of carbon nanotubes for gene delivery. They synthesized a modified carbon nanotube using the 1,

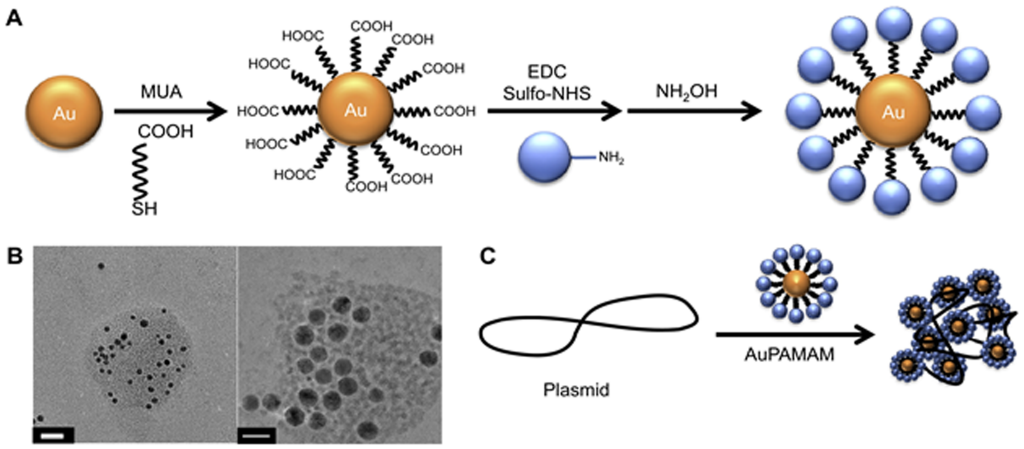

Figure 1.5: *Synthesis of MWCNT-CSFA NP hybrids. Reprinted with permission from ref. 164. E.R. Figueroa, A.Y. Lin, J. Yan, L. Luo, A. E. Foster, R. A. Drezek, Optimization of PAMAM-gold nanoparticle conjugation for gene therapy. Biomaterials, 35, 1725-1734 (2014). Copyright® 2014, Elsevier.*

3-dipolar cyclo-addition of azomethine. Both single walled carbon nanotubes (SWNTs) and multi-walled carbon nanotubes (MWNTs) were functionalized with a pyrrolidine ring bearing a free amine-terminal oligo-ethylene glycol moiety attached to the nitrogen atom. This functional group increased the solubility of carbon nanotubes and enhanced their ability to bind and condense DNA. CHO cells were transfected using these functionalized carbon nanotubes, delivering pDNA containing β-galactosidase as a marker gene[166]. Nunes et al.[167], have transfected lung epithelial (A549) using carboxylated MWNTs conjugated to the cationic polymers polyethylenimine (PEI), polyallylamine (PAA), or a mixture of the two polymers. Liu et al.[94], have reported the conjugation of MWNT with chitosan-folic acid nanoparticles and transfected cells using the gene reporter GFP (Figure 1.6). They observed an increase on transfection efficiency and reduction of cytotoxicity with this functionalization. Compared to the traditional delivery vehicles, the major advantages provided by carbon nanotubes are the following: 1) they are easily translocated across cell membrane 2) are capable of achieving spatially- and temporally- controlled release for targeted gene silencing, 3) their influence on conformation and conformational transitions of DNA/siRNA

due to their unique shape, modifiable surface chemistry, and their remarkable flexibility, and 4) their ability to be monitored for therapeutic effects of DNA/siRNA due to their extremely stable and strong Raman signal and NIR fluorescence emission[168].

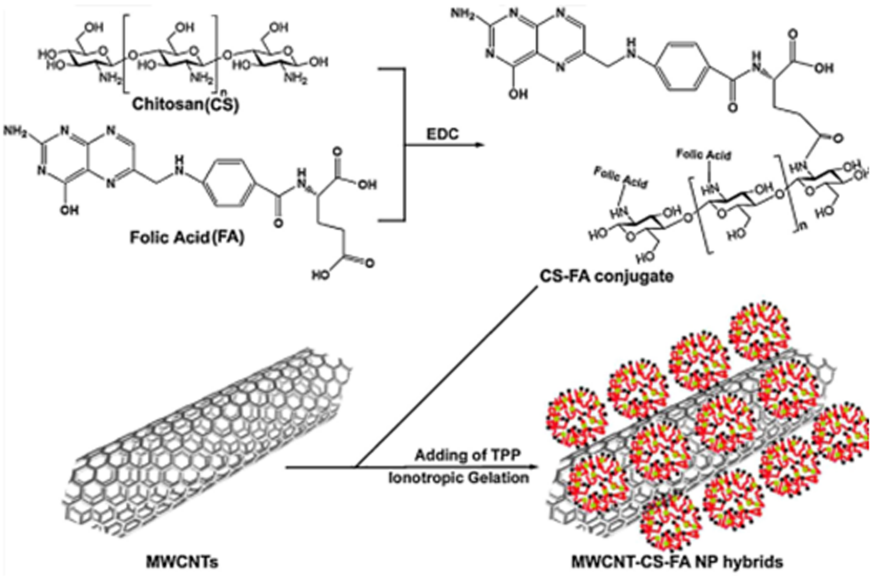

Figure 1.6: *Biocompatible multi-walled carbon nanotube-chitosanfolic acid nanoparticle hybrids as GFP gene delivery materials. The scheme demonstrating the synthesis of MWCNT-CSFA NP hybrids. Reprinted with permission from ref. 94, X. Liu, Y. Zhang, D. Ma, H. Tang, L. Tan, Q. Xie, S. Yao, Biocompatible multi-walled carbon nanotube-chitosanfolic acid nanoparticle hybrids as GFP gene delivery materials. Colloids Surf B Biointerfaces, 111, 224-231 (2013). Copyright® 2013, Elsevier.*

1.8 Summary

A significant number of diverse methods are currently available for pDNA delivery *in vitro*. Reports are emerging with great frequency describing modified or completely new transfection materials and protocols that do not require virus particles. For chemical carriers, there are several factors that can affect the transfection efficiency: cell type, carrier/DNA ratio, particle size, toxicity, solubility and stability in serum. Lipid and polymer base systems conjugated to peptides or inorganic nanoparticles seem to be the some of the most

promising non-viral vectors for pDNA gene delivery *in vitro*. It is important to critically analyze combination of these elements in order obtain high delivery efficiencies using the current generation of biomolecules. Researchers are undoubtedly trying to generate the next generation of amphiphilic cationic molecule capable of overcoming the extracellular and intracellular obstacles for *in vitro* and *in vivo* gene delivery taking into account the advantages and disadvantages of the current systems. Using current screening technologies this will be a time- and energy-intensive endeavor. The development of high-throughput methods for assessing transfection systems is needed and will be vital for optimizing the numerous parameters involved in this complex process.

Chapter 2

Branched amphiphilic cationic oligo-peptides form peptiplexes with DNA: A study of their biophysical properties and transfection efficiency

2.1 Introduction

The ability to deliver bioactive macromolecules into specific cell organelles holds the promise of treating a broad range of human diseases[3]. The first steps required for targeting sub cellular organelles involve traversing the plasma membrane and then gaining access to the cytosol. Macromolecules such as plasmid DNA (pDNA) are anionic and show greatly re-

duced membrane bilayer permeability[2]. Typically they need to be associated with molecular carriers to facilitate their translocation into the cell.

Adenovirus and retrovirus were the earliest systems used to deliver therapeutic pDNA and they still remain the first choices due to their high transfection efficiency[11]. Two disadvantages of viral gene delivery systems are the possibility of inactivating host genes through insertional mutagenesis and triggering severe immune responses[12]. In addition, previously established immunity to the virus vector and size limitations for packaging larger pDNAs have limited their clinical applications[13].

Safer, non-viral methods are being developed for DNA/RNA packaging and delivery systems[16]. While they have been reported to be less efficient than viral vectors, improvements in genome editing systems such as CRISPR/Cas9 and zinc-finger nuclease (ZFN), have greatly improved integration of corrective sequences by making them site specific[17,18]. Adding genome editing elements to pDNA and incorporating them into non-viral gene delivery systems has moved gene therapy closer to clinical applications.

A wide range of methods are currently available for pDNA delivery *in vitro*. Reports are emerging with increasing frequency describing modified or completely new transfection materials and protocols that do not require virus particles. Lipoplexes[169] (cationic lipid-DNA complexes) and polyplexes[38] (cationic polymer-DNA complexes) are examples of such non-viral gene delivery systems, which are potentially immunologically inert, as well as safe and effective gene delivery systems[170,171,153]. Lipoplexes constitute self-assembling nanosystems formed as a consequence of branched cationic lipids (e.g. DOTMA, DOTAP, etc.). Cationic lipids are amphiphilic molecules consisting of a positively charged polar head group connected to hydrophobic domain via a linker. They spontaneously react quantitatively with the negatively charged DNA molecules to form complexes, with the cationic lipids encasing the dsDNA[172,173]. Successful DNA delivery is known to be dependent on various factors that include the chemical structure and geometry of the cationic lipids as well as the supramolecular structure of the lipoplexes[57,20]. X-ray diffraction studies have revealed

the presence of a variety of structures for lipoplexes - including lamellar (L_α) phases with alternating lipid bilayer and DNA monolayers and inverted hexagonal (H_{II}) phase consisting of DNA coated with a lipid monolayer in a hexagonal lattice[174]. It has been argued that the H_{II} phase complexes have a much higher transfection activity then the L_α phase ones. One explanation could be that this phase promotes the lipoplex fusion with cellular membranes facilitating the cellular uptake[51]. However, the high affinity of cationic lipids to DNA reduces the successful transfection of eukaryotes cells once the DNA/lipid complex is internalized in the cytoplasm[175].

Polyplexes, are made of cationic polymers than bind DNA through electrostatic interactions between the phosphate groups present in the DNA and the cationic groups present in the polymer reagent[97]. Polyplexes can adopt diverse nano-structures: blends, toroids or rods, ranging from 50-100 nm in size. Regardless of the complex topology; it is size, charge and ability to escape the lysosome and enter the nucleus that appears to be the salient factors affecting transfection efficiency[96].

Peptiplexes, are peptide-DNA complexes that had emerged over the last decade as potential gene carriers systems[176]. A pure peptide-based transfection agent has several advantages over these systems. Peptides can be more stable with regards to oxidation, are easier to synthesize on a large scale than lipids and polymers, and are relatively easy to modify with cell specific recognition ligands. However, the mechanism of how they bind to and condense DNA is poorly documented in comparison to lipoplexes and polyplexes. Mann et al.[150] recently studied different patterns of DNA condensation in the presence of lysine and arginine based homo-peptides and observed a correlation between different shapes of the peptiplexes and gene delivery efficiency[177].

Recently, we reported results on a set of peptides that self-assemble to form stable nanocapsules[144] with lipid-like properties[145] that are able to encapsulate, retain and deliver (*in vitro*) a variety of solutes into cells, including the alpha-emitting ^{225}Actinium and its radioactive daughter radionuclides[146]. The Branched Amphiphilic Peptides Capsules, termed

BAPCs are potential drug/gene-delivery systems that can be tuned with added ligands to achieve targeted delivery. The capsules can adopt a range of sizes from 20 nm to several microns in diameter depending on assembly conditions and are capable of encapsulating various solutes within the hollow cavity defined by a pure peptide bilayer. Besides being extremely stable, water-soluble and simple to prepare, these peptide capsules are readily taken up by cells *in vitro*.

These amphiphilic peptide sequences were designed to mimic diacyl glycerol phospholipids in architecture and hence have a hydrophilic oligo lysine segment and two identical hydrophobic tails. The peptide capsules are prepared by mixing equimolar concentrations of two related peptides: bis(FLIVIGSII)-K-KKKK and bis(FLIVI)-K-KKKK (Fig.2.1). The hydrophobic core sequence is an internal fragment of the human dihydropyridine sensitive L-type calcium channel segment, CaIVS3. We refer to these peptides as bis(h_9)-K-K_4 and bis(h_5)-K-K_4 respectively, where h9 and h5 refer to the number of hydrophobic residues within the hydrophobic segment. The mixed peptides are referred to as bis(h_9:h_5)-K-K_4 and as BAPCs only when assembled into capsules or *bis(h_9:h_5)-K-K_4-peptiplexes* when bound to DNA.

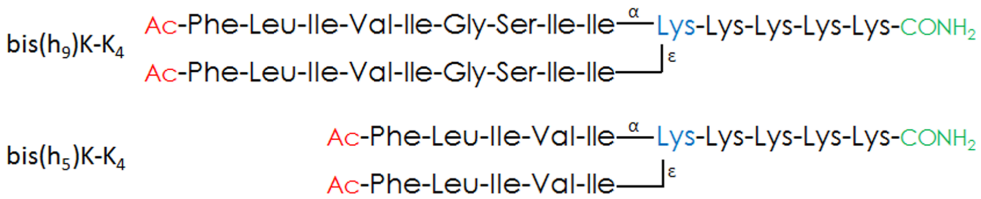

Figure 2.1: *The peptiplexes are comprised of an equimolar mixture of the N-terminal acetylated bis(h_9)-K-K_4 and bis(h_5)-K-K_4. The molecular weight (MW) of the peptides is 1912.29 and 1655.12, respectively.*

Initially we hypothesized that DNA would be encapsulated during the assembly process. However, we quickly realized that assembly was disfavored in the presence of the poly-anionic plasmid. We determined that when the peptides are added in great excess they appear to coat the poly-anionic surface of ds-DNA producing nano-fibers. However, at low peptide

concentrations we observed compaction of the DNA into nano-spheres type structures.

In this report, we investigated the interactions of these branched amphiphilic peptides with pDNA and the ability of the resulting peptiplexes to transfect HeLa cells. Different transfection efficiencies were obtained in each case, with the compacted peptiplexes showing the highest transfection rates.

2.2 Materials and Methods

2.2.1 Peptide synthesis

Peptides were synthesized as previously described[145]. The cleaved peptides were then washed three times with diethyl ether, dissolved in water, and then lyophilized before storing them at RT. The peptides were purified by reversed phase HPLC and characterized using matrix-assisted laser desorption/ionization-time of flight (MALDI TOF/TOF). For the mercury containing peptides, an additional cysteine was incorporated at the C-terminus of both the bis(FLIVIGSII)-K- K_4 and bis(FLIVI)-K-K_4 peptides. Following cleavage and deprotection, the cysteine thiol of the both peptides was reacted with 1 equivalent of methylmercury iodide as previously described[145,146].

For peptides covalently labeled with a fluorescent dye; the first amino acid coupled was N^{α}-t-Fmoc- N^{ε}-t-boc-Llysine on to a 4-Methylbenzhydrylamine (MBHA) resin (Anaspec Inc., Fremont, CA). After de-protection of the side chain amino group of the lysine using 80% TFA in dichloromethane chloride (DCM); the N-Hydroxysuccinimide ester of the 5/6-carboxy-tetramethyl rhodamine was used to couple the dye to the ε-amino site of a lysine residue in the presence of N,N-Diisopropylethylamine (DIEA). The rest of the synthesis was carried out as previously detailed[145,178].

2.2.2 Preparation of bis(h_9:h_5)-K-K_4 peptiplexes

The peptides, bis(h_9)-K-K_4 and bis(h_5)-K-K_4, were individually dissolved in neat 2,2,2,-Trifluoroethanol (TFE). Under these conditions the peptides adopt a helical conformation, thereby forcing the peptides into a monomeric state and ensuring complete mixing. Peptide concentrations were calculated using the molar absorptivity (ε) of phenylalanine in water at 257.5 nm (195 cm^{-1} M^{-1}). The bis(h_9)-K-K_4 and bis(h_5)-K-K_4 peptides were then mixed together in an equimolar ratio at 1.25, 2.5, 5, 10, 20, 40 and 50 μM final concentration, vortexed briefly and allowed to stand for a 10 minutes before removing the solvent under vacuum. The plasmid containing solution (2.5μg/mL) was added drop-wise into the dried peptide mixture in autoclaved 1.5 mL Eppendorf tubes and allowed to sit for 10 min at room temperature before adding $CaCl_2$ at 1.0 mM final concentration. After a 20 min incubation, the solution was added to the cell culture.

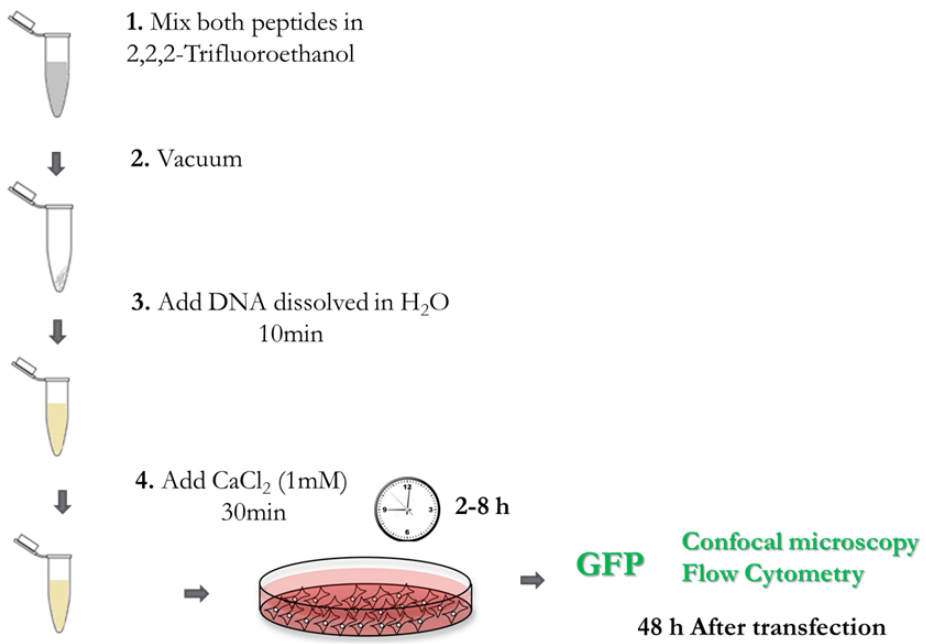

Figure 2.2: *A schema of the optimized method to prepare peptiplexes (described in detail within section 2.2.2*

2.2.3 Confocal Laser Scanning microscopy

Images in Figures 2A, 6, 7 and 8 were taken using a confocal LSM 700 laser-scanning microscope (Carl Zeiss, Gottingen, Germany). The cell boundary and structure was visualized using "Differential interference contrast microscopy (DIC)".

2.2.4 STEM sample preparation

For scanning transmission electron microscopy (STEM) analysis the bis(h_9:h_5)-K-K_4 peptiplexes were prepared as previously described in section (2.2.2) with one exception. The peptides samples were prepared by co-dissolving 0.7 mole equivalents of bis(h_9)-K-K_4 and bis(h_5)-K-K_4 along with 0.3 mole equivalents of their respective h_9 and h_5 cysteine containing Me-Hg labeled variants in water to a final concentration containing 0.1 mM each bis(h_5)-K-K_4 and bis(h_5)-K-K_4. The samples were negatively stained for 10 minutes using a multi isotope 2% Uranyl acetate (Uranium bis(acetato)-O-dioxodihydrate) (Sigma-Aldrich, St. Louis, MO) aqueous solution. Sample solutions (6 μL) were spotted on to grids and allowed to stand for 5 min, after which, excess solution was wicked off the grid with a tissue and allowed to air dry before loading it into the FEI Tecnai F20XT Field Emission Transmission Electron Microscope (FEI North America, Hillsboro, Oregon) with a 0.18 nm STEM HAADF resolution and a 150X-2306X-106X range of magnification. Scanning transmission electron microscopy was carried out in the annular dark field mode with a single tilt of 17°.

2.2.5 Atomic force microscopy (AFM)

The plasmid DNA sample was prepared as described by Li *et al.*[179].For the peptide/DNA sample, 15 μL of Opti-MEM® I Reduced Serum Media containing the bis(h_9:h_5)-K-K_4 peptiplexes at a ratio equal to 10.4 were deposited onto freshly cleaved mica substrates and incubated for 15 minutes at room temperature. AFM topography images of immobilized DNA and peptides were acquired in liquid media using the contact mode on an Innova

(AFM) from Bruker, USA. The AFM scanner was calibrated using a TGZ1 silicon grating from NT-MDT, USA. We used MLCT-E cantilevers with their respective nominal spring constants of 0.1 N/m, and using set point contact forces of 1 nN or less. The AFM topography data were flattened by subtracting the background and then plotting them using a second order equation incorporated in the Gwyddion analysis software[180].

2.2.6 Determination of zeta potential

The bis(h_9:h_5)-K-K_4 peptiplexes were prepared as previously described at different charge ratios and then dissolved in a final volume of 1 mL Opti-MEM® I Reduced Serum Media (Life Technologies, Grand Island, NY). Zeta-potential for all dispersions were determined using a Zeta-Potential Analyzer (Brookhaven Instruments Corporation, Holtsville, NY) equipped with a 677 nm laser. Zeta-potentials (ζ) were determined from the electrophoretic mobility and Smoluchowski equation, $\zeta = \mu\eta/\varepsilon$, where η and ε are the viscosity and the dielectric constant of the medium, respectively. All measurements were performed in triplicates.

2.2.7 Gel Electrophoresis

The bis(h_9:h_5)-K-K_4 peptiplexes were prepared as previously described at different charge ratios and then dissolved in a final volume of 1 mL Opti-MEM® I Reduced Serum Media. 15 μL of these solutions were loaded on a 0.8% agarose gel containing 0.012% Ethidium bromide, and run at 60 V for 40 min. A 1 kb ladder was used as reference (Fisher Scientific, Pittsburgh PA, USA). After electrophoresis, the resulting DNA migration bands were visualized using a MultiDoc-it, Digital Imaging System (Ultra-Violet Products, Upland, CA, USA).

2.2.8 Plasmid digestion with DNase-1

The bis(h_9:h_5)-K-K_4 peptiplexes were prepared as reported above. The nuclease, RQ-1 RNase-free DNase-1 (Promega Corp., Madison, WI) treated samples were prepared according to the protocol supplied by the manufacturer. Briefly, 30 μL samples of the bis(h_9:h_5)-K-K_4 peptiplexes dissolved in Opti-MEM® I Reduced Serum Media were digested using 1 μL of the nuclease, followed by 4 μL of a 10x reaction buffer (provided by manufacturer). This sample was incubated for 30 min at 37 °C. At the end of the reaction, 4 μL of the stop solution (provided by manufacturer) was added and the sample incubated for an additional 10 min at 65°C to inactivate the DNase. All samples were run in a 0.8% agarose gel containing 0.012% Ethidium bromide, run at 60 V for 40 min. A 1 kb ladder was used as reference (Fisher Scientific, Pittsburgh PA, USA). After electrophoresis, the resulting DNA migration bands were visualized using a MultiDoc-it, Digital Imaging System (Ultra-Violet Products, Upland, CA, USA).

2.2.9 Cell Culture

HeLa cells were purchased from ATCC (CCL-2). HeLa cells were grown in Dulbeccos Modified Eagle Medium DMEM (Life Technologies, Grand Island, NY) supplemented with 10% (v/v) fetal bovine serum (Life Technologies, Grand Island, NY) and cells were kept in a humidified 5% CO_2 humidified atmosphere at 37 °C. All cell lines were passaged by tripsinization with TrypLE^{TM} Express (Life Technologies, Grand Island, NY) every 3rd-4th day. No antibiotics were added.

2.2.10 Temperature Dependence on Cellular uptake and Lysosomal co-localization of bis(h_9:h_5)-K-K_4 peptiplexes

HeLa cells were seeded on 22 mm culture dishes at a density of 1x10^5 cells per mL and grown to roughly 60% confluence. Fresh media at 4 °C was added and subsequently, 100 μL

of media was replaced by a temperature controlled solution containing the bis(h_9:h_5)-K-K_4 peptiplexes prepared with 30% Rhodamine B label on the bis(h_5)-K-K_4 peptide. Subsequently, cells were incubated for 2 h at 4 °C, then washed twice with PBS at 4 °C and analyzed using confocal microscopy. The same cell samples were then incubated for an additional 2 h at 37 °C, washed twice with PBS at 37 °C and then reanalyzed by confocal microscopy. For the lysosomal immunostaining post incubation with the bis(h_9:h_5)-K-K_4 peptiplexes cells were fixed in 4% paraformaldehyde (PFA) at RT for 2 h followed by washes with phosphate-buffered saline containing 1% Triton X-100 (PBS-T, Thermo Fisher Scientific Inc.). Subsequently, the cells were incubated with mouse anti-lamp 1 antibody (G1/139/5) for 1 h. The (G1/139/5) hybridoma, developed by Hauri HP.[181] was obtained from Developmental Studies Hybridoma Bank at the University of Iowa. After the incubation, cells were washed three times with PBS-T. Subsequently, were incubated for 3 h with Alexa 488® labeled goat anti-mouse IgG (Molecular Probes, Carlsbad, CA). Stained tissues were washed again with PBST and mounted in glycerol containing the nuclear stain 4′,6′-diamino-2-phenylindole (DAPI; 2 μg mL-1; Sigma).

2.2.11 pEGFP-N3 plasmid transfection

Transfection experiments were carried out by mixing a 4.7 kb pDNA, which encodes for the enhanced green fluorescent protein (EGFP), with bis(h_9:h_5)-K-K_4-peptide equimolar mixture. The plasmid pEGFP-N3 was obtained from Dr. Dolores Takemoto lab (purchased from Clontech, Mountain View, CA). HeLa cells were seeded on 22 mm culture dishes at a density of 1x10^5 cells per mL, 24 h later at 60% confluence, all medium was removed from the wells and 800 μL of Opti-MEM® I Reduced Serum Media was added. Next, 200 μL of the different bis(h_9:h_5)-K-K_4 peptiplexes were added to cells and allowed to incubated in normoxic conditions for 2-6 h. After this incubation, media and transfection reagent was removed and replaced with 1 mL of fresh DMEM containing 10 % FBS in each well. The cells were returned to the incubator for 48 h. For the positive control cells

were transfected with Lipofectin® (Invitrogen, Carlsbad, CA), according to the protocol supplied by the manufacturer. Some parameters were adjusted to reach optimum results in HeLa cells. Briefly, lipoplexes where formed in 200 μL Opti-MEM® I Reduced Serum Media mixing 4 μL of pDNA (2 μg), 8 μL of the transfection reagent and 188 μL of media. Higher volumes of the reagent led to cell death and lower volumes reduced transfection efficiency. The lipoplexes were added to the cells and allowed to incubate for 6 h at 37 °C. Transfection efficiency and mean fluorescence intensity were then measured by fluorescence-activated cell sorting (FACS). Briefly, cell culture medium was removed and cells were washed once with PBS. Cells were detached by the addition of TrypLE^{TM} Express. The resuspended cells were transferred to 1.5 mL tube and centrifuged for removal of trypsin. Cells were then resuspended in 250 μL of PBS containing 2% (v/v) FBS and 0.1% (v/v) propidium iodide (Life Technologies). Analyses were performed on a FACS Calibur, (Becton Dickinson, Franklin Lakes, NJ, USA). The EGFP-positive/PI-negative cells were counted as positively transfected cells. The data were analyzed using ANOVA with Bonferroni post-test. Also, transfection efficiency was monitored by direct counting using confocal microscopy. Experiments were performed in triplicates.

2.2.12 Cell viability assay

Cell toxicity assays were carried out based on cell death using exclusion of the fluorescent dye trypan blue. Cells were seeded on 22 mm culture dishes at a density of 1x10^5 cells per mL and grown to roughly 60% confluence. Subsequently, 200 μL of the media was replaced with a media free solution containing bis(h_9:h_5)-K-K_4 peptiplexes. After 6 h incubation with the bis(h_9:h_5)-K-K_4 peptiplexes all media was removed and replaced with 1 mL of fresh media per well. After 48 h, all media was removed and cells were washed three times with PBS. Next, cells were treated for 5 min with 100 L TrypLE^{TM} Express to release the cells from the surface of the wells. The cells were centrifuged and the supernatant was discarded and the pellet resuspended in 500 μL of PBS. To check for cell viability, 10 μL of

the resuspended cells were mixed with 10 μL of 2x trypan blue solutions and allowed to sit for 2 min before counting them in a Cellometer® AutoT4 automated cell counter (Nexcelom Bioscience LLC, Lawrence, MA). The data were analyzed using ANOVA with Bonferroni post-test. All experiments were performed in triplicates.

2.3 Results and Discussion

2.3.1 Gene delivery and viability assays of bis(h_9:h_5)-K-K_4 peptiplexes

Here, we investigated the ability of bis(h_9:h_5)-K-K_4 peptides to deliver plasmid DNA into eukaryotic cells. We hypothesized that pDNA could be trapped inside the capsules formed by the peptides even in the presence of a strong electrostatic interaction between the peptide's oligo lysyl amines and the anionic DNA backbone phosphates. Modeling studies provided an estimate of 1600-2000 peptides required for the assembly of our 20 nm diameter capsules[144,145,146].

According to this estimation, transfection experiments were carried out expecting encapsulation to occur by providing enough peptides to form one capsule/pDNA strand. The charge ratio (N:P) between the number of NH_3^+'s (N) contained in the oligolysine tails of the ~2000 peptides per 20 nm capsule and the number of PO^{4-}'s (P) in the 4.7 kb ds pDNA was calculated to be 65.5. These parameters were used throughout the experiment however, only ~2% of transfection efficiency was observed. This value was deemed quite low and no more experiments were conducted using these concentrations. Subsequently, we examined the effect of reduced peptide concentrations with a fixed pDNA concentration (N:P ratios). Surprisingly at lower N:P ratios the transfection rate in HeLa cells increased nearly 10 fold (Fig.2.3).

In this experiment HeLa cells were incubated 4 hours with the peptide/DNA complexes

at different ratios in reduced serum media. Calcium chloride ($CaCl_2$) was added at 1 mM final concentration to improve transfection efficiency. It has been reported that adding $CaCl_2$ to Cell Penetrating Peptides (CPP)/DNA complexes can reduce particle size and maximize gene delivery *in vitro*[182]. However, ($CaCl_2$) by itself is capable of transfecting mammalian cells *in vitro* at certain conditions[183].To account for this possibility, we studied the effect of different concentrations (250 μM to 20 mM) of $CaCl_2$ mixed with DNA in HeLa cells. No GFP expression was observed with $CaCl_2$ final concentrations 1 mM for 6-8 hr incubations.

Gene delivery efficiency was monitored qualitatively by confocal microscopy and quantified using fluorescence-activated cell sorting (FACS). Propidium Iodide (PI) was used to identify and then exclude dead cells from the analysis. The GFP-positive/PI-negative cells were counted as positively transfected cells. As a positive control, cells were transfected with the commercial transfection reagent Lipofectin® using conditions optimized for this cell line. Transfection efficiency was reported as the percentage od cells that have been transfected, despite of the difference in the level of protein production among each cell.

FACS analysis showed that the N:P ratios of 2.6 and 10.4 yielded the highest gene expression with minimal toxicity. Subsequently, for these two ratios, different transfection conditions were tested to maximize gene delivery and expression.

We investigated how incubation time affects the transfection rates (Fig. 2.3 B). It was observed that a 6 h incubation with the peptide/DNA mixture led to the best transfection rate, particularly for the ratio N:P =10.4. Different buffers were also tested for the 2.6 and 10.4 ratios, being Opti-MEM® I Reduced Serum Media where the peptide/DNA complexes appeared to be more efficient (Fig. 2.3 C). Fig. 2.3 D shows the effect of 1 mM calcium with the optimized transfection incubation time and buffer, where according to the Bonferroni post-test there is no significant difference between the values from the groups 10.4 w/$CaCl_2$ and Lipofectin®.

It is important to note that optimal GFP expression was observed only when the plasmid

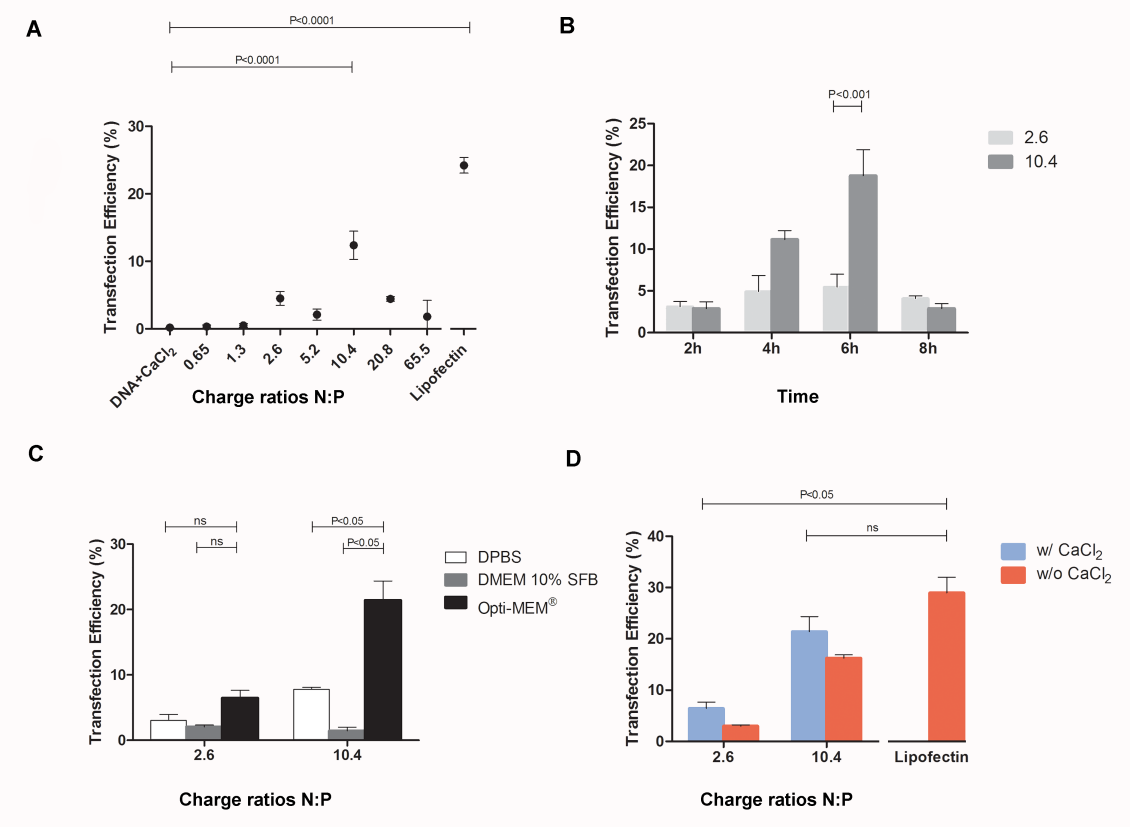

Figure 2.3: *Comparison of transfection efficiency of bis(h_9:h_5)-K-K_4 peptiplexes in HeLa cells. (A) Different peptide to DNA charge ratios (N:P) after 4 h of incubation time with the complexes in reduced serum media and 1 mM $CaCl_2$ (B) Different incubation times for the charge ratios 2.6 and 10.4 in reduced serum media and 1 mM $CaCl_2$ (C) Different media compositions used for transfection after 6 h of incubation with the complexes in reduced serum media and 1 mM $CaCl_2$. (D) Effect of $CaCl_2$ after 6 h of incubation time with in reduced serum media and 1 mM $CaCl_2$. Data are presented as means SEM (standard error of the mean). Differences between values were compared by ANOVA using Bonferroni as post test. Non-statistical significance (ns) was considered when P>0.05. DPBS: Dulbecco's Phosphate-Buffered Saline, calcium and magnesium free*

was delivered in the presence of the both branched peptides. The plasmid by itself, when added directly to the media with or without 1 mM calcium showed no GFP expression. Transfection with just one of the peptides, either bis(h_9)-K-K_4, bis(h_5)-K-K_4 or the linear sequences FLIVIGSII-K_4 and FLIVI-K_4 showed minimal GFP expression in comparison with the bis(h_9:h_5)-K-K_4 peptiplexe with the N:P ratio of 10.4 (Appendix A Fig.A.1). These results preclude the possibility that the transfection properties of the complex are only due

to the cationic oligo-lysine segment. Nevertheless, the control sequences mentioned above are capable of condensing pDNA and facilitating translocation across the cell membrane (Appendix A Fig. A.2A and A.2B). A possible explanation of why the mixture of the two branched peptides works better than the linear sequence or just one of them, could be that both peptides are required to promote the endosomal release of the peptide/DNA complex. It has been suggested for cationic lipids that incorporation of aliphatic chains with different numbers and length can improve transfection efficiency by promoting endosomal escape[184,33]. These control sequences were tested under the same transfection conditions that yielded the highest transfection rates.

When one considers the average (n = 3) total number of viable cells per mL (Fig. 2.4A) after transfecting with bis(h_9:h_5)-K-K_4 peptiplexes at N:P 10.4 and Lipofectin®, the GFP yield for the peptiplex is 1.7-fold higher than with the commercial reagent. Our results show that cell viability is minimally affected by the bis(h_9:h_5)-K-K_4 peptiplexe at the most effective N:P ratio.

Confocal analysis of living cells (Fig. 2.4B and 2.4C) revealed that the cell morphology appeared normal after transfection with the peptide/DNA complexes, whereas Lipofectin® treated cells appeared to have altered morphologies. FACS analysis clearly indicates the higher efficiency and minimal toxicity of the peptiplexes as compared to the commercial reagent at its optimized efficiency (Fig 2.4D and 2.4E, respectively). Cationic lipids containing quaternary nitrogen functional groups can bind and inhibit enzymes such as PKC, which could explain their toxicity[60]. In addition, cationic lipids can trigger immune responses and perturb the cell membrane[185]. Very little has been reported in regard to the toxicity of peptide carriers causing cell death[185]. According to results reported by others[79,141,32] our system appears to be one of the least toxic transfection systems for cells when compared to several other lipid- and polymer-based transfection methods, suggesting that it might be safely used for *in vivo* applications.

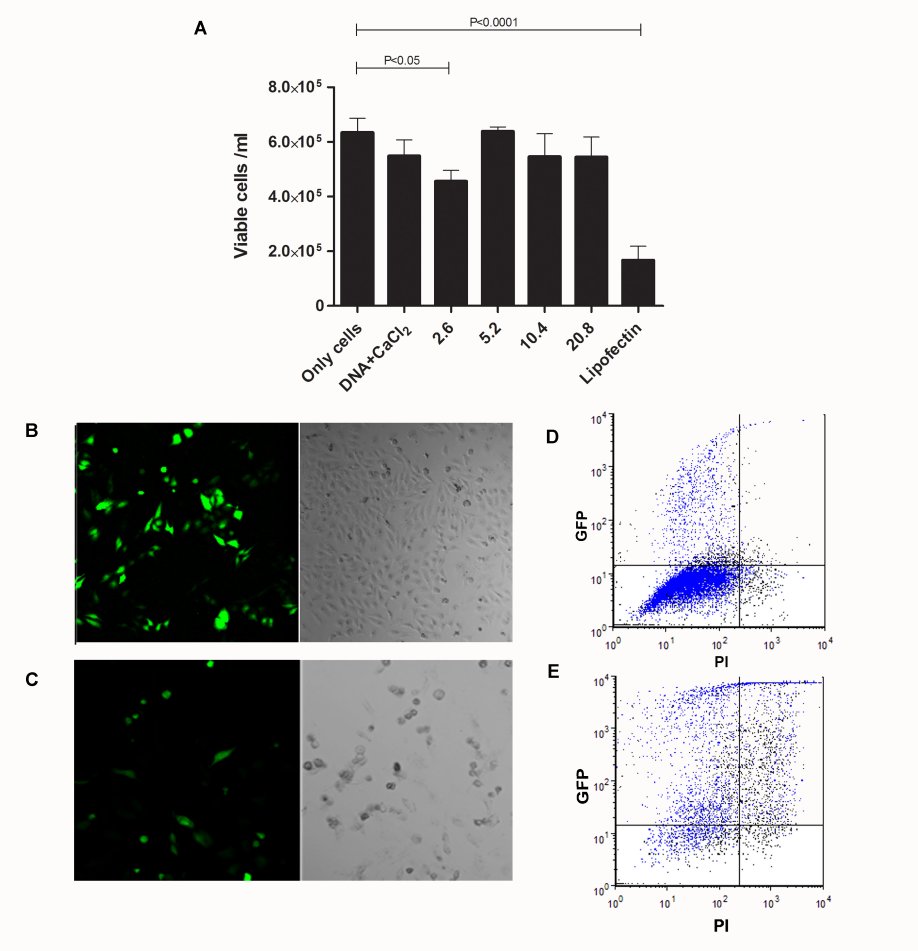

Figure 2.4: *(A) Cell viability as determined by trypan blue analysis. (B) Confocal microscopy images of HeLa cells after transfection with pDNA encoding GFP using the peptiplex at N:P = 10.4 after 6 h of incubation in reduced serum media and (C) Lipofectin®. FACS analysis of cells transfected with the peptiplex at N:P = 10.4 (D) Lipofectin® (E) using the same conditions used for the confocal studies. Data are presented as means SEM The overall P value was determined using 1-way ANOVA using Bonferroni as post test, (ns) was considered when P>0.05*

2.3.2 Biophysical characterization of bis(h_9:h_5)-K-K_4 peptiplexes

Transmission electron microscopy (TEM) of the bis(h_9:h_5)-K-K_4 peptiplexes at charge ratio of 10.4 revealed compact nanostructures (Fig. 2.5A) compared to plasmid alone (Fig. 2.5B), whereas the analysis of the ratio where we expected to see encapsulation of the DNA along the BAPCs (N:P 65.5), generated long strands of DNA. At this high peptide to DNA charge

ratio the branched peptides appeared to coat the negatively charged backbone phosphate groups of the dsDNA forming nano-fibers (Fig. 2.5C).

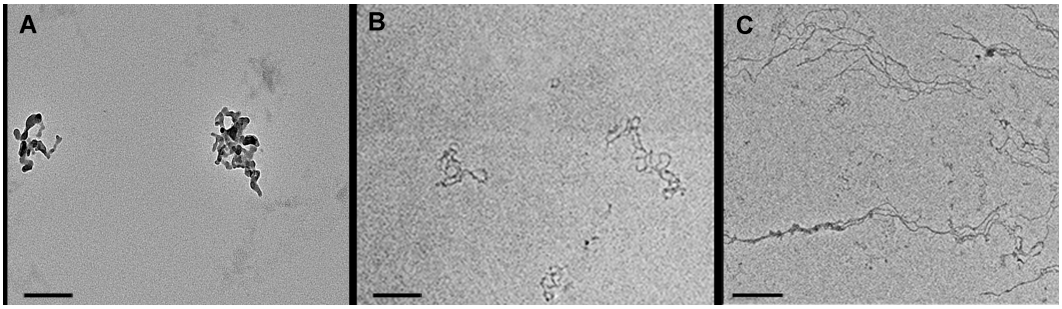

Figure 2.5: *TEM images of the peptiplexes at different peptide to DNA ratios. (A) Nano-omplexes formed at lower charge ratio N:P = 10.4. (B) Plasmid DNA in the absence of peptide and is shown to compare the different supramolecular structures. (C) Nano-fibers structures at charge ratio N:P = 65.5. Scale bar = 200 nm*

Mann et al.[150] reported different patterns of DNA condensation with polylysine and polyarginine peptides. Their results showed rod and sphere shaped complexes depending on the charge ratio. However, their results showed an opposite effect when compared to our results. At higher charge ratios they obtained mostly spheres whereas fibers were obtained at lower concentrations. These results suggest that our system relies on more than just electrostatic interactions.

We envision two possible mechanisms that could explain this result. At low N:P ratios the lysyl groups of monomeric branched peptides associate with the phosphates in the DNA backbone. Adjacent peptides can then associate through the hydrophobic interactions of the beta-structure hydrophobic segments thereby constraining the DNA segments in a compacted conformation. It is also conceivable that small micelle-like patches of peptides form through the association of multiple hydrophobic segments to shield themselves from water. This structure leaves the lysines solvent exposed where they are able to interact electrostatically with different portions of the DNA strands and through bridging, stabilize the compacted DNA structure. In the case of the high N:P ratio where we see nano-fibers, the peptides are in large excess over the phosphates and capable of forming bilayers along

the DNA surface. In the case the DNA becomes a template for the self-assembly of the peptides and becomes encased (see Fig. 2.6). This model suggests that by adjusting the N:P ratios different structures can be generated for the complexes. Both models protect DNA from nuclease cleavage (Appendix A Fig. A.3). The nuclease used in this assay; DNase-1 cleaves single stranded, double stranded and chromatin DNA and preferentially cleaves at the 5' phosphodiester linkages adjacent to pyrimidine nucleotides[186].

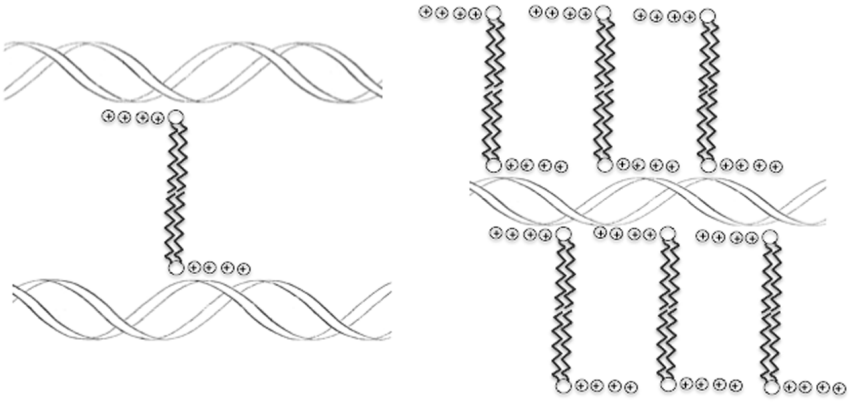

Figure 2.6: *The left panel shows a scenario in which the branched peptide sequences bridge the DNA at low N:P ratios allowing them to be pulled together. The right panel shows a hypothetical structure where the DNA is encased within a peptide bilayer. Lysines are represented by positive charges in the circles*

AFM was used to assess the dimensions of the bis(h_9:h_5)-K-K_4 peptiplexes using the N:P ratio of 10.4:1. Relatively uniform dimensions were observed for the complexes. The nanostructures displayed heights 70-85 nm and the lateral sizes of around 200-250 nm (Fig. 2.7A and 2.7B). Plasmid DNA vertical height was only about 1 nm (Fig. 2.7C). The significant change in compaction of the plasmid DNA demonstrates the peptides ability to interact with and condense DNA.

The zeta potential (ZP) of the nanostructures was also determined at several peptide to DNA charge ratios previously tested for transfection efficiency (Fig. 2.8B). The ZP can be defined as the charge that develops at the interface between a solid surface and its liquid medium. A positive ZP can enhance the interaction with cell membranes however, values

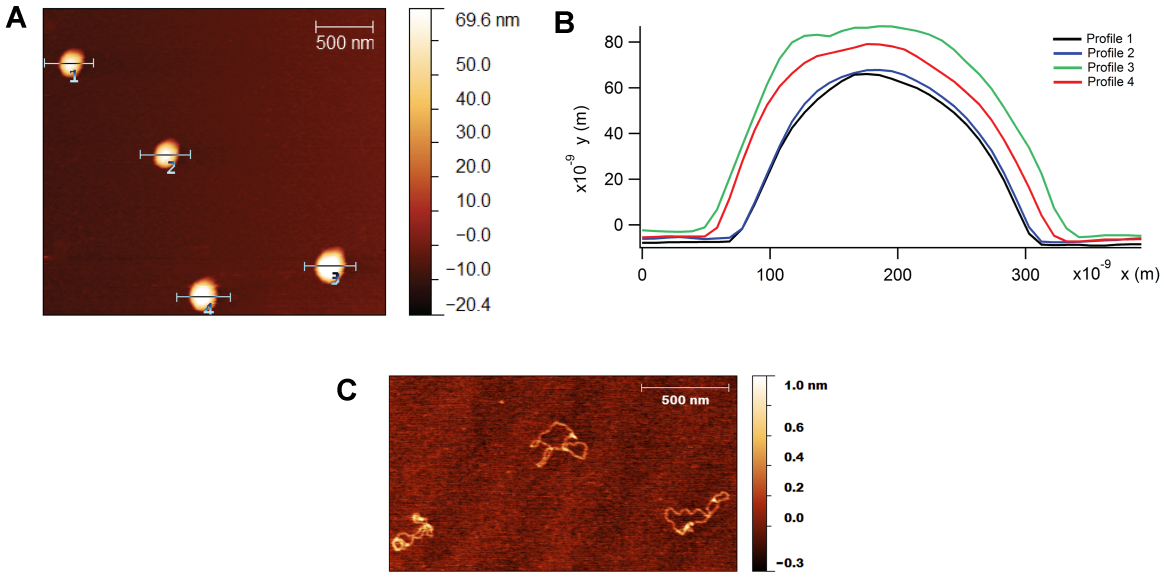

Figure 2.7: *AFM images of the peptiplexes. (A) 3 x 2.4 µm image of the nano-structure form at N:P of 10.4:1. (B) Cross section analyses of the peptiplex shown in panel A. (C) Plasmid DNA alone*

above 45 mV can be toxic for cells. Particles with negative ZP might not interact efficiently with the negatively charge cell surface. The surface charge for the nanostructure at N:P=10.4 that led to the highest transfection rate is 5mV, a value suitable to facilitate interactions with negatively cell membrane surfaces but not too high to cause cell damage[187,21].

To further confirm the changes in charge and size of the complexes, we analyzed their electrophoretic mobility in a 0.8% agarose gel (Fig. 2.8A). The first lane shows a 1 kb dsDNA ladder, lane 2 and 3 contains free pEGFP-N3 plasmid DNA in water and Opti-MEM® I Reduced Serum Media respectively. Lane 4, represents DNA combined with $CaCl_2$ at 1 mM final concentration. For 2.6 and 10.4 charge ratios (lanes 5 and 6) a gel shift for the complex is observed. This shift suggests the formation of a new structure through the association of peptides with the dsDNA; although only for the N:P = 10.4 is a total DNA retardation observed. As the peptide/DNA ratio increases, N:P=20.8 (Lane 7) the DNA is fully coated by a peptide bilayer and ethidium bromide cannot penetrate the complex therefore DNA is

not visible.

Both methods (electrophoretic mobility and ZP) are analytical measurements that confirm the formation of peptide-DNA complexes. In the case of the ZP, the DNA displayed a negative potential (∼-20 mV) whereas as mentioned above for the peptiplexes at N:P = 2.6 and N:P = 10.4 the ZP is -5 mv and 5mV respectively. This represent a significant difference in the charge surface between the peptiplexes and DNA. In the agarose gel, different electrophoretic mobility was observed for only DNA and DNA mixed with different peptide concentrations.

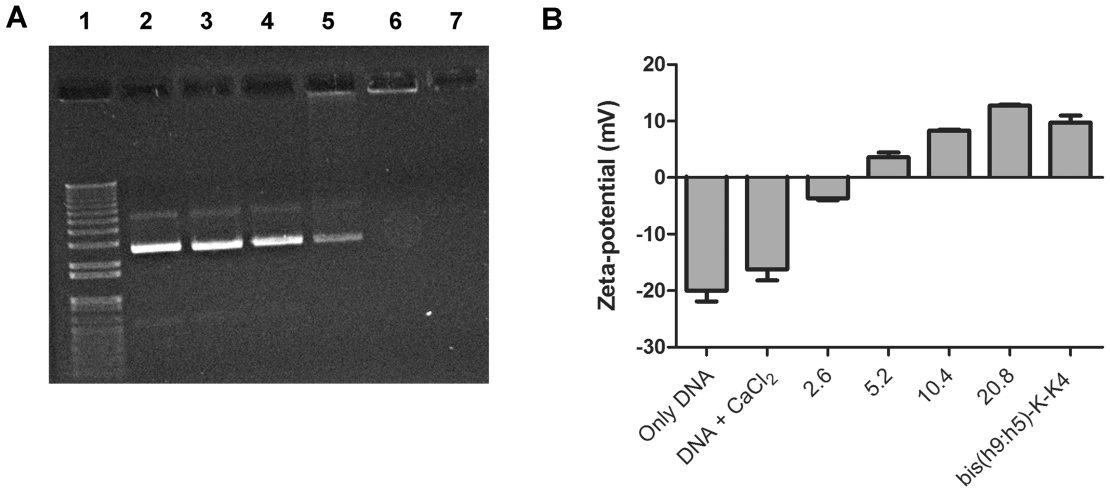

Figure 2.8: *A) Zeta potential of bis(h_9:h_5)-K-K_4 peptiplexes at different peptide to DNA ratios. (B) Agarose gel electrophoresis of peptide complexes at different ratios, each lane contains 80 ng of pEGFP-N3. Lane 1 corresponds to 1kb dsDNA Ladder, lane 2 and 3 contains only pEGFP-N3 plasmid in water and Opti-MEM® I Reduced Serum Media respectively. Lane 4 contains DNA + $CaCl_2$ and lanes 5-7 are bis(h_9:h_5)-K-K_4 peptiplexes at 2.6,10.4 and 20.8 respectively.*

2.3.3 Uptake and cellular co-localization of bis(h_9:h_5)-K-K_4 peptiplexes

Cellular uptake of the peptide/DNA complex that displayed the best transfection rate was monitored using confocal microscopy. For this analysis, the peptide was labeled with Rhodamine B to permit visualization. To determine whether uptake of bis(h_9:h_5)-K-K_4 peptiplexes follows an endocytotic or non-endocytotic route, we employed the most direct and commonly used method: low temperature (4 °C) followed by return to 37 °C[188]. At this temperature, energy depended endocytotic pathways are inhibited while non-endocytotic pathways are not[102]. Non-endocytotic uptake includes (a) membrane fusion and (b) cell penetration, which is seen in certain cationic peptides containing TAT-like sequences that can directly penetrate the cell membrane in an energy independent manner[189]. HeLa cells were incubated for 2 h at 4 °C with the bis(h_9:h_5)-K-K_4 peptiplexes at charge ratio N:P of 10.4 before being washed and imaged. The same cells are then transitioned back to 37 °C and allowed to incubate for an additional 2 h before being re imaged a second time. Confocal images of living cells incubated at 4 °C failed to internalize the labeled peptide/DNA complex (Fig. 2.9A) however they appear to be attached to the surface of the cell. Once the cells were returned to 37 °C, normal uptake of the labeled peptide capsules was observed (Fig. 2.9B). These results indicate that the uptake occurs via a temperature dependent process such as endocytosis. At low temperatures the peptide remains bound to the cell surface even after two washes. Upon raising the incubation temperature, the bound complexes are readily taken up by the cells. Based on nuclear morphology, cells in (Fig. 2.9A) do not seem healthy. Cells that were incubated for 2 h at 4°C showed abnormal nuclear morphology, certainly dropping the temperature might compromise cell survival an it is beyond the scope of this study to determine how this could interfere with the internalization route of the peptiplexes.

To examine the sub-cellular localization of the bis(h_9:h_5)-K-K_4 peptiplexes after 6 h of incubation with HeLa cells, both the lysosomes (green) and peptide/pDNA complex (red)

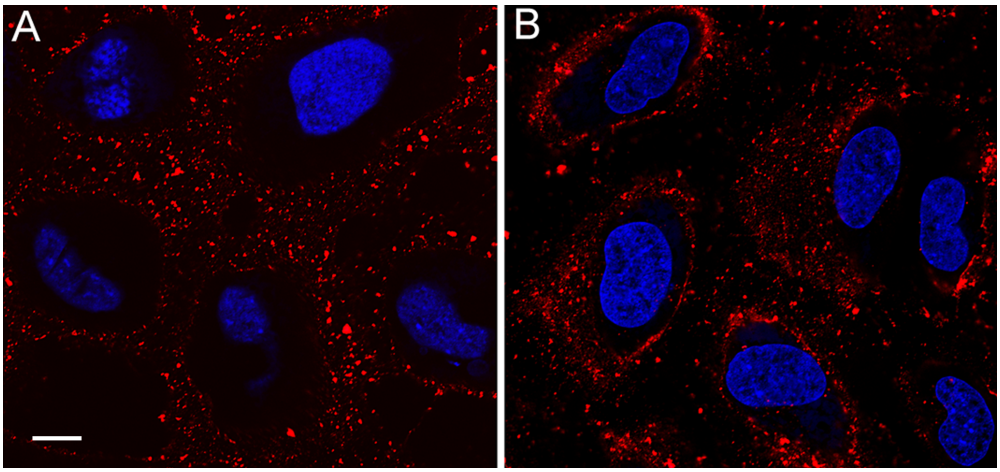

Figure 2.9: *Cellular uptake of bis(h_9:h_5)-K-K_4 peptiplexes at different temperatures. The nuclei was stained with DAPI (blue) and the peptide bis(h_9:h_5)-K-K_4 was partially labeled (30%) with Rhodamine B (red). The experiment was done on living cells. (A) Failed cellular uptake of peptide/DNA complexes at 4 °C. (B) Incubation of cells with peptide/DNA complexes at 37 °C shows internalization of the peptide. Scale bar = 10 μm*

were visualized (Fig. 2.10 panels A-D). Fig. 2.10C shows the merged images of panels A (complexes) and B (lysosomes). Both co-localized and non-co-localized bis(h_9:h_5)-K-K_4 peptiplexes with lysosomes are observed. These results suggest that the complexes enter the cell through the endosomal pathway yet at some point they escape most likely due to endosomal lysis.

The exact endocytic pathway utilized in internalizing the peptide/DNA complex has not been defined. However, regardless the exact route of entry the peptide/DNA complexes remain inside the cells without apparent degradation. In Fig. 2.11 cells were transfected with bis(h_9:h_5)-K-K_4 peptiplexes and after 48 h peptides appear to localize in the peri-nuclear area with EGFP expression in some of the cells.Cellular uptake at 37 °C was observed using branched peptides containing only D-amino acids (Data no shown). The uptake of the D-peptide containing complex, suggests that a specific binding interaction does not occur. We believe that binding of the complex to the cells surface occurs primarily through an electrostatic interaction.

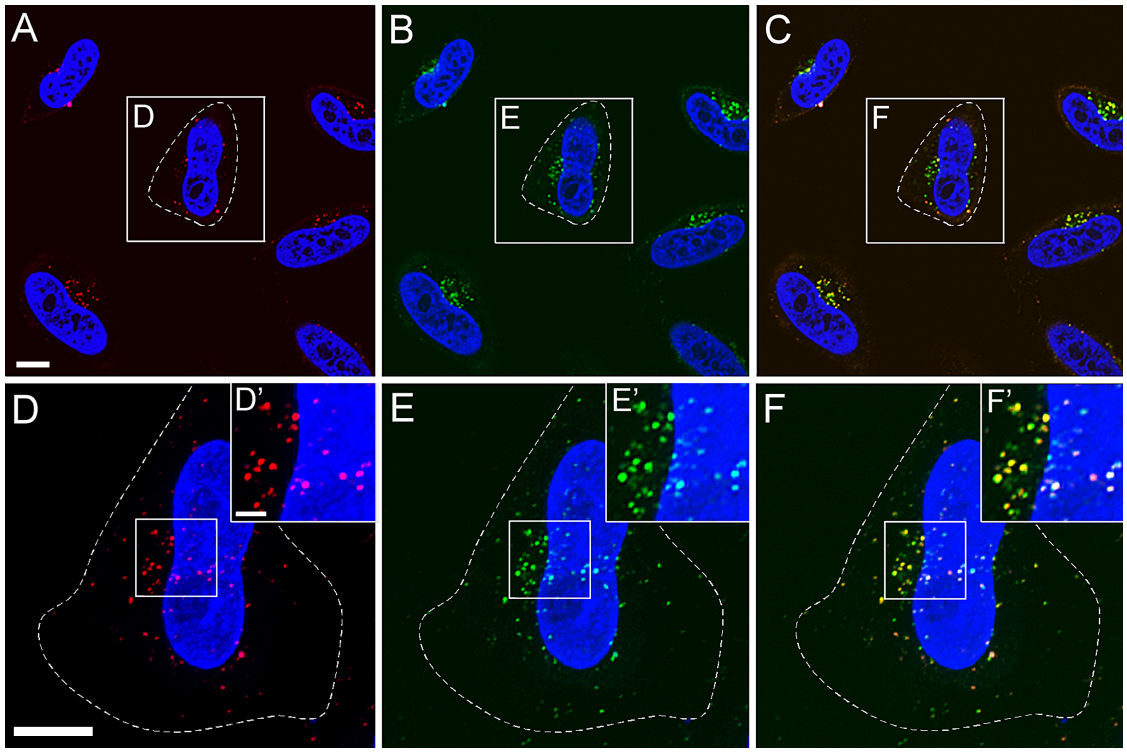

Figure 2.10: *Lysosomal co-localization of bis(h_9:h_5)-K-K_4 peptiplexes incubated at 37 °C with 50 µM 30% Rhodamine B label (A) Red channel for rhodamine (B) Green channel for lysosomal stain (C) Merge image showing co-localization of bis(h_9:h_5)-K-K_4 peptiplexes and the lysosomes (yellow). D,D', EE' and FF' are magnification to analyze in more detail the co-localization of the bis(h_9:h_5)-K-K_4 peptiplexes and the lysosomes . Scale bar upper panel = 20 µm, lower panel = 10 µm*

2.4 Conclusions

Here we report on the formulation of an alternative plasmid DNA/peptide complex that successfully transfers DNA into cultured cells with good efficiency and low cytotoxicity. As previously reported the branched peptides bis(h_9:h_5)-K-K_4-peptides form capsules in water and act as hollow nano-carriers for small solutes[144,145,146]. In the case of large anionic molecules like nucleic acids, capsule formation is not observed. Instead, different structures are generated based on the charge ratios (N:P) between the peptides and the ds-DNA. At very high charge ratios the peptides appear to coat the poly-anionic surface of the ds-DNA forming what appear under TEM long nano fibers. At low charge ratios we observed that

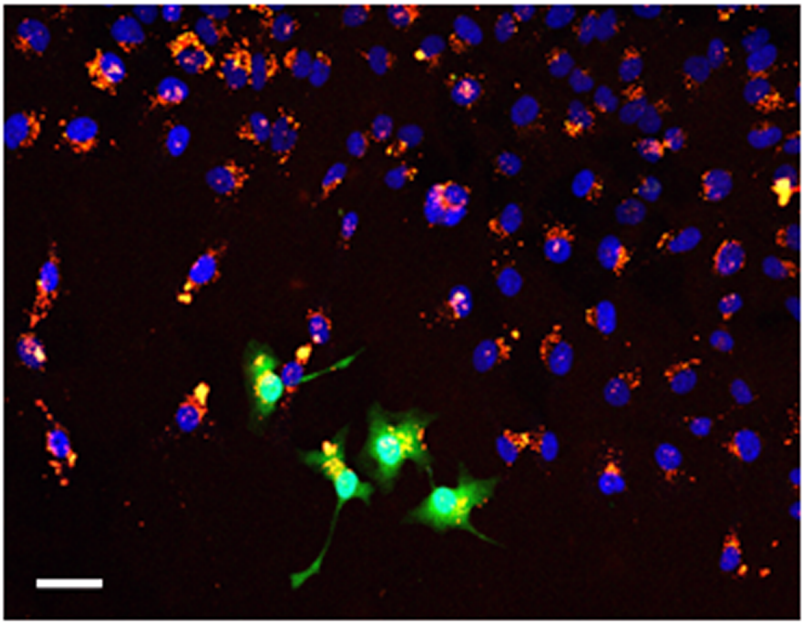

Figure 2.11: *Transient EGFP expression (green) and the peptide bis(h_9:h_5)-K-K_4 partially labeled (30%) with Rhodamine B (red) in HeLa cells visualized by confocal microscope. Yellow spots are the merge of EGFP expression and the peptide. Scale bar=40μM.*

the DNA was condensed in compacted structures within different sizes (200-300 nm). The highest transfection rate was obtained at lower ratios 2.6 and 10.4 in the presence of 1 mM calcium chloride. Transfection efficiencies superior to the commercial transfection agent, Lipofectin® were observed when the total number of living transfected cells is taking into account. The simplicity of the method, low cost ($\sim$1 cent per 1x10^6 cells) and minimal cytotoxicity may make this system suitable for *in vitro* gene delivery where the transformed cells are to be clonally expanded[190]. Another potential application could be the use of this system for *in vivo* delivery of DNA vaccines, where safe and efficient delivery of plasmid DNA to initiate immune response is critical for the success of the therapy[5]. Unlike other lipid reagents, which are non-degradable, the non-toxic nature of these peptide-base nanostructures could potentially facilitate *in vivo* applications.

Chapter 3

Branched Amphiphilic Peptide Capsules (BAPCs) for delivery of plasmid DNA vaccines.

3.1 Introduction

Nucleic acid-based vaccination offers an attractive option to traditional vaccine strategies composed principally of attenuated viruses, inactivated pathogens, inactivated bacterial toxins or recombinant proteins[5]. Compared to traditional vaccines, DNA vaccines can generate long-term humoral and cellular immunity[191]. In addition, DNA vaccines potentially allow for both prophylactic and therapeutic vaccination[5]. Furthermore they are relative inexpensive for manufacture and storage[6]. It has been shown that injections of naked DNA into skeletal muscle in animal models result in the expression of the proteins coded by the added DNA however at low and extremely variable levels, making difficult the design of a robust and reproducible vaccination system[10]. Also, the same success achieved in animal models has not been reported for studies done in humans[192]. Complexion of DNA with a biomaterial can improve pDNA-based vaccination. Biocompatible materials such

lipids, peptides and polymers can enhance DNA stability and cellular uptake[5,193]. Recently, peptides have emerged as potential vaccine gene carriers systems[194]. A pure peptide-based gene delivery agent would have several advantages over these other biomaterials. Peptides display stability in regard oxidation and storage and are easier to synthesize on a large scale than lipids and polymers, and are relatively easy to modify with specific ligands that can help for targeting purposes[129]. As far as we know, peptides are the family that has been less explored as vehicles for DNA vaccine delivery[194]. P. Locher et al.[195] have reported the enhancement of a human immunodeficiency virus env DNA vaccine using a peptide-based formulation . This formulation is made of poly-lysines capable to interact electrostatically with the DNA vaccines. Imidazole moieties were conjugate to the peptide sequence to facilitate endosomal escape and avoid early intracellular degradation of the DNA. They reported higher expression of the antigen in comparison to naked DNA delivered by the intradermal route in BALB/c mice.

Recently, we reported a new class of peptide base nano-capsules termed BAPCs (Branched Amphiphilic Peptide Capsules). BAPCs are formed by the self-assembly of two branched peptide sequences bis(FLIVI)-K-K_4 and bis(FLIVIGSII)-K-K_4 (Fig. 2.1 and 3.1). These sequences are similar in geometry to phospholipids, the branch point lysine in the sequence orients the two peptide segments at $\sim$90° angle, as occur with the phosphate bond present in the diacyl phospholipids. They show other biophysical properties in common with lipids such the ability to fuse, encapsulate solutes and the possibility to be re-sized.

BAPCs display a uniform size of 20 nm when prepared at 25°C for 30 min followed by moving them to 4°C. These BAPCs retain their size when moved to elevated temperatures[145]. They are taken up by cells *in vitro* and showed resistance to nucleases and the cell's degradative machinery. BAPCs are resistant as well to detergents, proteases and chaotropes. Recent studies showed the ability of BAPCs to withstand the α-particle emission and the recoil of daughter radionuclides, *in vivo* studies demonstrated that the ^{225}Ac containing BAPCs remained in circulation for 24 h[146]. The biodistribution of the ^{225}Ac

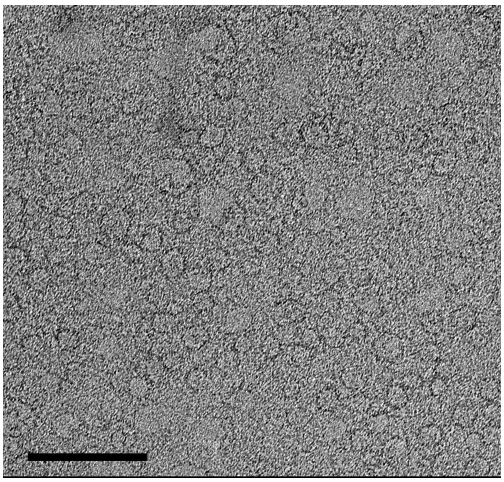

Figure 3.1: *S/TEM image of BAPCs incubated 30 min in water at 25°C. To improve contrast, the peptide sequence bis(FLIVI)-K-K_4 was labeled with Hg and mixed at 3:1 ratio with the no labeled sequence. Scale bar = 100nm*

containing BAPCs was different than that observed with free radionuclide. In this report, we studied the ability of BAPCs to deliver pDNA vaccines capable of targeting Human Papillomavirus(HPV)-induced tumors in mice.

This pDNA vaccine encodes a fused HPV-16 E7 oncoprotein with the herpes virus gD protein and it was designed by Dr. Luís C.S. Ferreira from the vaccine development laboratory at University of São Paulo[196]. The aim of the fusion was to maximize the antitumoral effect. The fusion promotes the enhancement of antigen-specific cytotoxic $CD8^+$ T-cell responses associated with antitumor protective effects[197]. The protein E7 is expressed early in the HPV life cycle and among other proteins from the same family is responsible for the HPV oncogenic properties. The vaccine promoted the antitumor therapeutic effects based on the obstruction of coinhibitory signals and the coactivation mechanisms[198]. The effect of the vaccine was tested in the C57BL/6 mouse strain. Before vaccination, TC-1 cell epithelial lung cells expressing the HPV-16 E7 oncoprotein were inoculated into the animals intravenously, resulting in a single tumor cell mass at the body flank or pulmonary nodules[199]. Significant antitumor therapeutic effects compared with naked DNA vaccines were achieved when BAPCs were used as a deliver vehicle of the vaccine.

In our earlier study on using the branched amphiphilic peptides to interact directly with DNA we saw that the DNA to peptide ratio influenced not only the type of structure generated but also transfection efficiencies of a double stranded plasmid DNA in cultured cells (2). Here the peptide capsules were preformed prior to the addition of the pDNA. These complexes were able to transfect HeLa cells and stably express EGFP in with gene delivery rates higher that that observed with the commercial reagent Lipofectin® while showing minimal toxicity.

3.2 Materials and Methods

3.2.1 Peptide synthesis

Peptides were synthesized as previously described[145]. The cleaved peptides were then washed three times with diethyl ether, dissolved in water, and then lyophilized before storing them at RT. The peptides were purified by reversed phase HPLC and characterized using matrix-assisted laser desorption/ionization-time of flight (MALDI TOF/TOF).

3.2.2 BAPCs preparation

The peptides, bis(h_9)-K-K_4 and bis(h_5)-K-K_4, were individually dissolved in pure 2,2,2,-Trifluoroethanol (TFE) and then mixed together in an equimolar ratio in at 500 μM final concentration. Peptide concentrations were calculated using the molar absorptivity (ξ) of phenylalanine in water at 257.5 nm (195 cm^{-1} M^{-1}). After mixing were allowed to stand for 10 minutes before removing the solvent under vacuum. 1 mL of water was added drop-wise into the dried peptide mixture in autoclaved 1.5 mL Eppendorf tubes and allowed to sit for 30 min at 25°C to form capsules. Subsequently, the capsule containing solution was incubated for 1 h at 4°C to stop the capsule fusion. After 1 h, the peptide sample was then returned to 25°C for 30 min before mixing with pDNA.

3.2.3 Preparation of BAPCs-DNA complexes

A plasmid containing solution (2.5μg/mL) was added drop-wise into different tubes containing BAPCs at different final concentrations (2.5, 5, 10, 20, 40 and 50 μM). This concentrations correspond to the N:P = 1.3, 2.6, 5.2, 10.4, 20.8 and 41.6 respectively. Solutions were mixed carefully with pipette and allow staying for 10 min before adding $CaCl_2$ at 1.0 mM final concentration. After 30 min incubation, the solution was added to the cell culture.

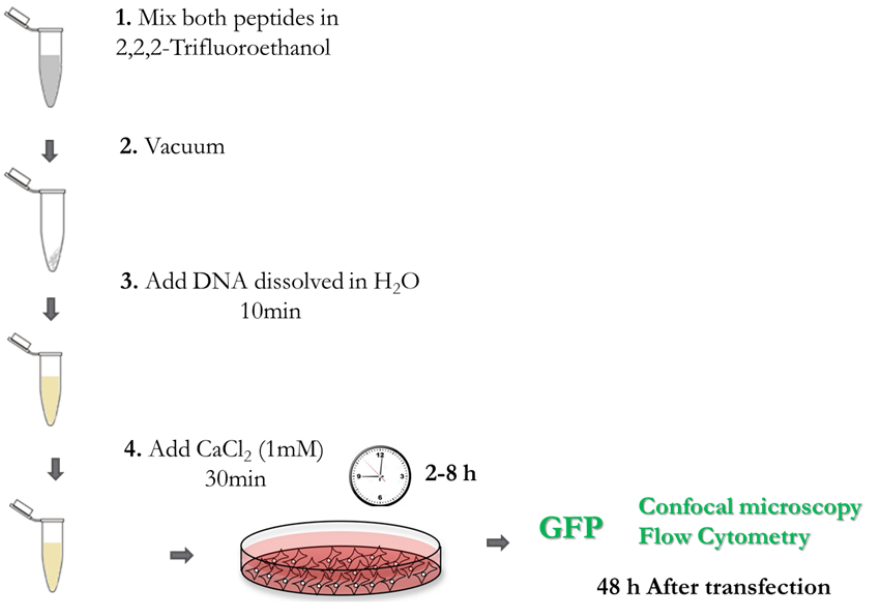

Figure 3.2: *A schema of the optimized method to prepare peptiplexes (described in detail within section 3.2.2*

3.2.4 STEM sample preparation

For scanning transmission electron microscopy (STEM) BAPCs-DNA complexes were prepared as previously described in 3.2.3. The samples were negatively stained for 10 minutes using a multi isotope 2% Uranyl acetate (Uranium bis(acetato)-O-dioxodihydrate) (Sigma-Aldrich, St. Louis, MO) aqueous solution. Sample solutions (6 μL) were spotted on to grids

and allowed to stand for 5 min, after which, excess solution was wicked off the grid with a tissue and allowed to air dry before loading it into the FEI Tecnai F20XT Field Emission Transmission Electron Microscope (FEI North America, Hillsboro, Oregon) with a 0.18 nm STEM HAADF resolution and a 150X 2306 x 106X range of magnification. Scanning transmission electron microscopy was carried out in the annular dark field mode with a single tilt of 17°.

3.2.5 Atomic force microscopy (AFM)

The plasmid DNA sample was prepared as described by Li et al.[179]. For the peptide/DNA samples, 10 μL of the BAPCs-DNA complex at N:P = 20.8 was deposited onto freshly cleaved mica substrates. After a 15 min incubation, the sample was dried under a nitrogen atmosphere. AFM topography images of immobilized DNA and/or peptides were acquired in air using the contact mode on an Innova Atomic Force Microscope (AFM) from Bruker, USA. The AFM scanner was calibrated using a TGZ1 silicon grating from NT-MDT, USA. We used MLCT-E cantilevers with their respective nominal spring constants of 0.05 N/m and 0.1 N/m, and using set point contact forces of 1 nN or less. The AFM topography data were flattened by subtracting the background and using second order line by line fitting methods incorporated within the Gwyddion software[180].

3.2.6 Determination of zeta potential

BAPCs-DNA complexes were prepared as previously described in 3.2.3 at different charge ratios and then dissolved in a final volume of 1 mL Opti-MEM® I Reduced Serum Media (Life Technologies, Grand Island, NY). Zeta-potential was measured as described in 2.2.6. All measurements were performed in triplicates.

3.2.7 Plasmid digestion with DNase-1

BAPCs-DNA complexes were prepared as reported above (3.2.3) and digested as described in 2.2.8. All samples were run in a 0.8% agarose gel containing 0.012% Ethidium bromide, run at 60 V for 40 min. A 1 kb ladder was used as reference (Fisher Scientific, Pittsburgh PA, USA). After electrophoresis, the resulting DNA migration bands were visualized using a MultiDoc-it, Digital Imaging System (Ultra-Violet Products, Upland, CA, USA).

3.2.8 DNA/Capsule interaction study with two BAPC temperature variants

Two different capsule preparation (1.0 mM) schemes were used in this study. One sample was prepared at 25°C for 30 min followed by incubation a 4°C for 1 h, before returning it to 25°C for another 30 min (25-4-25°C BAPCs). The second sample was prepared at 4°C for 30 min and then transferred to 25°C (4-25°C BAPCs). Encapsulation of the auto quenching fluoresce dye Eosin Y (2.13 mM) occurred during BAPC formation and washed as previously described[145]. The washed capsules were suspended in water and mixed with 2.5 μg of pDNA, The samples were analyzed in the fluorometer with excitation at 490nm with emissions recorded from 495 to 800 nm for 4 h at 15 min intervals using a CARY Eclipse spectrophotometer (scan rate, 600 nm/min; PMT detector voltage, 800 V; excitation slit, 5 nm; emission slit, 5 nm).

3.2.9 Cell Culture

HeLa cells were purchased from ATCC (CCL-2) and maintained as described in 2.2.9.

3.2.10 Confocal Laser Scanning microscopy

Images in Figure 3B and Suplementary data Fig 1 were taken using a confocal LSM 700 laser-scanning microscope (Carl Zeiss, Gottingen, Germany). The cell boundary and structure

was visualized using "Differential interference contrast microscopy (DIC)".

3.2.11 pEGFP-N3 plasmid transfection

Transfection experiments were carried out by mixing a 4.7 kb pDNA, encoding the enhanced green fluorescent protein (EGFP). The plasmid pEGFP-N3 was obtained from Dr. Dolores Takemoto lab (purchased from Clontech, Mountain View, CA). HeLa cells were seeded on 22 mm culture dishes at a density of 1x105 cells per mL, 24 h later at 60% confluence, all medium was removed from the wells and 800 μL of Opti-MEM® I Reduced Serum Media was added. Next, 200 μL BAPCs-DNA complexes were added to cells and allowed to incubated in normoxic conditions for 2-6 h. After this incubation, media and transfection reagent was removed and replaced with 1 mL of fresh DMEM containing 10% FBS in each well. The cells were returned to the incubator for 48 h. For the positive control cells were transfected with Lipofectin® (Invitrogen, Carlsbad, CA), according to the protocol supplied by the manufacturer. Some parameters were adjusted to reach optimum results in HeLa cells. Briefly, lipoplexes where formed in 190 μL Opti-MEM® I Reduced Serum Media and mixed with 2 μg of pDNA and 10 μL of the transfection reagent (Higher volumes of the reagent led to cell death and lower volumes reduced transfection efficiency). The lipoplexes were added to the cells and allowed to incubate for 6 h at 37°C. Transfection efficiency was evaluated as previously described (2.2.11).

3.2.12 Transfection with pEGFP-N3 plasmid previously treated with DNase I

BAPCs-DNA complexes at charge ratio of 10.4 and 20.8 were digested for 30 min with DNase I as previously described in a total volume of 1 mL of Opti-MEM® I Reduced Serum Media. Subsequently, cell were washed two with PBS and the solution was placed transferred to cells and incubate for 4 h. 48 h later transfection was monitored by confocal microscopy

3.2.13 Cell viability assay

Cell toxicity assays were carried out based on cell death using exclusion of the fluorescent dye trypan blue and PI as previously described (2.2.11 and 2.2.12) at N:P = 1.3, 2.6, 5.2, 10.4, 20.8 and 41.6 values.

3.2.14 DNA vaccine

The circular plasmid DNA vaccine (5.6kb) encoding HPV-16 E7 genetically fused after amino acid 244 of the HSV-1 gD protein has been described previously by Lasaro et al.[200] . To form the BAPCs-vaccine complexes at different N:P ratios (0.65, 1.3 and 2.6), BAPCs were prepared as we described earlier, and then mixed at 200, 400 and 800 μM with 40 μg of the DNA vaccine. Each animal was inoculated with a final volume of 100 μL in saline solution of these complexes

3.2.15 Tumor cell challenge

All animal experiments were conducted with the permission of Biomedical Sciences Institute of the University of São Paulo and housed at the Parasitology Department of the University of Sao Paulo following the recommendations for proper use and care of laboratory animals. Groups of 410 mice were injected subcutaneously to the rear flank of the animal with 7.5 X 104 104 TC-1 cells suspended in 100 μl of serum-free medium. The mice were vaccine with the peptide/DNA formulation three days after the tumoral cell inoculation. Tumor evolution was checked by visual inspection and palpation for a period of 60 days. The animals were scored as tumor-bearing when the tumors reached a size of approximately 2 mm in diameter. The mice were euthanized once the tumors showed a diameter of 1 cm or became necrotic.

3.2.16 Intracellular cytokine staining

Intracellular IFN-γ staining was done using blood samples from the mice collected 14 days after vaccine administration following the protocol previously described by Diniz et al.[196] for the 0.65 and 1.3 charge ratios.

3.3 Results and discussion

3.3.1 *In vitro* Transfection Efficiency of the BAPCs-DNA complexes

We assessed the ability of BAPCs to deliver the plasmid pEGFP-N3 in HeLa cells. Cells were incubated 4 hours with the peptide/DNA complexes at different charge ratios in reduced serum media (Fig. 3.3A). We define charge ratio (N:P) as the number of NH^{3+}'s (N) contained in the oligolysine and the number of PO^{4-}'s (P) in the 4.7 kb pEGFP-N3 plasmid. We tested 6 different formulations based on previous transfection experiments where the same peptides sequences are mixed directly with the DNA at 25°C (2).

This treatment condition does not result in capsules formation, instead, depending of the peptide/DNA ratios; the peptides either coat the plasmid surface forming nano-fibers or condense the plasmid into nano-sized spherical structures. Calcium chloride ($CaCl_2$) was added at 1 mM final concentration to improve transfection efficiency. It has been reported that adding $CaCl_2$ to Cell Penetrating Peptides (CPP)/DNA complexes can reduce particle size and maximize gene delivery *in vitro*[182]. Transfected cells expressing EGFP were visualized by confocal microscopy and quantified using fluorescence-activated cell sorting (FACS). Propidium Iodide (PI) was used to identify and then exclude dead cells from the analysis. The EGFP-positive/PI-negative cells were counted as positively transfected cells. As a positive control, cells were transfected with the commercial transfection reagent Lipofectin® using conditions optimized by the manufacturer for this cell line. FACS analysis showed that

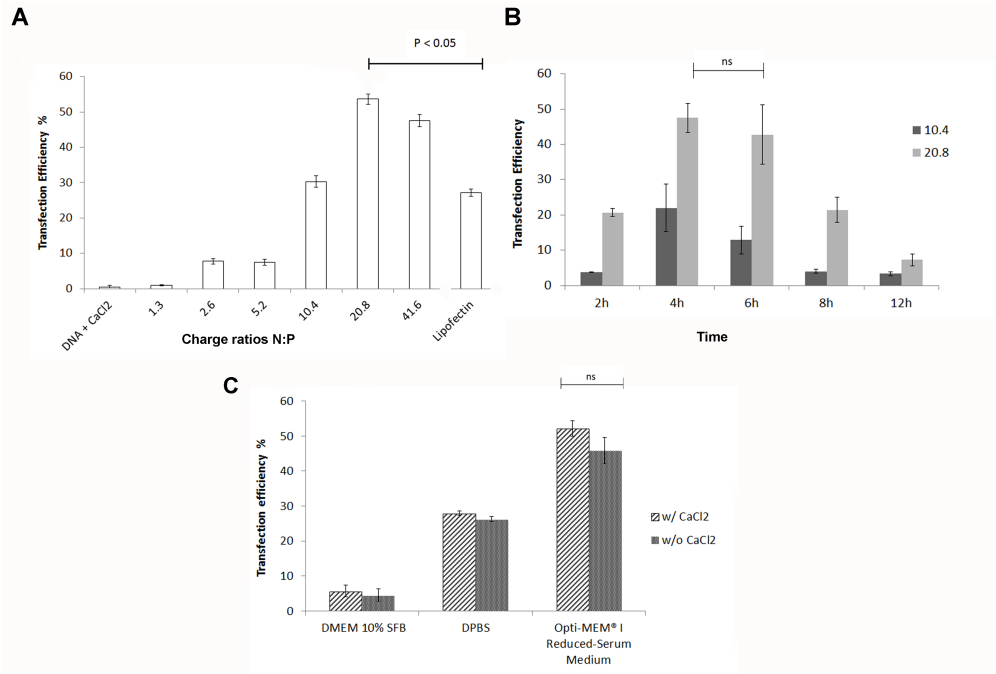

Figure 3.3: *Comparison of transfection efficiency of BAPCs-DNA in HeLa cells. (A) Different peptide to DNA charge ratios (N:P) after 4 h of incubation time with the complexes in reduced serum media and 1 mM $CaCl_2$ (B) Different incubation times for the charge ratios 10.4 and 20.8 in reduced serum media and 1 mM $CaCl_2$ (C) Different media compositions used for transfection of the BAPCs-DNA complexes at N:P = 20.8, after 6 h of incubation in the absence and presence of $CaCl_2$. Data are presented as means SEM (standard error of the mean). Differences between values were compared by ANOVA using Bonferroni as post test. Non-statistical significance (ns) was considered when P>0.05. DPBS: Dulbecco's Phosphate-Buffered Saline, calcium and magnesium free.*

transfection efficiency differs significantly depending on the peptide to DNA charge ratio. The ratios that yielded the highest transfection rates were N:P = 20.8 and 41.6, however cell viability at N:P = 41.6 was almost two-fold lower than the viability observed using 20.8 ratio. Therefore, we discontinued using the higher ratio and we studied how other parameters might affect the transfection efficiency of the 10.4 and 20.8 ratios, We investigated how incubation time affects the transfection rates (Fig. 3.3B). It was observed that the optimal incubation time with the complexes was between 4 to 6 h. Although there was no statistically significant difference between the two time intervals, cell viability was better when the incubation time is only 4 hours (Data not shown). Once we fixed the suitable charge ratio

and incubation time, different buffers were also tested in the presence and absence of $CaCl_2$. We found that transfection rate is the best when Opti-MEM® I Reduced Serum Media is used as a buffer for the transfection (Fig. 3.3C). According to Bonferroni Test, there is no significant difference between the complexes incubated with or without $CaCl_2$. Nevertheless, we observed after carried out three different experiments a slightly improvement in the transfection rate (∼8%) based on this observation we have decided to add $CaCl_2$ regardless the minimal effect on the overall transfection rate. Ultimately these optimized conditions generated transfection rates approaching 55%, almost twice the transfection rate observed for the commercial reagent Lipofectin®.

3.3.2 *In vitro* toxicity of BAPCs-DNA complexes

The *in vitro* cytotoxicity of the peptide-DNA complexes was evaluated in HeLa cells based on the dead cell fluorescent marker dyes Trypan blue and propidium iodide (PI) (Fig. 3.4A and Supplementary data Fig. B.1). The results showed that cell viability is minimally affected using the DNA/BAPC complex at the N:P ratio yielding the highest transfection efficiency while the lipid-based transfection reagent caused cell death approaching 50%. Additionally, confocal analysis shows a normal morphology for those cells that were treated with DNA/BAPCs whereas treated with Lipofectin displayed abnormal cell structures (2.4B and 2.4C).

3.3.3 Biophysical characterization of DNA/BAPC complexes

As previously reported, BAPCs will retain their size (∼20-30 nm) upon incubation at 4°C. Based on this fact, we hypothesized that BAPCs could act as cationic nucleation centers around which DNA could wind, in an analogous fashion to histones compacting DNA to form nucleosomes. The lysine residues exposed on the outside layer of BAPCs have a net positive charge thereby facilitating electrostatic interactions with the negatively charge phosphate groups on DNA polymer. After inspection of 40 images, a well-resolved and

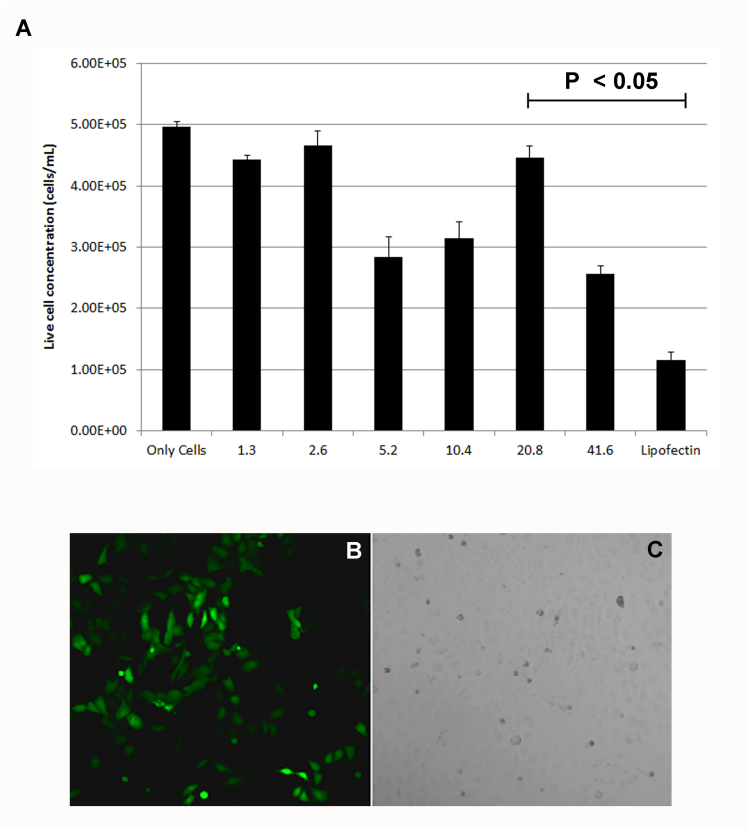

Figure 3.4: *(A) Cell viability after treatment with DNA/BAPC complexes at different N:P charge ratios as determined by the trypan blue analysis. Viability experiments were done using the same conditions than transfection. (B) Confocal microscopy images of HeLa cells after transfection with plasmid DNA encoding the green fluorescent protein (GFP) using BAPCs: DNA at N:P = 20.8. (C) Bright field images after transfection with plasmid DNA encoding the green fluorescent protein (GFP) using BAPCs: DNA at N:P = 20.8. Data are presented as means SEM (standard error of the mean). Differences between values were compared by ANOVA using Bonferroni as post test. Non-statistical significance (ns) was considered when P>0.05.*

representative transmission electron microscopy (TEM) image of the complex revealed a uniform coating of single BAPCs with what appears to be a double stranded DNA (Fig. 3.5). However, complexes made up of several BAPCs were more prevalent, suggesting that the multi-mers comprised of multiple BAPCs and more than one DNA molecule are involve in the supra-molecular structure of the nanoparticles. The total number of nanostructures analyzed within the 40 images was 312 and the proportion multi-mers to single BAPCs was approximately 5:1. According to the polymer random walk model[201] pDNA had an

estimated size of ∼50 nm. However, free DNA molecules generally adopt a much larger size in solution (∼200 nm)[202]. For a single 20 nm BAPC, the curvature could be too high for a single DNA chain to wrap tightly however, since the bending energy is inversely proportional to the square of the bending circle radius[203]. Bending of DNA around larger nanoparticle clusters requires much lower energies. This might explain the presence predominantly of clusters with average size between 50-100 nm.

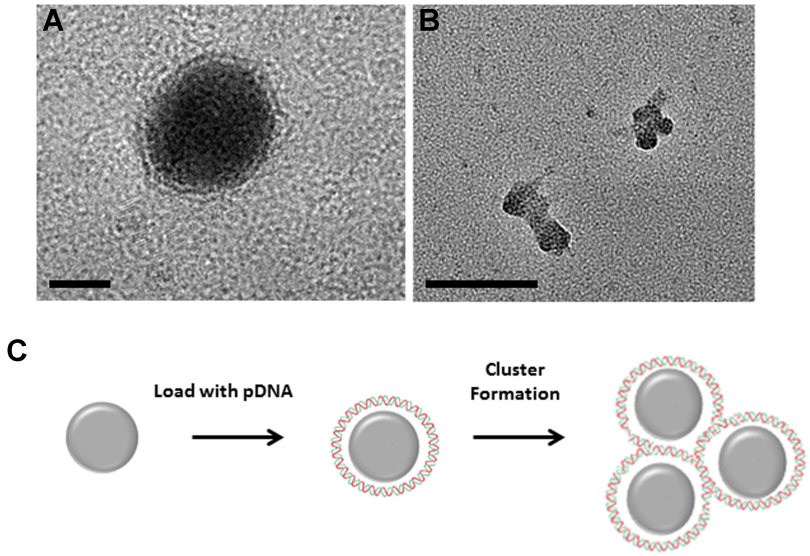

Figure 3.5: *TEM images of the BACP:DNA assemblies at N:P = 20.8. (A) Single BAPCs interacting with pDNA (Scale bar = 5 nm). (B) Cluster of BAPCs interacting with DNA. (C) Schematic representation of the BAPCs-DNA interaction (Scale bar = 100 nm).*

AFM imaging was used as a second technique to confirm the topologies of the BAPCs-DNA complexes at the ratio that displayed the best transfection rate. Using AFM, one can visualize surface-dependent molecular events in three dimensions on a nanometer scale. At the N:P = 20.8 using AFM we visualized mostly clusters of several BAPCs interacting with DNA (Fig. 3.6A). The size distribution of the clusters observed in Fig 3.6A is predominately between 50-200 nm and match perfectly to what was observed in TEM (Fig. 3.5). Plasmid DNA "thickness" (or vertical height) is about 1 nm or below (2.7C). A minimum thickness of the "cluster" is about 5 nm and around 10 nm what confirms that peptide and DNA are

interacting and forming complexes.

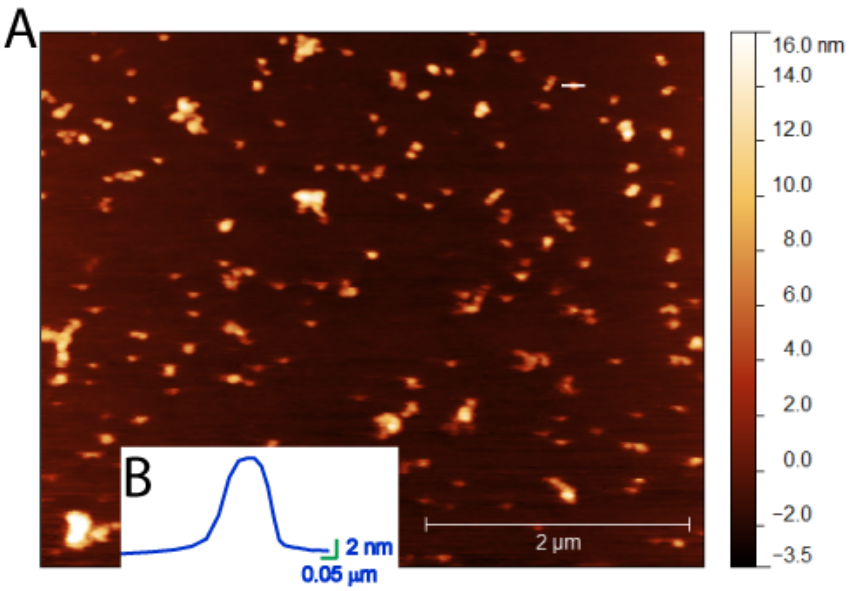

Figure 3.6: *AFM images of the DNA/BAPCs at N:P = 20.8. (A) 5 x 4 µm image of the nano-structure form at N:P of 20.8. (B) Cross section analyses of the DNA/BAPCs complex shown in panel A, where the nanostructure show a height of ∼ 10nm and length of ∼ 20nm.*

According to the two different imaging techniques, BAPCs when are mixed with DNA, form compact clusters with sizes ranging predominately from 50 nm to 200 nm in average with a few forming larger assemblies. Among several factors influencing transfection efficiency, particle size is one of the most critical. It impacts both the rate and route of uptake and cytotoxicity. Rejman et al.[204] demonstrated that nanoparticles with a size of 50 nm are taken up 34 times faster than 100 nm particles and 810 times faster than 500 nm particles. In regard to cytotoxicity, Yin et al.[205] have proposed that the interaction area of bigger particles is greater than the smaller ones, causing stronger stimulus on the cells, therefore more chemical reactivity. Most DNA/BAPC complexes appear to be in the suitable range of size to stimulate transfection.

We investigated the ability of BAPCs to protect bound DNA against nuclease degradation (Fig. 3.7A). Deoxyribonuclease I (DNase I) was used as a nuclease for this assay and

cleaves non-specifically at the 5' phosphodiester linkages adjacent to pyrimidine nucleotides of double strand DNA[186]. Results were visualized using agarose gel electrophoresis. The N:P ratios of 10.4 and 20.8 (lanes 6 and 8 respectively) were able to form tight complexes with DNA that appeared to avoid endonuclease digestion. No difference was observed when the bands are compared with the negative controls (lane 5 and 7) of complexes not treated with the nuclease. The first lane shows a 1 kb dsDNA ladder and lane 2 the free pEGFP-N3 plasmid. Lane 3 contains plasmid mixed only with $CaCl_2$ 1mM, conditions where the DNA is not condensed by the salt. Lane 4 shows the plasmid mixed with $CaCl_2$ and treated with DNase-1, were no enzyme protection was detected. To further confirm protection, DNase-1 treated DNA/BAPC complexes were checked for transfection efficiency in HeLa cells. Under these conditions a significant reduction in the transfection rate was observed (data no shown), suggesting that DNA could be partially degraded or nicked by the nuclease, most likely due to the fact that some scissile bonds of the DNA remain exposed in the DNA/BAPC complex.

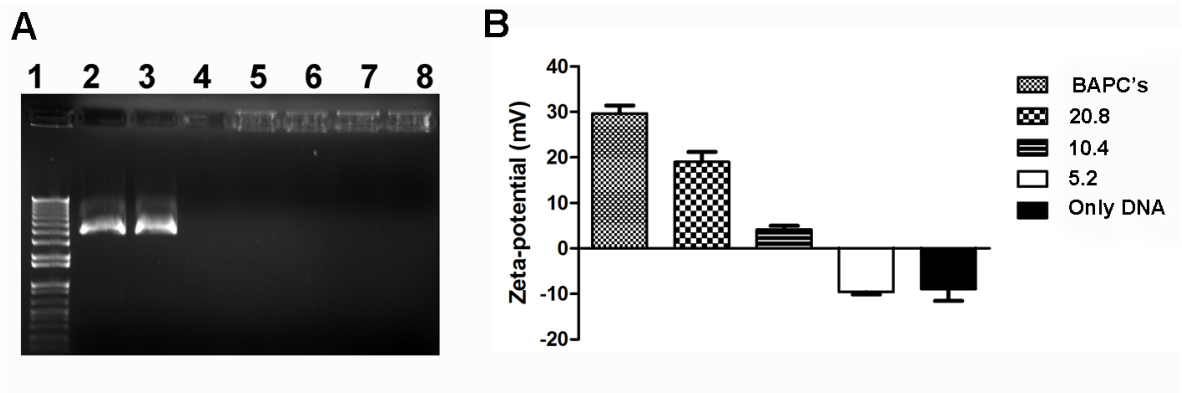

Figure 3.7: *Gel shifts and Zeta potentials of DNA/BAPCs (A) Agarose gel electrophoresis of peptide complexes at different ratios, each lane contains 80 ng of pEGFP-N3. Lane 1 corresponds to 1kb dsDNA Ladder, lane 2 contains only pEGFP-N3 plasmid, lane 3: DNA + $CaCl_2$, lane 4: DNA + $CaCl_2$ + DNase I, lane 5: BAPCs:DNA at N:P = 10.4, lane 6: BAPCs:DNA at N:P = 10.4 + DNase I, lane 7: BAPCs:DNA at N:P = 20.8, lane 8: BAPCs:DNA at N:P = 20.8 + DNase I. (B) Zeta potential of BAPCs-DNA complexes at different peptide to DNA ratios.*

The BAPCs-DNA complexes zeta potential (ZP) changes from negative to positive when

the N:P ratio increases, being ∼22mV for the N:P= 20.8, appropriate value to promote cell surface interaction but not cell damage (Fig. 3.7B). The ZP is a function of the surface charge which changes when any material is placed in solution. Values above 45 mV could be toxic for cells and values with a high negative ZP might not interact efficiently with the negatively charge cell surface.

3.3.4 DNA/Capsule interaction study with two BAPC temperature variants

After 30 min hydration, BAPCs are a water filled spheres with a homogeneous size of ∼20-30 nm in diameter (Fig. 3.1). Longer incubation times result in capsule fusion and after 24 h BAPCs can reach sizes up to 1 μm in diameter. Lowering the temperature to 4°C for 1 h is sufficient to prevent capsule fusion and therefore provides a method to control size. After this temperature treatment, increasing the temperature or incubation time does not affect capsule size or cargo release. In our initial vaccine trial 25-4-25°C BAPCs were used with success. However in a second trial 4-25°C BAPCs were used without success. Based on these results, fluorescence studies looking at the effect of DNA binding with these two temperature variants were undertaken.

In this experiment 25-4-25°C BAPCs showed no appreciable change in fluorescence, suggesting that the capsule's size remained similar (Fig. 3.8). We have come to refer to this temperature dependent conformation as the "locked conformation". A different behavior in fluorescence intensity was observed when the 4-25°C BAPCs were mixed with DNA. In this case, fluorescence rapidly decreased and appeared to reach an endpoint within the first 60 min. This decrease in fluorescence indicates an increase in dye concentration within the capsule. It should be noted that more capsules form at 4°C thus accounting for the higher initial fluorescence intensity[206]. This increases in concentration could only occur if the 4-25°C BAPCs decreased in diameter with the presumed expulsion of water. These results suggest that the "locked" BAPCs are better for DNA vaccine use.

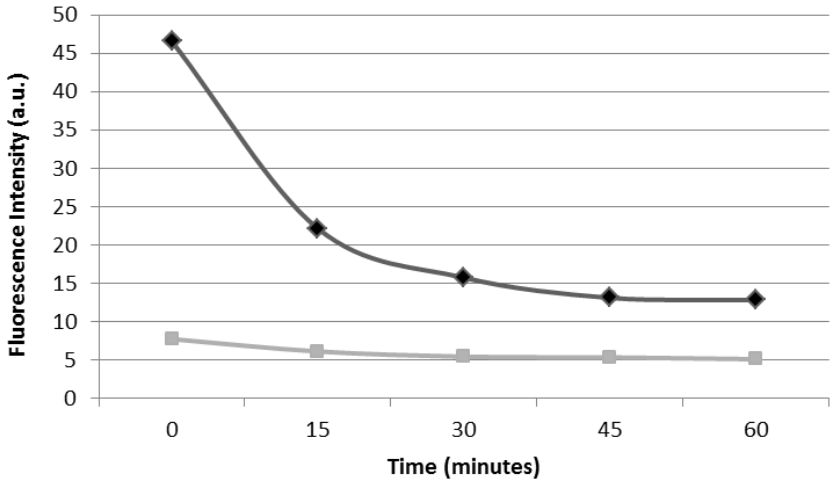

Figure 3.8: *DNA/capsule interaction study. Washed Eosin Y entrapped 25-4-25°C (grey) and 4-25°C (black) BAPCs were mixed with DNA at N:P = 20.8. at 25°C. The florescence emission at nm was measured every 15 min for 60 min*

3.3.5 Delivery of HPV-Specific therapeutic antitumor DNA vaccines

Diniz et al.[196] reported the design of a DNA vaccine capable of targeting HPV tumors. The vaccine is a 5.6 kb circular plasmid DNA encoding the HPV-16 E7 oncoprotein genetically fused to the HSV gD protein. This is a pioneer design that has proven to be extremely efficient in triggering immune responses against HPV-16 tumors. In our study, the ability of BAPCs to act as a gene carrier and increase potency for the pDNA vaccine was studied. We administrated BAPCs at different N:P ratios based on the *in vitro* results previously showed. For the vaccine delivery at N:P = 1.3 ratio conferred the highest antitumor protection (80%) to C57BL/6 mice with previously transplanted TC-1 tumor cells (Fig. 3.9). Surprisingly, lower ratios displayed better transfection *in vivo*. Around 60% of tumor protection was detected in animals injected only with DNA + $CaCl_2$ and approximately 20% was achieved by the peptide-DNA complexes with an N:P = 0.65 and 2.6. The control with only saline solution showed no tumor protection. The vaccines were tested in groups of five mice and vaccines were administrated 3 days after the injection of tumor cells.

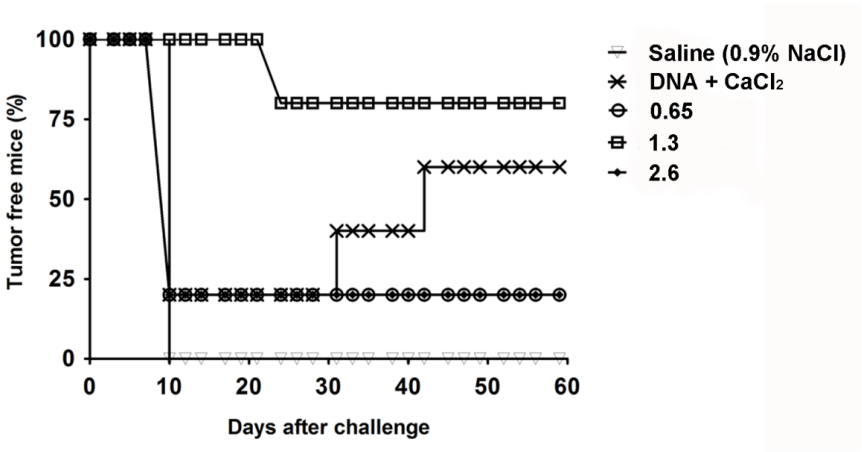

Figure 3.9: *Administration of a single vaccine dose containing DNA/BACP's complexes at different N:P charge ratios. Vaccines were administered intramuscularly 3 days after injecting the TC-1 cells. Figure provided by Dr. Luís C.S. Ferreira and Luana R. M. M. Aps from the vaccine development laboratory at University of São Paulo*

The induction of antigen-specific $CD8^+$ T-cells response was measured as well since it directly related with the therapeutic tumor protection. $CD8^+$ T-cells exert antitumor cytolytic activity and are also implicated in the destruction of virally infected cells. Figure 3.10 shows that the administration of the vaccine complexes with BAPCs increased the activation of E7-specific IFN-γ producing $CD8^+$ T cells in mice 3 days after the TC-1 cell challenge, particularly for the charge ratio of 1.3. No significant immune response was detected for the control group (only saline). Lower responses were detected for only DNA or the 0.65 and 2.6 N:P groups. These results confirmed the enhanced therapeutic antitumor protection observed in the mice immunized with the DNA/BAPC complexes. Greater cytotoxic activity against tumor cells and reduction in tumor mass was detected when BAPCs were co-administrated with the enhance DNA vaccine.

3.4 Conclusions

In summary, we report the ability of a peptide capsules to safely deliver plasmid DNA *in vitro* and *in vivo*. These pre-formed peptide capsules are prepared in water at 25°C and

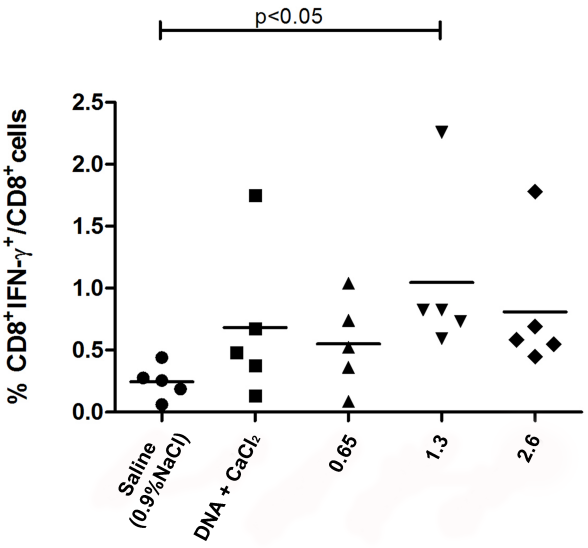

Figure 3.10: *Percentage of CD8$^+$ IFN-γ^+ cells of total CD8$^+$ T cells in mice immunized with different DNA/BAPC complexes at different N:P charge ratios. Data represent results of one immunization of two experiments with similar results, each data point represent one animal. Differences between values were compared by ANOVA using Bonferroni as post test. Non-statistical significance (ns) was considered when P>0.05.Figure provided by Dr. Luís C.S. Ferreira and Luana R. M. M. Aps from the vaccine development laboratory at University of São Paulo*

subsequently cooled to 4°C to prevent fusion and preserve the particle size around 20-30 nm. They interact with plasmid DNA acting as a cationic nucleation centers were DNA wraps around, generating DNA/BAPCs complexes with a size ranging mainly between 50-250 nm that displayed a positive zeta potential. Both of these parameters are appropriate for gene delivery. One possible explanation for the increase in transfection rates in comparison with the method that was previously reported (2) might be the reduction in size of the peptide/DNA complex. Also the presence of a cationic surface should enhance cellular uptake and subsequent release from the late endosomes. The AFM images show some larger clusters that appear to be around 500 nm. It is unclear whether these participate complexes participate in the delivery process.

HeLa cells transfected with the DNA/BAPCs complexes showed around 55% for GFP expression, almost two-fold that observed for the same gene and same cell line by the

commercial reagent Lipofectin®. Taking into account the viable cells per mL ($4.5x10^5$), the protein yield is almost four times when compared to Lipofectin®. While some transfection reagents displayed high transfection efficiencies *in vitro*, they often lose their ability to reach the same results for *in vivo* applications[207]. BAPCs are capable to enhancing the therapeutic effect of an optimized DNA vaccine that encodes for the oncoprotein E7. The TC-1 cell transplantation model was using to monitor E7-specific $CD8^+$ T-cell responses against and tumor development. After 60 days of the T-cell transplantation, 80% of the mice were tumor free. This represents a clear improvement in the antitumor protection vs. the group of mice treated only with naked DNA (60

Chapter 4

Conclusions

We developed a new peptide-base method to deliver plasmid DNA into eukaryotic cells. DNA is a large anionic molecule with limited ability to penetrate cells without the presence of a carrier or shocking the cell. Synthetic non-viral DNA carriers are cationic molecules that bind to DNA, predominantly through electrostatic interactions and promote the cell membrane translocation. In these studies two relatively short branched peptide sequences were prepared that proved to function as a synthetic non-viral carriers of plasmid DNA. The sequences bis(FLIVIGSII)-K-KKKK and bis(FLIVI)-K-KKKK, are capable of self-assembling into extremely stable nano-capsules that are able to encapsulate, retain and deliver (*in vitro*) a variety of solutes into cells. To date, these include the alpha-emitting 225Actinium and its radioactive daughter radionuclides and various fluorescent dyes[146].

Initially, we hypothesized that pDNA could be trapped inside the capsules formed by the peptides. Based on this premise, transfection experiments were carried out expecting encapsulation to occur by providing enough peptides to form one capsule/pDNA strand. The charge ratio (N:P) between the number of NH^{3+}'s (N) contained in the oligolysine tails of the ∼2000 peptides per 20 nm capsule and the number of DNA backbone phosphates (P) in the 4.7 kb ds pDNA was calculated to be 65.5. These parameters were used throughout the experiment however, only a ∼2% transfection efficiency was observed. When these pep-

tide/DNA complexes were analyzing using TEM, we observed long nano-fibrils with lengths of 0.5-1 microns. However, since transfection efficiencies were quite low no more experiments were conducted using these proportions. Subsequently, we examined the effect of reduced peptide concentrations at a fixed pDNA concentration. Surprisingly, at lower N:P ratios transfection rate in HeLa cells increased nearly 10 fold reaching rates nearly 25%. Structural analyses of the peptide/DNA complexes for these ratios reveled spheric morphologies with sizes ranging from 100-500 nm in diameter. For this nanostructure we used AFM in liquid phase as a second technique to confirm the structure pattern of the complexes. In both cases (fibers and nano-spheres), the DNA in water was added to the dried peptides with an incubation time of 30 min before adding them to *in vitro* cultured HeLa cells. Although we managed to increase the transfection rate by modifying the peptide/DNA charge ratio, we felt higher transfection rates could be obtained that would be comparable to those obtained using commercial synthetic transfection reagents. Pursuing this, we discovered that if the peptide capsules, termed BAPCs were pre-formed in water for 30 min at 25°C followed by cooling at 4°C for 1 h and then before adding DNA at 25°C, better transfection rates might be achieved. We refer to this temperature shift regime as 25-4-25°C and was identified previously by Sukthankar[208]. Here BAPCs displayed a uniform size of ∼20 nm and they retain their size at elevated temperatures and are resistant to disruption by organic solvents. Images generated by TEM and AFM for the resulting DNA/BAPC complexes revealed that BAPCs remained intact and bound plasmid DNA acting as a cationic nucleation centers were DNA wraps around, generating peptide-DNA complexes with a size between 50-250nm. The size reduction of the DNA/BAPC complexes might be a possible explanation for the increase in transfection rates in comparison with the methods previously described. Among several factors influencing transfection efficiency, the particle size is one of the most critical since have an impact in the rate and route of uptake and their cytoxicity. Rejman et al.[204] demonstrated that nanoparticles with a size of 50 nm are taken up 34 times faster than 100 nm particles and 810 times faster than 500 nm particles. In regard cytotoxicy, Yin et al.[205]

have proposed that the interaction area of bigger particles is greater than the smaller ones, causing stronger stimulus on the cells, therefore more chemical reactivity and potentially more toxic effects. In summary, we discovered different patterns of DNA condensation by the peptide sequences bis(FLIVIGSII)-K-KKKK and bis(FLIVI)-K-KKKK FLIVV depending on the peptide/DNA charge ratio and the method of preparation (4.1). Each conformation displayed different gene delivery efficiency. The structure where the DNA wraps around display much higher transfection efficiencies in HeLa cells in comparison with the other two morphologies and the commercial lipid reagent Lipofectin®. Similarly, pDNA was delivered *in vivo*, as a vaccine DNA encoding E7 oncoproteins of HPV-16. It elicited an immune response activating $CD8^+$ T cells and provided anti-tumor protection in murine models.

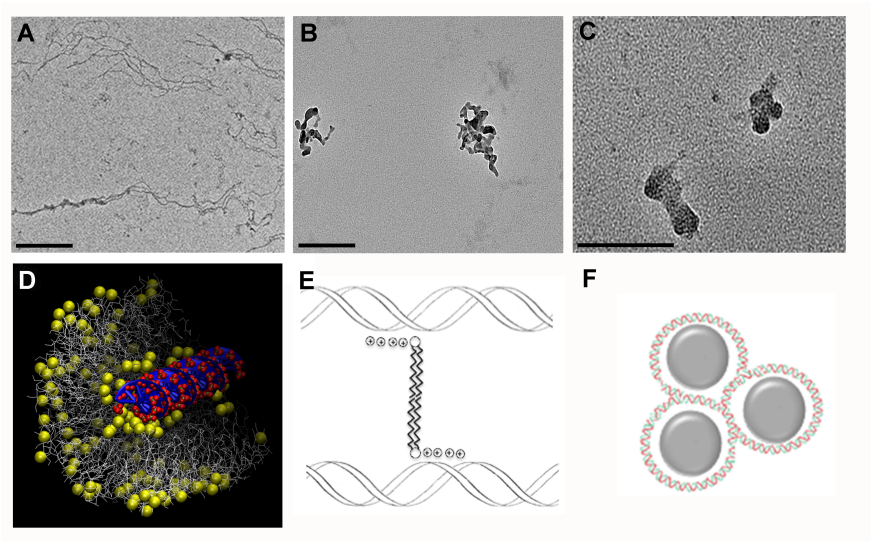

Figure 4.1: *(A) Peptiplexes forming nano-fibers structures at N:P = 65.5, scale bar = 200nm (B) Peptiplexes forming nano-spheres complexes formed at N:P = 10.4, scale bar = 200nm.(C) BACP:DNA assemblies at N:P = 20.8, scale bar = 100nm. D, E and F are schematic plots of the different DNA/peptide assemblies respectively.*

4.1 Future Directions

Several factors can influence transfection efficacy such as cell type, carrier/DNA charge ratio, particle size, particle charge, toxicity, solubility and stability in serum[185]. For *in vitro* delivery the parameters described here were optimized exclusively for HeLa cells using a reporter gene GFP. It would be relevant to test our delivering method in different cells types and using different plasmids, or even different type of nucleic acids such a RNA. BAPCs are relatively easy and cheap to synthesize in comparison with some polymers that often require extra purification steps[209,210,211]. Compared to lipids, these peptide sequences appear to be less toxic and more stable (for instance less susceptible to oxidation), giving an advantage for manufacture and storage[29,212].Other peptides systems have showed to be efficient transfection reagents, however for some cases high concentration of peptide is needed causing reduction in cell viability[88,213]. Also, often peptides must be conjugate to other molecules such lipids or polymers in order to reach high transfection rates[213]. Potentially, BAPCs could be a commercial alternative for the current market of transfection reagents due to their low toxicity, stability and relatively high transfection rate.

While some transfection reagents displayed high transfection efficiencies *in vitro*, they often lose their ability to reach the same results for *in vivo* applications. BAPCs have been improved the therapeutic effect of an optimized DNA vaccine that encodes for the oncoprotein E7. Studies are currently in progress to find out if a second round of the same vaccine formulation will enhance the antitumoral effect. Also, preliminary data using blood biomarkers for three organs (heart, liver and kidney) in mice demonstrated that BAPCs are not toxic in the concentration range used for vaccination. Several vaccines against HPV-induced tumors have been tested in clinical studies, however none of them have reach licensing for human use[214]. Problems associated with reproducibility and antitumor protection emerged in some of theses methods[215,216,217]. If we succeed in optimize the vaccine formulation to reach values near to 100% of tumor protection and reproducibility, this vaccine method could find application in future clinical trials on HPV and other viral

mediated cancers.

In another series of experiments DNA/BAPCs were able to transfect Drosophila melanogaster cell lines (data no shown), suggesting that BAPCs are capable of penetrate a variety of cell types. We are currently testing the ability of BAPC's to transfect gram positive or gram negative bacteria. Other experiments being considered involve using BAPCs to deliver DNA and dsRNA orally.

Bibliography

[1] T. Friedmann. A brief history of gene therapy. *Nature Genetics*, 2:93–98, 1992.

[2] K.A. Whitehead, R. Langer, and D.G. Anderson. Knocking down barriers: advances in sirna delivery. *Nature Reviews Drug Discovery*, 8:129–138, 2009.

[3] M. Elsabahy, A. Nazarali, and M. Foldvari. Non-viral nucleic acid delivery: key challenges and future directions. *Current Drug Delivery*, 8:235–244, 2011.

[4] R. Kole, A.R. Krainer, and S. Altman. RNA therapeutics, beyond RNA interference and antisense oligonucleotides. *Nature Reviews Drug Discovery*, 11:125–140, 2012.

[5] D.N. Niguyen, J.J. Green, R.L. Chan, and D.G. Anderson. Polymeric materials for gene delivery and dna vaccination. *Advanced Materials*, 21:847867, 2009.

[6] J. Rice, C. H. Ottensmeier, and F. K. Stevenson. DNA vaccines, precision tools for activating effective immunity against cancer. *Nature Reviews Cancer*, 8:108–120, 2008.

[7] T. M. Fu, J. B. Ulmer, M. J. Caulfield, R. R. Deck, A. Friedman, S. Wang, X. Liu, J. J. Donnelly, and M. A. Liu. Priming of cytotoxic t lymphocytes by dna vaccines: Requirement for professional antigen presenting cells and evidence for antigen transfer from myocytes. *Molecular Medicine*, 3:362371, 1997.

[8] A. P. Lam and D. A. Dean. Progress and prospects: nuclear import of nonviral vectors. *Gene Therapy*, 17:439–447, 2010.

[9] D. Karra and R. Dahm. Transfection techniques for neuronal cells. *The Journal of neuroscience : the official journal of the Society for Neuroscience*, 30:6171–6177, 2010.

[10] J. Villemejane and L. M. Mir. Physical methods of nucleic acid transfer: general concepts and applications. *British journal of pharmacology*, 157:207–219, 2009.

[11] T. Fukazawa, J. Matsuoka, T. Yamatsuji, Y Y. Maeda, M.L. Durbin, and Y. Naomoto. Adenovirus-mediated cancer gene therapy and virotherapy. *International Journal Molecular Medicine*, 25:3–10, 2010.

[12] I.M. Verma and N. Somia. Gene therapy – promises, problems and prospects. *Nature*, 389:239–242, 1997.

[13] S. Li and L. Huang. Nonviral gene therapy: promises and challenges. *Gene Theraphy*, 7:31–34, 2000.

[14] D. Escors and K. Breckpot. Lentiviral vectors in gene therapy: their current status and future potential. *Archivum Immunologiae et Therapiae Experimentalis*, 58:107–119, 2010.

[15] N. Yang. Nonviral gene delivery system. *International Journal of Pharmaceutical Investigation*, 2:97–98, 2012.

[16] C.X. He, Y. Tabata, and J.Q. Gao. Non-viral gene delivery carrier and its three-dimensional transfection system. *International Journal of Pharmaceutics*, 386:232–242, 2010.

[17] P. Mali, K.M. Esvelt, and G.M. Church. Cas9 as a versatile tool for engineering biology. *Nature Methods*, 10:957–963, 2013.

[18] D. Carroll. Genome engineering with zinc-finger nucleases. *Genetics*, 188:773782, 2011.

[19] V. P. Torchilin. Multifunctional nanocarriers. *Advance Drug Delivery Reviews*, 58: 1532–1555, 2006.

[20] C. Tros de Ilarduya, Y. Sun, and N. Duzgunes. Gene delivery by lipoplexes and polyplexes. *European journal of pharmaceutical sciences: official journal of the European Federation for Pharmaceutical Sciences*, 40:159–170, 2010.

[21] M. Jafari, M. Soltani, S. Naahidi, D. N. Karunaratne, and P. Chen. Nonviral approach for targeted nucleic acid delivery. *Current medicinal chemistry*, 19:197–208, 2012.

[22] A. Elouahabi and J.M. Ruysschaert. Formation and intracellular trafficking of lipoplexes and polyplexes. *Molecular Therapy*, 11:336–347, 2005.

[23] N. Perrimon U. Hacker, K. Nybakken. Heparan sulphate proteoglycans: The sweet side of development. *Nature Reviews Molecular Cell Biology*, 6:530–41, 2005.

[24] Z. ur Rehman, I. S. Zuhorn, and D Hoekstra. How cationic lipids transfer nucleic acids into cells and across cellular membranes: Recent advances. *Journal Controlled Release*, 166:46–56, 2013.

[25] H. Uludag C.Y. Hsu. Nucleic-acid based gene therapeutics: delivery challenges and modular design of nonviral gene carriers and expression cassettes to overcome intracellular barriers for sustained targeted expression. *Journal of Drug Target*, 20:301328, 2012.

[26] M. Marsh and H. T. McMahon. The structural era of endocytosis. *Science*, 285: 215–220, 1999.

[27] E. Koren and V. P. Torchilin. Cell-penetrating peptides: breaking through to the other side. *Trends in molecular medicine*, 18:385–393, 2012.

[28] K. Von Gersdorff, N. N. Sanders, R. Vandenbroucke, S. C. De Smedt, E. Wagner, and M. Ogris. The internalization route resulting in successful gene expression depends on both cell line and polyethylenimine polyplex type. *Molecular Theraphy*, 1148:745–753, 2006.

[29] C. Lonez, M. Vandenbranden, and J.M. Ruysschaert. Cationic liposomal lipids: From gene carriers to cell signaling. *Progress in Lipid Research*, 47:340347, 2008.

[30] S. Choksakulnimitr, S. Masuda, H. Tokuda, Y. Takakura, and M. Hashida. In-vitro cytotoxicity of macromolecules in different cell-culture systems. *J Control Release*, 34: 233241, 1995.

[31] E. V. van Gaal, R. van Eijk, R. S. Oosting, R. J. Kok, W. E. Hennink, D. J. Crommelin, and E. Mastrobattista. How to screen non-viral gene delivery systems *in vitro*. *Journal Control Release*, 154:218–232, 2011.

[32] S. Yamano, J. Dai, C. Yuvienco, S. Khapli, A. M. Moursi, and J. K. Montclare. Modified tat peptide with cationic lipids enhances gene transfection efficiency via temperature-dependent and caveolae-mediated endocytosis. *Journal of controlled release : official journal of the Controlled Release Society*, 152:278–285, 2011.

[33] D. Zhi, S. Zhang, B. Wang, Y. Zhao, B. Yang, and S. Yu. Transfection efficiency of cationic lipids with different hydrophobic domains in gene delivery. *Bioconjugate chemistry*, 21:563–577, 2010.

[34] Q.D. Huang, W.J. Ou, H. Chen, Z.H. Feng, J.Y. Wang, J. Zhang, W. Zhu, and X.Q. Yu. Novel cationic lipids possessing protonated cyclen and imidazolium salt for gene delivery. *European Journal of Pharmaceutics and Biopharmaceutics*, 78:326–335, 2011.

[35] M. A. Ilies, B. H. Johnson, F. Makori, A. Miller, W. A. Seitz, E. B. Thompson, and A. T. Balaban. Pyridinium cationic lipids in gene delivery: an *in vitro* and *in vivo* comparison of transfection efficiency versus a tetraalkylammonium congener. *Archives of Biochemistry and Biophysics*, 435:217–226, 2005.

[36] D. Zhi, S. Zhang, F. Qureshi, Y. Zhao, S. Cui, B. Wang, H. Chen, Y. Wang, and D. Zhao. Synthesis and biological activity of carbamate-linked cationic lipids for gene delivery *in vitro*. *Bioorganic and Medicinal Chemistry Letters*, 22:3837–3841, 2012.

[37] A. Masotti, G. Mossa, C. Cametti, G. Ortaggi, A. Bianco, N. D. Grosso, D. Malizia, and C. Esposito. Comparison of different commercially available cationic liposome-DNA lipoplexes: Parameters influencing toxicity and transfection efficiency. *Colloids and Surfaces B Biointerfaces*, 68:136–144, 2009.

[38] P.L. Felgner, T.R. Gadek, M. Holm, R. Roman, H.W. Chan, M. Wenz, J.P Northrop, G.M. Ringold, and M. Danielsen. Lipofection: a highly efficient, lipid-mediated dna-transfection procedure. *Proceedings of the National Academy of Sciences of the United States of America*, 84:7413–7417, 1987.

[39] F. Tang and J. A. Hughes. Synthesis of a single-tailed cationic lipid and investigation of its transfection. *Journal of controlled release : official journal of the Controlled Release Society*, 62:345–358, 1999.

[40] M. Mevel, N. Kamaly, S. Carmona, M. H. Oliver, M. R. Jorgensen, C. Crowther, F. H. Salazar, P. L. Marion, M. Fujino, Y. Natori, M. Thanou, P. Arbuthnot, J. J. Yaouanc, P. A. Jaffres, and A. D. Miller. DODAG; a versatile new cationic lipid that mediates efficient delivery of pDNA and siRNA. *Journal of controlled release : official journal of the Controlled Release Society*, 143:222–232, 2010.

[41] R. S. Shirazi, K.K.Ewert, C. Leal, R.N. Majzoub, N.F. Bouxsein, and C.R. Safinya. Synthesis and characterization of degradable multivalent cationic lipids with disulfide-bond spacer for gene delivery. *Biochimica et Biophysica Acta (BBA) - Molecular and Cell Biology of Lipids*, 1808:2156–2166, 2011.

[42] D. A. Medvedeva, M. A. Maslov, R. N. Serikov, N. G. Morozova, G. A. Serebrenikova, D. V. Sheglov, A. V. Latyshev, V. V. Vlassov, and M. A. Zenkova. Novel cholesterol-based cationic lipids for gene delivery. *Journal of medicinal chemistry*, 52:6558–6568, 2009.

[43] M. Berchel, T. Le Gall, H. Couthon-Gourves, J. P. Haelters, T. Montier, P. Midoux,

P. Lehn, and P. A. Jaffres. Lipophosphonate/lipophosphoramidates: a family of synthetic vectors efficient for gene delivery. *Biochimie*, 94:33–41, 2012.

[44] Q. Liu, W.J. Yi, Y.M. Zhang, J. Zhang, L. Guo, and X.Q. Yu. Biotinylated cyclen-contained cationic lipids as non-viral gene delivery vectors. *Chemical Biology and Drug Design*, 82:376–386, 2013.

[45] A. D. Bangham and R. W. Horne. Negative staining of phospholipids and their structural modification by surface-active agents as observed in the electron microscope. *Journal of Molecular Biology*, 8:660–668, 1964.

[46] W.T. Godbey D.A. Balazs. Liposomes for use in gene delivery. *Journal of drug delivery*, 10:e1155, 2011.

[47] A. Jesorka and O. Orwar. Liposomes: technologies and analytical applications. *Annual review of analytical chemistry (Palo Alto, Calif.)*, 1:801–832, 2008.

[48] L. G. Barron, L. Gagne, and F. C. Szoka Jr. Lipoplex-mediated gene delivery to the lung occurs within 60 minutes of intravenous administration. *Human Gene Therapy*, 10:1683–1694, 1999.

[49] M.B. Bally P. Harvie, F.M. Wong. Use of poly(ethylene glycol)lipid conjugates to regulate the surface attributes and transfection activity of lipiddna particles. *Journal of Pharmaceutical Sciences*, 89:652–663, 2000.

[50] I. Koltover, T. Salditt, J. O. Radler, and C. R. Safinya. An inverted hexagonal phase of cationic liposome-DNA complexes related to dna release and delivery. *Science (New York, N.Y.)*, 281:78–81, 1998.

[51] R. Koynova and T. Tenchov. Cationic phospholipids: structure-transfection activity relationships. *Soft Matter*, 5:31873200, 2009.

[52] W.A. Talbot, L.X. Zheng, and B.R. Lentz. Acyl chain unsaturation and vesicle curvature alter outer leaflet packing and promote poly(ethylene glycol)-mediated membrane fusion. *Biochemistry*, 36:5827–5836, 1997.

[53] Z. ur Rehman, D. Hoekstra, and I.S. Zuhorn. Protein kinase a inhibition modulates the intracellular routing of gene delivery vehicles in hela cells, leading to productive transfection. *Journal Control Release*, 156:76–84, 2011.

[54] D. Simberg, S. Weisman, Y. Talmon, and Y. Barenholz. Dotap (and other cationic lipids): chemistry, biophysics, and transfection. *Critical Reviews in Therapy Drug Carrier Systems*, 21:257–317, 2004.

[55] F. Cardarelli, D. Pozzi, A. Bifone, C. Marchini, and G. Caracciolo. Cholesterol-dependent macropinocytosis and endosomal escape control the transfection efficiency of lipoplexes in cho living cells. *Molecular Pharmaceutics*, 9:334–340, 2012.

[56] M. S. Al-Dosari and X. Gao. Nonviral gene delivery: principle, limitations, and recent progress. *The AAPS journal*, 11:671–681, 2009.

[57] A. S. Ulrich. Biophysical aspects of using liposomes as delivery vehicles. *Bioscience reports*, 22:129–150, 2002.

[58] R.S. Shirazi, K.K. Ewert, B.F. Silva, C. Leal, Y. Li, and C.R. Safinya. Structural evolution of environmentally responsive cationic liposomeDNA complexes with a reducible lipid linker. *Langmuir*, 28:10495–10503, 2012.

[59] A. C. Hunter and S. M. Moghimi. Cationic carriers of genetic material and cell death: a mitochondrial tale. *Biochimica et biophysica acta*, 1797:1203–1209, 2010.

[60] R. Bottega and R. M. Epand. Inhibition of protein kinase c by cationic amphiphiles. *Biochemistry*, 31:9025–9030, 1992.

[61] W. Yan, W. Chen, and L. Huang. Mechanism of adjuvant activity of cationic liposome: phosphorylation of a MAP kinase, ERK and induction of chemokines. *Molecular Immunology*, 44:3672–3681, 2007.

[62] L. Huang W. Chen, W. Yan. A simple but effective cancer vaccine consisting of an antigen and a cationic lipid. *Cancer Immunology Immunotherapy*, 57:517–530, 2008.

[63] T. Tanaka, A. Legat, E. Adam, J. Steuve, J.S. Gatot, M. Vandenbranden, L. Ulianov, C. Lonez, J.M. Ruysschaert, E. Muraille, M. Tuynder, M. Goldman, and A. Jacquet. Dic14-amidine cationic liposomes stimulate myeloid dendritic cells through toll-like receptor 4. *European Journal of Immunology*, 38:13511357, 2008.

[64] M. Ouali, J.M. Ruysschaert, C. Lonez, and M. Vandenbranden. Cationic lipids involved in gene transfer mobilize intracellular calcium. *Molecular Membrane Biology*, 24:225–232, 2007.

[65] B.M. Tandia, C. Lonez, M. Vandenbranden, J.M. Ruysschaert, and A. Elouahabi. Lipid mixing between lipoplexes and plasma lipoproteins is a major barrier for intravenous transfection mediated by cationic lipids. *Journal of Biological Chemistry*, 280: 12255–12261, 2005.

[66] R.A. Daynes and D.C. Jones. Emerging roles of ppars in inflammation and immunity. *Nature Reviews Immunology*, 2:748–759, 2002.

[67] A. Aied, U. Greiser, A. Pandit, and W. Wang. Polymer gene delivery: overcoming the obstacles. *Drug Discovery Today*, 18:e1016, 2013.

[68] O. Boussif, F. Lezoualc'h, M. A. Zanta, M. D. Mergny, D. Scherman, B. Demeneix, and J. P. Behr. A versatile vector for gene and oligonucleotide transfer into cells in culture and *in vivo*: polyethylenimine. *Proceedings of the National Academy of Sciences of the United States of America*, 92:7297–7301, 1995.

[69] Y.B. Lim, C.H. Kim, K. Kim, S.W. Kim, and J.S. Park. Developement of a safe gene delivery system using biodegradable polymer, poly[alpha-(4-aminobutyl)-l-glycolic acid. *Journal of the American Chemical Society*, 122:6524 6525, 2000.

[70] D. M. Lynn and R. Langer. Degradable poly(-amino esters): Synthesis, characterization, and self-assembly with plasmid DNA. *Journal of the American Chemical Society*, 122:10761–10768, 2000.

[71] P. van de Wetering, J.Y. Cherng, H. Talsma, D.J. Crommelin, and W.E. Hennink. 2-(dimethylamino)ethyl methacrylate based (co)polymers as gene transfer agents. *Journal of Control Release*, 53:145–153, 1998.

[72] H. Lv, S. Zhang, B. Wang, S. Cui, and J. Yan. Toxicity of cationic lipids and cationic polymers in gene delivery. *Journal of Control Release*, 114:100–109, 2006.

[73] C. Dufés, I. F. Uchegbu, and A. G. Schatzlein. Dendrimers in gene delivery. *Advanced Drug Delivery Reviews*, 57:2177–2202, 2005.

[74] T.G. Park, J.H. Jeong, and S.W. Kim. Current status of polymeric gene delivery systems. *Advance Drug Delivery Rev*, 58:467–486, 2006.

[75] M. Lee and S.W. Kim. Polyethylene glycol-conjugated copolymers for plasmid DNA delivery. *Pharm Res*, 22:1–10, 2005.

[76] M. Papi, V. Palmieri, G. Maulucci, G. Arcovito, E. Greco, G. Quintiliani, M. Fraziano, and M. Spirito. Controlled self assembly of collagen nanoparticle. *Journal of Nanoparticle Research*, 13:6141–6147, 2011.

[77] W-T. Kuo, H-Y. Huang, M.J. Chou, M-C. Wu, and Y-Y. Huang. Surface modification of gelatin nanoparticles with polyethylenimine as gene vector. *Journal of Nanomaterials*, 10:e646538, 2011.

[78] Jiyoung M. Danga and Kam W. Leong. Natural polymers for gene delivery and tissue engineering. *Advance Drug Delivery Reviews*, 58:487–499, 2004.

[79] B. Newland, Y. Zheng, Y. Jin, M. Abu-Rub, H. Cao, W. Wang, and A. Pandit. Single cyclized molecule versus single branched molecule: a simple and efficient 3D "knot" polymer structure for nonviral gene delivery. *Journal of the American Chemical Society*, 134:4782–4789, 2012.

[80] J. Zhou, J. Liu, C. J. Cheng, T. R. Patel, C. E. Weller, J. M. Piepmeier, Z. Jiang, and W. M. Saltzman. Biodegradable poly(amine co ester) terpolymers for targeted gene delivery. *Nature materials*, 11:82–90, 2011.

[81] M. Keeney, J. J. van den Beucken, P. M. van der Kraan, J. A. Jansen, and A. Pandit. The ability of a collagen/calcium phosphate scaffold to act as its own vector for gene delivery and to promote bone formation via transfection with VEGF(165). *Biomaterials*, 10:2893–2902, 2010.

[82] H. Shen, J. Tan, and W. M. Saltzman. Surface-mediated gene transfer from nanocomposites of controlled texture. *Nature materials*, 3:569–574, 2004.

[83] D. Luo, E. Han, N. Belcheva, and W. M. Saltzman. A self-assembled, modular dna delivery system mediated by silica nanoparticles. *Journal Control Release*, 95:333–341, 2004.

[84] M. M. O. Sullivan, J. J. Green, and T. M. Przybycien. Development of a novel gene delivery scaffold utilizing colloidal gold-polyethylenimine conjugates for DNA condensation. *Gene Therapy*, 10:1882–1890, 2003.

[85] M. Thomas and A. M. Klibanov. Conjugation to gold nanoparticles enhances polyethylenimine's transfer of plasmid DNA into mammalian cells. *Proceedings of the National Academy of Sciences*, 100:91389143, 2003.

[86] I. J. Majoros, T. P. Thomas, C. B. Mehta, and J. R. Baker Jr. Poly(amidoamine) dendrimer-based multifunctional engineered nanodevice for cancer therapy. *Journal of Medicinal Chemistry*, 48:58925899, 2005.

[87] Park T Yoo H. Folate-receptor-targeted delivery of doxorubicin nano-aggregates stabilized by doxorubicinpegfolate conjugate. *Journal of Control Release*, 100:247–256, 2004.

[88] S. Yamano, J. Dai, and A. M. Moursi. Comparison of transfection efficiency of nonviral gene transfer reagents. *Molecular biotechnology*, 46:287–300, 2010.

[89] M. A. Gosselin, W. Guo, and R.J. Lee. Efficient gene transfer using reversibly cross-linked low molecular weight polyethylenimine. *Bioconjugate Chemistry*, 12:989–994, 2001.

[90] S. F. Peng, M. J. Yang, C. J. Su, H. L. Chen, P. W. Lee, M. C. Wei, and H. W. Sung. Effects of incorporation of poly(gamma-glutamic acid) in chitosan/dna complex nanoparticles on cellular uptake and transfection efficiency. *Biomaterials*, 30:1797–1808, 2009.

[91] W. F. Lai. Cyclodextrins in non-viral gene delivery. *Biomaterials*, 35:401–411, 2014.

[92] S. Pan, D. Cao, R. Fang, W. Yi, H. Huang, S. Tian, and M. Feng. Cellular uptake and transfection activity of DNA complexes based on poly(ethylene glycol)-poly-(l-glutamine) copolymer with PAMAM G2. *Journal of Materials Chemistry B*, 1:5114–5127, 2013.

[93] K. Sarkara, A. Chatterjeeb, G. Chakrabortib, and P. P. Kundu. Blood compatible n-maleyl chitosan-graft-PAMAM copolymer for enhanced gene transfection. *Carbohydrate Polymers*, 98:596 606, 2013.

[94] X. Liu, Y. Zhang, D. Ma, H. Tang, L. Tan, Q. Xie, and S. Yao. Biocompatible multi-walled carbon nanotube-chitosan-folic acid nanoparticle hybrids as gfp gene delivery materials. *Colloids and surfaces.B, Biointerfaces*, 111C:224–231, 2013.

[95] G. T. Zugates, D. G. Anderson, and R. Langer. High-throughput methods for screening polymeric transfection reagents. *Cold Spring Harbor protocols*, 2013: 10.1101/pdb.prot078634, 2013.

[96] D. W. Pack, A. S. Hoffman, S. Pun, and P. S. Stayton. Design and development of polymers for gene delivery. *Nature Reviews Drug Discovery*, 4:581–593, 2005.

[97] T. Zhou, A. Llizo, C. Wang, G. Xu, and Y. Yang. Nanostructure-induced DNA condensation. *Nanoscale*, 5:8288–8306, 2013.

[98] R. W. Wilson and V. A. Bloomfeld. Counterion-induced condensation of deoxyribonucleic acid. a light-scattering study. *Biochemistry*, 18:21922196, 1979.

[99] C. Pichon, L. Billiet, and P. Midoux. Chemical vectors for gene delivery: uptake and intracellular trafficking. *Current opinion in biotechnology*, 21:640–645, 2010.

[100] C. Reilly. Polyplexes traffic through caveolae to the golgi and endoplasmic reticulum en route to the nucleus. *Molecular Pharmaceutics*, 9:12801290, 2012.

[101] S. Xiang, H.Tong, Q. Shi, J. C. Fernandes, T Jin, K. Dai, and X. Zhang. Uptake mechanisms of non-viral gene delivery. *Journal Control Release*, 158:371378, 2012.

[102] S. Hong, A. U. Bielinska, A. Mecke, B. Keszler, J. L. Beals, X. Shi, L. Balogh, B. G. Orr, J. R. Baker Jr, and M. M. Banaszak Holl. Interaction of poly(amidoamine) dendrimers with supported lipid bilayers and cells: hole formation and the relation to transport. *Bioconjugate chemistry*, 15:774–782, 2004.

[103] C. K. Chen, C. H. Jones, P. Mistriotis, Y. Yu, X. Ma, A. Ravikrishnan, M. Jiang, S. T. Andreadis, B. A. Pfeifer, and C. Cheng. Poly(ethylene glycol)-block-cationic

polylactide nanocomplexes of differing charge density for gene delivery. *Biomaterials*, 34:9688–9699, 2013.

[104] H. A. Staab. Proton sponges and the geometry of hydrogen bonds: Aromatic nitrogen bases with exceptional basiciticies. *Angewanate Chemie*, 27:865879, 1988.

[105] A. Akinc, M. Thomas, A. M. Klibanov, and R. Langer. Exploring polyethylenimine-mediated DNA transfection and the proton sponge hypothesis. *The journal of gene medicine*, 7:657–663, 2005.

[106] J. D. Ziebarth and Y. Wang. Understanding the protonation behavior of linear polyethylenimine in solutions through monte carlo simulations. *Biomacromolecules*, 11:29–38, 2010.

[107] R. V. Benjaminsen, M. A. Mattebjerg, J. R. Henriksen, S. M. Moghimi, and T. L. Andresen. The possible "proton sponge" effect of polyethylenimine (PEI) does not include change in lysosomal ph. *Molecular therapy : the journal of the American Society of Gene Therapy*, 21:149–157, 2013.

[108] H., J.S. Remy, G. Loussouarn, S. Demolombe, J.P. Behr, and D. Escande. Polyethylenimine but not cationic lipids promotes transgene delivery to the nucleus in mammalian cells. *J Biol Chem*, 273:75077511, 1998.

[109] G. Breuzard, M. Tertil, C. Goncalves, H. Cheradame, P. Geguan, C. Pichon, and P. Midoux. Nuclear delivery of NFkappaB-assisted DNA/polymer complexes: plasmid DNA quantitation by confocal laser scanning microscopy and evidence of nuclear polyplexes by FRET imaging. *Nucleic acids research*, 36:e71, 2008.

[110] Y. Matsumoto, K. Itaka, T. Yamasoba, and K. Kataoka. Intranuclear fluorescence resonance energy transfer analysis of plasmid dna decondensation from nonviral gene carriers. *The journal of gene medicine*, 11:615–623, 2009.

[111] A.K. Salem, P.C. Searson, and K. W. Leong. Multifunctional nano rods for gene delivery. *Nature Materials*, 2:668–671, 2003.

[112] S. M. Moghimi, P. Symonds, J. C. Murray, A. C. Hunter, G. Debska, and A. Szewczyk. A two-stage poly(ethylenimine)-mediated cytotoxicity: implications for gene transfer/therapy. *Molecular therapy : the journal of the American Society of Gene Therapy*, 11:990–995, 2005.

[113] A. M. Klibanov M. Thomas. Enhancing polyethylenimine's delivery of plasmid DNA into mammalian cells. *Proceedings of the National Academy of Sciences*, 99:14640–14645, 2002.

[114] Y. He, G. Cheng, L. Xie, Y. Nie, B. He, and Z. Gu. Polyethyleneimine/dna polyplexes with reduction-sensitive hyaluronic acid derivatives shielding for targeted gene delivery. *Biomaterials*, 34:1235–1245, 2013.

[115] K. L. Aillon, Y. Xie, N. El-Gendy, C. J. Berkland, and M. L. Forrest. Effects of nanomaterial physicochemical properties on *in vivo* toxicity. *Advanced Drug Delivery Reviews*, 61:457–466, 2009.

[116] K. Jain, P. Kesharwani, U. Gupta, and N. K. Jain. Dendrimer toxicity: Let's meet the challenge. *International journal of pharmaceutics*, 394:122–142, 2010.

[117] N.A. Stasko, C.B. Johnson, M.H. Schoenfisch, T.A. Johnson, and E.L. Holmuhamedov. Cytotoxicity of polypropylenimine dendrimer conjugates on cultured endothelial cells. *Biomacromolecules*, 8:38533859, 2007.

[118] A. Diaz-Moscoso, L. Le Gourrierec, M. Gomez-Garcia, J. M. Benito, P. Balbuena, F. Ortega-Caballero, N. Guilloteau, C. Di Giorgio, P. Vierling, J. Defaye, C. Ortiz Mellet, and J. M. Garcia Fernandez. Polycationic amphiphilic cyclodextrins for gene delivery: synthesis and effect of structural modifications on plasmid DNA complex

stability, cytotoxicity, and gene expression. *Chemistry (Weinheim an der Bergstrasse, Germany)*, 15:12871–12888, 2009.

[119] C. Ortiz Mellet, J. M. Garcia Fernandez, and J. M. Benito. Cyclodextrin-based gene delivery systems. *Chemical Society Reviews*, 40:1586–1608, 2011.

[120] S. A. Cryan, A. Holohan, R. Donohue, R. Darcy, and C. M. O'Driscoll. Cell transfection with polycationic cyclodextrin vectors. *European journal of pharmaceutical sciences : official journal of the European Federation for Pharmaceutical Sciences*, 21: 625–633, 2004.

[121] R. Donohue, A. Mazzaglia, B. J. Ravoo, and R. Darcy. Cationic beta-cyclodextrin bilayer vesicles. *Chemical communications (Cambridge, England)*, (23):2864–2865, 2002.

[122] N. Duceppe and M. Tabrizian. Advances in using chitosan-based nanoparticles for *in vitro* and *in vivo* drug and gene delivery. *Expert opinion on drug delivery*, 7:1191–1207, 2010.

[123] J. M. Dang and K. W. Leong. Natural polymers for gene delivery and tissue engineering. *Advanced Drug Delivery Reviews*, 58:487–499, 2006.

[124] Y. Liu, M. Kong, X. J. Cheng, Q. Q. Wang, L. M. Jiang, and X. G. Chen. Self-assembled nanoparticles based on amphiphilic chitosan derivative and hyaluronic acid for gene delivery. *Carbohydrate Polymers*, 94:309–316, 2013.

[125] L. Casettari, D. Vllasaliu, J. K. Lam, M. Soliman, and L. Illum. Biomedical applications of amino acid-modified chitosans: a review. *Biomaterials*, 33:7565–7583, 2012.

[126] F. Said Hassane, A. F. Saleh, R. Abes, M. J. Gait, and B. Lebleu. Cell penetrating

peptides: overview and applications to the delivery of oligonucleotides. *Cellular and molecular life sciences : CMLS*, 67:715–726, 2010.

[127] R. Brasseur and G. Divita. Happy birthday cell penetrating peptides: already 20 years. *Biochimica et biophysica acta*, 1798:2177–2181, 2010.

[128] A. Chugh, F. Eudes, and Y. S. Shim. Cell-penetrating peptides: Nanocarrier for macromolecule delivery in living cells. *IUBMB life*, 62:183–193, 2010.

[129] M. E. Martin and K. G. Rice. Peptide-guided gene delivery. *The AAPS journal*, 9: E18–29, 2010.

[130] S. Futaki, T. Suzuki, W. Ohashi, T. Tanaka, K. Ueda, and Y. Sugiura. Arginine-rich peptides. an abundant source of membrane-permeable peptides having potential as carriers for intracellular protein delivery. *Journal of Biology Chemistry*, 276:58365840, 2011.

[131] D. Derossi, A.H. Joliot, G. Chassaing, and A. Prochiantz. The third helix of the antennapedia homeodomain translocates through biological membranes. *Journal of Biology Chemistry*, 269:1044410450, 1994.

[132] K.T. Jeang, H. Xiao, and E.A. Rich. Multifaceted activities of the HIV-1 transactivator of transcription, tat. *Journal of Biology Chemistry*, 274:2883728840, 1999.

[133] M. Pooga, M. Hallbrink, M. Zorko, and U. Langel. Cell penetration by transportan. *FASEB J*, 12:6777, 1998.

[134] J. Oehlke, A. Scheller, B. Wiesner, E. Krause, M. Beyermann, E. Klauschenz, M. Melzig, and M. Bienert. Cellular uptake of an alpha-helical amphipathic model peptide with the potential to deliver polar compounds into the cell interior non-endocytically. *Biochimica et Biophysica Acta (BBA) - Molecular and Cell Biology of Lipids*, 1414:127139, 1998.

[135] T.B. Wyman, F. Nicol, O. Zelphati, P. V. Scaria, C. Plank, and F. C. Szoka. Design, synthesis and characterization of a cationic peptide that binds to nucleic acids and permeabilizes bilayers. *Biochemistry*, 36:3008 3017, 1997.

[136] S. T. Henriques and M. A. Castanho. Translocation or membrane disintegration? implication of peptide-membrane interactions in pep-1 activity. *Journal of Peptide Sciences*, 14:482487, 2008.

[137] S. Trabulo, A. L. Cardoso, M. Mano, and M. C. Pedroso de Lima. Cell-penetrating peptidesmechanisms of cellular uptake and generation of delivery systems. *Pharmaceuticals*, 3:961–993, 2010.

[138] V.P. Torchilin, R. R.V. Weissig, and T. S. Levchenko. TAT peptide on the surface of liposomes affords their efficient intracellular delivery even at low temperature and in the presence of metabolic inhibitors. *Proceedings of the National Academy of Sciences*, 98:8786–8791, 2001.

[139] B. Gupta, T. S. Levchenko, and V. P. Torchilin. TAT peptide-modified liposomes provide enhanced 7gene delivery to intracranial human brain tumor xenografts in nude mice. *Oncology Research*, 8:351–359, 2000.

[140] V. P. Torchilin, T. S. Levchenko, R. Rammohan, N. Volodina, B. Papahadjopoulos-Sternberg, and G. G. M. D'Souza. Cell transfection *in vitro* and *in vivo* with nontoxic tat peptide-liposome-DNA complexes. *Proceedings of the National Academy of Sciences*, 100:1972–1977, 2003.

[141] S. R. Sarker, Y. Aoshima, R. Hokama, T. Inoue, K. Sou, and S. Takeoka. Arginine-based cationic liposomes for efficient *in vitro* plasmid DNA delivery with low cytotoxicity. *International journal of nanomedicine*, 8:1361–1375, 2013.

[142] J. Nguyen, X. Xie, M. Neu, R. Dumitrascu, R. Reul, J. Sitterberg, U. Bakowsky, R. Schermuly, L. Fink, T. Schmehl, T. Gessler, W. Seeger, and T. Kissel. Effects of

cell-penetrating peptides and pegylation on transfection efficiency of polyethylenimine in mouse lungs. *The Journal of Gene Medicine*, 10:1236–1246, 2008.

[143] A. Kwok, G. A. Eggimann, J. L. Reymond, T. Darbre, and F. Hollfelder. Peptide dendrimer/lipid hybrid systems are efficient DNA transfection reagents: Structure activity relationships highlight the role of charge distribution across dendrimer generations. *ACS Nano*, 28:4668–4682, 2013.

[144] S. Gudlur, P. Sukthankar, J. Gao, L. A. Avila, Y. Hiromasa, J. Chen, T. Iwamoto, and J. M. Tomich. Peptide nanovesicles formed by the self-assembly of branched amphiphilic peptides. *PloS one*, 7:e45374, 2012.

[145] P. Sukthankar, S. Gudlur, L. A. Avila, S. K. Whitaker, B. B. Katz, Y. Hiromasa, J. Gao, P. Thapa, D. Moore, T. Iwamoto, J. Chen, and J. M. Tomich. Branched oligo peptides form nanocapsules with lipid vesicle characteristics. *Langmuir: the ACS journal of surfaces and colloids*, 29:14648–14654, 2013.

[146] P. Sukthankar, L. A. Avila, S. K. Whitaker, T. Iwamoto, A. Morgenstern, C. Apostolidis, K. Liu, R. P. Hanzlik, E. Dadachova, and J. M. Tomich. Branched amphiphilic peptide capsules: Cellular uptake and retention of encapsulated solutes. *Biochimica et biophysica acta*, 1838:2296–2305, 2014.

[147] S. L. Hart. Multifunctional nanocomplexes for gene transfer and gene therapy. *Cell biology and toxicology*, 26:69–81, 2010.

[148] S. B. Fonseca, M. P. Pereira, and S. O. Kelley. Recent advances in the use of cell-penetrating peptides for medical and biological applications. *Advanced Drug Delivery Reviews*, 61:953–964, 2009.

[149] S. H. Lee, B. Castagner, and J. C. Leroux. Is there a future for cell-penetrating peptides in oligonucleotide delivery? *European journal of pharmaceutics and biophar-*

maceutics : official journal of Arbeitsgemeinschaft fur Pharmazeutische Verfahrenstechnik e.V, 85:5–11, 2013.

[150] A. Mann, G. Thakur, V. Shukla, A.K. Singh, R. Khanduri, R. Naik, Y. Jiang, N. Kalra, U. Langel B.S. Dwarakanath, and M. Ganguli. Differences in DNA condensation and release by lysine and arginine homopeptides govern their DNA delivery efficiencies. *Molecular Pharmaceutics*, 8:17291741, 2011.

[151] H. Hillaireau and P. Couvreur. Nanocarriers' entry into the cell: relevance to drug delivery. *Cellular and molecular life sciences : CMLS*, 66:2873–2896, 2009.

[152] M. Lundberg and M Johansson. Positively charged DNA-binding proteins cause apparent cell membrane translocation. *Biochemical and Biophysical Research Communications*, 291:367371, 2002.

[153] L. Wasungu and D. Hoekstra. Cationic lipids, lipoplexes and intracellular delivery of genes. *Journal of controlled release: official journal of the Controlled Release Society*, 116:255–264, 2006.

[154] F. Duchardt, M. Fotin-Mleczek, H. Schwarz, R. Fischer, and R. Brock. A comprehensive model for the cellular uptake of cationic cell penetrating peptides. *Traffic*, 8: 848866, 2007.

[155] M. V. Yezhelyev, L. Qi, R. M. O'Regan, S. Nie, and X. Gao. Proton-sponge coated quantum dots for sirna delivery and intracellular imaging. *Journal of the American Chemical Society*, 130:9006–9012, 2008.

[156] M. Lewin, N. Carlesso, C. H. Tung, X. W. Tang, D. Cory, D. T. Scadden, and R. Weissleder. Tat peptide-derivatized magnetic nanoparticles allow *in vivo* tracking and recovery of progenitor cells. *Nature biotechnology*, 18:410–414, 2000.

[157] A.M.S. Cardoso, S. Trabulo, A.L. Cardoso, A. Lorents, C. M. Morais, P. Gomes, C. Nunes, M. Lcio, S. Reis, K. Padari, M. Pooga, M. C. Pedroso de Lima, and A. S. Jurado. S4(13)-PV cell-penetrating peptide induces physical and morphological changes in membrane-mimetic lipid systems and cell membranes: Implications for cell internalization. *Biochimica et Biophysica Acta (BBA) - Molecular and Cell Biology of Lipids*, 1818:877888, 2012.

[158] X.H. Peng, X. Qian, H. Mao, A. Y. Wang, Z. G. Chen, S. Nie, and D. M. Shin. Targeted magnetic iron oxide nanoparticles for tumor imaging and therapy. *International Journal of Nanomedicine*, 3:311–321, 2008.

[159] H.I. Labouta and M. Schneider. Interaction of inorganic nanoparticles with the skin barrier: current status and critical review. *Nanomedicine: NBM*, 9:39–54, 2013.

[160] T. D. Tetley A. J. Thorley. New perspectives in nanomedicine. *Pharmacology and Therapeutics*, 140:2176–2185, 2013.

[161] R. Levy, U. Shaheen, Y. Cesbron, and V. See. Gold nanoparticles delivery in mammalian live cells: a critical review. *Nano reviews*, 1:10.3402/nano.v1i0.4889. Epub 2010 Feb 22, 2010.

[162] D. Pissuwan, T. Niidome, and M. B. Cortie. The forthcoming applications of gold nanoparticles in drug and gene delivery systems. *Journal of controlled release : official journal of the Controlled Release Society*, 149:65–71, 2011.

[163] P. M. Tiwari, K. Vig, V. A. Dennis, and S. R. Singh. Functionalized gold nanoparticles and their biomedical applications. *Nanomaterials*, 1:31–63, 2011.

[164] E. R. Figueroa, A. Y. Lin, J. Yan, L. Luo, A. E. Foster, and R. A. Drezek. Optimization of PAMAM-gold nanoparticle conjugation for gene therapy. *Biomaterials*, 35:1725–1734, 2014.

[165] D. Pantarotto, R. Singh, D. McCarthy, M. Erhardt, J. P. Briand, M. Prato, K. Kostarelos, and A. Bianco. Functionalized carbon nanotubes for plasmid DNA gene delivery. *Angewandte Chemie (International ed.in English)*, 43:5242–5246, 2004.

[166] W. Cheung, F. Pontoriero, O. Taratula, A. M. Chen, and H. He. DNA and carbon nanotubes as medicine. *Advanced Drug Delivery Reviews*, 62:633–649, 2010.

[167] A. Nunes, N. Amsharov, C. Guo, J. Van den Bossche, P. Santhosh, T. K. Karachalios, S. F. Nitodas, M. Burghard, K. Kostarelos, and K. T. Al-Jamal. Hybrid polymer-grafted multiwalled carbon nanotubes for *in vitro* gene delivery. *Small (Weinheim an der Bergstrasse, Germany)*, 6:2281–2291, 2010.

[168] R. Singh, D. Pantarotto, D. McCarthy, O. Chaloin, J. Hoebeke, C. D. Partidos, J. P. Briand, M. Prato, A. Bianco, and K. Kostarelos. Binding and condensation of plasmid DNA onto functionalized carbon nanotubes: toward the construction of nanotube-based gene delivery vectors. *Journal of the American Chemical Society*, 127:4388–4396, 2005.

[169] G.Y. Wu and C.H. Wu. Receptor-mediated gene delivery and expression *in vivo*. *The Jorunal of Biological Chemistry*, 263:14621–14624, 1988.

[170] P. Pires, S. Simoes, S. Nir, R. Gaspar, N. Duzgunes, and M.C. Pedroso de Lima. Interaction of cationic liposomes and their dna complexes with monocytic leukemia cells. *Biochimica et Biophysica Acta*, 1418:71–84, 1999.

[171] S. Simoes, V. Slepushkin, P. Pires, R. Gaspar, M.P. de Lima, and N. Duzgunes. Mechanisms of gene transfer mediated by lipoplexes associated with targeting ligands or ph-sensitive peptides. *Gene Therapy*, 6:1798–1807, 1999.

[172] R. I. Zhdanov, O. V. Podobed, and V. V. Vlassov. Cationic lipid-DNA complexes-lipoplexes-for gene transfer and therapy. *Bioelectrochemistry (Amsterdam, Netherlands)*, 58:53–64, 2002.

[173] C.Nicolau and D.E. Papahadjopoulos. *In Gene therapy: liposomes and gene delivery – a perspective*, volume 1. Elsevier, 1998.

[174] C. R. Safinya. Structures of lipid-DNA complexes: supramolecular assembly and gene delivery. *Current opinion in structural biology*, 11:440–448, 2001.

[175] K. Ewert, N.L. Slack, A. Ahmad, H.M. Evans, A.J. Lin, C.E. Samuel, and C.R. Safinya. Cationic lipid-DNA complexes for gene therapy: Understanding the relationship between complex structure and gene delivery pathways at the molecular level. *Current Medicinal Chemistry*, 11:133–149, 2004.

[176] H.L. Åmand, B. Nordén, and K. Fant. Functionalization with C-terminal cysteine enhances transfection efficiency of cell-penetrating peptides through dimer formation. *Biochemical and Biophysical Research Communications*, 3:469–74, 2012.

[177] M. C. Branco and J. P. Schneider. Self-assembling materials for therapeutic delivery. *Acta biomaterialia*, 5:817–831, 2009.

[178] L.C. Gruen. Stoichiometry of the reaction between methylmercury(II) iodide and soluble sulphides. *Analytica Chemical Acta*, 50:299–303, 1970.

[179] C. Li, F. Zhao, Y. Huang, X. Liu, Y. Liu, R. Qiao, and Y. Zhao. Metal-free DNA linearized nuclease based on PASP-polyamine conjugates. *Bioconjugate chemistry*, 23: 1832–1837, 2012.

[180] D. Necas and P. Klapetek. Gwyddion: an open-source software for SPM data analysis. *Central European Journal of Physics*, 10:181–188, 2012.

[181] A. Schweizer, J. A. Fransen, T. Bachi, L. Ginsel, and H. P. Hauri. Identification, by a monoclonal antibody, of a 53-kD protein associated with a tubulo-vesicular compartment at the cis-side of the Golgi apparatus. *The Journal of cell biology*, 107: 1643–1653, 1988.

[182] A. Baoum, D. Ovcharenko, and C. Berkland. Calcium condensed cell penetrating peptide complexes offer highly efficient, low toxicity gene silencing. *International Journal of Pharmaceutics*, 1:134–42, 2012.

[183] R.E. Kingston, C.A. Chen, and J.K. Rose. *Calcium Phosphate Transfection. Current Protocols in Molecular Biology*, volume 1. Elsevier, 2003.

[184] H. S. Rosenzweig, V. A. Rakhmanova, T. J. McIntosh, and R. C. MacDonald. O-alkyl dioleoylphosphatidylcholinium compounds: the effect of varying alkyl chain length on their physical properties and in vitro DNA transfection activity. *Bioconjugate chemistry*, 11:306–313, 2000.

[185] L.A. Avila, S.Y. Lee, and J. Tomich. Synthetic *In Vitro* delivery systems for plasmid DNA in eukaryotes. *Journal of Nanopharmaceutics and Drug Delivery*, 2:1–19, 2014.

[186] S. Moore. *Pancreatic DNase in The Enzymes*, volume 14. Academic Press, 1981.

[187] S. Honary and F. Zahir. Effect of zeta potential on the properties of nano-drug delivery systems. *Tropical Journal of Pharmaceutical Research*, 2:265–273, 2013.

[188] I. A. Ignatovich, E. B. Dizhe, A. V. Pavlotskaya, B. N. Akifiev, S. V. Burov, S. V. Orlov, and A. P. Perevozchikov. Complexes of plasmid DNA with basic domain 47-57 of the HIV-1 tat protein are transferred to mammalian cells by endocytosis-mediated pathways. *The Journal of biological chemistry*, 278:42625–42636, 2003.

[189] B. Gupta, T. S. Levchenko, and V. P. Torchilin. Intracellular delivery of large molecules and small particles by cell-penetrating proteins and peptides. *Advanced Drug Delivery Reviews*, 57:637–651, 2005.

[190] L. Y. Xue, S. M. Chiu, and N. L. Oleinick. Atg7 deficiency increases resistance of mcf-7 human breast cancer cells to photodynamic therapy. *Autophagy*, 6:248–255, 2010.

[191] L. Xu, Y. Liu, Z. Chen, W. Li, Y. Liu, L. Wang, Y. Liu, X. Wu, Y. Ji, Y. Zhao, L. Ma, Y. Shao, and C. Chen. Surface-engineered gold nanorods: promising DNA vaccine adjuvant for HIV-1 treatment. *Nano letters*, 12:2003–2012, 2012.

[192] S. P. Kasturi, K. Sachaphibulkij, and K. Roy. Covalent conjugation of polyethyleneimine on biodegradable microparticles for delivery of plasmid DNA vaccines. *Biomaterials*, 26:6375–6385, 2005.

[193] Malou Henriksen-Lacey, Karen Smith Korsholm, Peter Andersen, Yvonne Perrie, and Dennis Christensen. Liposomal vaccine delivery systems. *Expert Opinion on Drug Delivery*, 8:505–519, 2011.

[194] L. Li, F. Saade, and N. Petrovsky. The future of human DNA vaccines. *Journal of Biotechnology*, 162:171–182, 2012.

[195] C. P. Locher, D. Putnam, R. Langer, S. A. Witt, B. M. Ashlock, and J. A. Levy. Enhancement of a human immunodeficiency virus env DNA vaccine using a novel polycationic nanoparticle formulation. *Immunology letters*, 90:67–70, 2003.

[196] M. O. Diniz, F. A. Cariri, L. R. Aps, and L. C. Ferreira. Enhanced therapeutic effects conferred by an experimental DNA vaccine targeting human papillomavirus-induced tumors. *Human Gene Therapy*, 24:861–870, 2013.

[197] M. O. Lasaro, N. Tatsis, S. E. Hensley, J. C. Whitbeck, S. W. Lin, J. J. Rux, E. J. Wherry, G. H. Cohen, R. J. Eisenberg, and H. C. Ertl. Targeting of antigen to the herpesvirus entry mediator augments primary adaptive immune responses. *Nature medicine*, 14:205–212, 2008.

[198] A. P. Lepique, T. Rabachini, and L. L. Villa. HPV vaccination: the beginning of the end of cervical cancer? - a review. *Memorias do Instituto Oswaldo Cruz*, 104:1–10, 2009.

[199] K. Y. Lin, F. G. Guarnieri, K. F. Staveley-O'Carroll, H. I. Levitsky, J. T. August, D. M. Pardoll, and T. C. Wu. Treatment of established tumors with a novel vaccine that enhances major histocompatibility class II presentation of tumor antigen. *Cancer research*, 56:21–26, 1996.

[200] M. O. Lasaro, M. O. Diniz, A. Reyes-Sandoval, H. C. Ertl, and L. C. Ferreira. Anti-tumor DNA vaccines based on the expression of human papillomavirus-16 e6/e7 oncoproteins genetically fused with the glycoprotein d from herpes simplex virus-1. *Microbes and infection / Institut Pasteur*, 7:1541–1550, 2005.

[201] J. P. Peters 3rd and L. J. Maher. DNA curvature and flexibility *in vitro* and *in vivo*. *Quarterly reviews of biophysics*, 43:23–63, 2010.

[202] H. G. Garcia, P. Grayson, L. Han, M. Inamdar, J. Kondev, P. C. Nelson, R. Phillips, J. Widom, and P. A. Wiggins. Biological consequences of tightly bent DNA: the other life of a macromolecular celebrity. *Biopolymers*, 85:115–130, 2007.

[203] D. Boal. *Mechanics of the Cell*, volume 1. Cambridge University Press, 2012.

[204] J. Rejman, V. Oberle, I. S. Zuhorn, and D. Hoekstra. Size-dependent internalization of particles via the pathways of clathrin- and caveolae-mediated endocytosis. *The Biochemical journal*, 377:159–169, 2004.

[205] H. Yin, H. P. Too, and G. M. Chow. The effects of particle size and surface coating on the cytotoxicity of nickel ferrite. *Biomaterials*, 26:5818–5826, 2005.

[206] P. Sukthankar, Susan K. Whitaker, B.B. Katz, and J.M. Tomich. Thermally induced conformational transitions in branched amphiphilic peptide capsules. *Langmuir*, 1: Submitted, 2014.

[207] Y. Zhang, A. Satterlee, and L. Huang. *In Vivo* gene delivery by nonviral vectors: Overcoming hurdles? *Nature: Molecular Therapy*, 20:12981304, 2012.

[208] P. Sukthankar. *Biophysical Characterization of Branched Amphiphilic Peptide Capsules and Their Potential Application in Radiotherapy*, volume 1. Ph.D. Dissertation Kansas State University, 2014.

[209] M. Keeney, S. G. Ong, A. Padilla, Z. Yao, S. Goodman, J. C. Wu, and F. Yang. Development of poly(beta-amino ester)-based biodegradable nanoparticles for nonviral delivery of minicircle DNA. *ACS nano*, 7:7241–7250, 2013.

[210] S. Pan, C. Wang, X. Zeng, Y. Wen, H. Wu, and M. Feng. Short multi-armed polylysine-graft-polyamidoamine copolymer as efficient gene vectors. *International journal of pharmaceutics*, 420:206–215, 2011.

[211] J. Guerra, A. C. Rodrigo, S. Merino, J. Tejeda, J. C. García-Martínez, P. Sánchez-Verdú, V. Cea, and Julin Rodríguez-López. PPVPAMAM hybrid dendrimers: Self-assembly and stabilization of gold nanoparticles. *Macromolecules*, 46:7316–7324, 2013.

[212] F. Shahidi and Y. Zhong. Lipid oxidation and improving the oxidative stability. *Chemical Society Reviews*, 39:4067–4079, 2010.

[213] A. del Pozo-Rodriguez, S. Pujals, D. Delgado, M. A. Solinis, A. R. Gascon, E. Giralt, and J. L. Pedraz. A proline-rich peptide improves cell transfection of solid lipid nanoparticle-based non-viral vectors. *Journal of controlled release : official journal of the Controlled Release Society*, 133:52–59, 2009.

[214] B. Ma, Y. Xu, C.F. Hung, and T.C. Wu. Hpv and therapeutic vaccines: where are we in 2010? *Current Cancer Therapy Reviews*, 6:81–103, 2010.

[215] S. E. Goldstone, J. M. Palefsky, M. T. Winnett, and J. R. Neefe. Activity of hspe7, a novel immunotherapy, in patients with anogenital warts. *Diseases of the colon and rectum*, 45:502–507, 2002.

[216] M. J. Welters, G. G. Kenter, S. J. Piersma, A. P. Vloon, M. J. Lowik, D. M. Berends van der Meer, J. W. Drijfhout, A. R. Valentijn, A. R. Wafelman, J. Oostendorp, G. J. Fleuren, R. Offringa, C. J. Melief, and S. H. van der Burg. Induction of tumor-specific cd4+ and cd8+ t-cell immunity in cervical cancer patients by a human papillomavirus type 16 e6 and e7 long peptides vaccine. *Clinical cancer research : an official journal of the American Association for Cancer Research*, 14:178–187, 2008.

[217] E. E. Sheets, R. G. Urban, C. P. Crum, M. L. Hedley, J. A. Politch, M. A. Gold, L. I. Muderspach, G. A. Cole, and P. A. Crowley-Nowick. Immunotherapy of human cervical high-grade cervical intraepithelial neoplasia with microparticle-delivered human papillomavirus 16 e7 plasmid DNA. *American Journal of Obstetrics and Gynecology*, 188:916–926, 2003.

Appendix A

Supplementary Data for Chapter 2

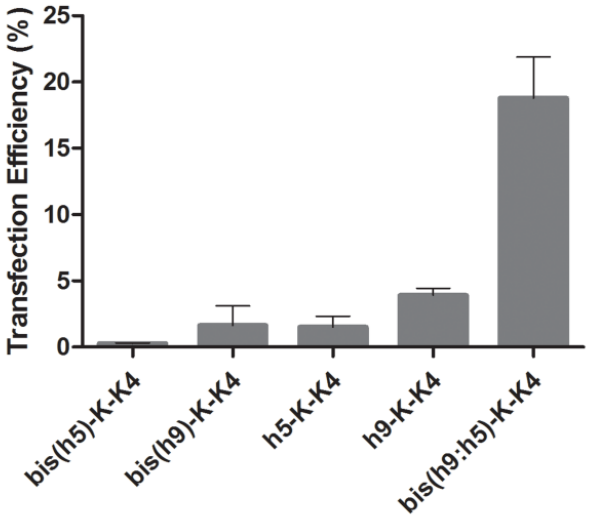

Figure A.1: *Comparison of transfection efficiency of bis(h_9:h_5)-K-K_4 peptiplex and different peptide control sequences at the same N:P ratio of 10.4. Peptide-DNA complexes were incubated 6 h in reduced serum media and 1.0 mM $CaCl_2$. Data are presented as means SEM (standard error of the mean).*

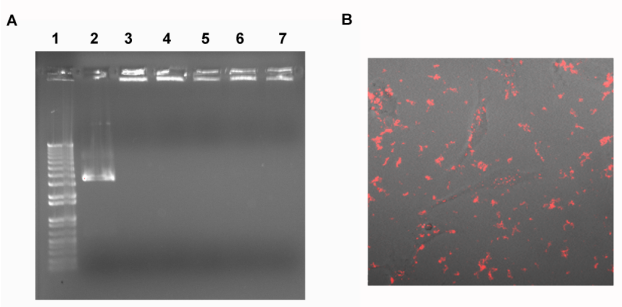

Figure A.2: *(A) Agarose gel electrophoresis of peptide complexes with different peptide sequences at N:P=10.4, each lane contains 100 ng of pEGFP-N3. Peptiplexes were in Opti-MEM® I Reduced Serum with 1 mM $CaCl_2$. Lane 1: 1kb dsDNA Ladder, lane 2: bis(h_9:h_5)-K-K_4 peptiplex, Lane 3: Branched sequence bis(h_5)-K-K_4 only, Lane 4: Branched sequence bis(h_9)-K-K_4 only, Lane 5: Linear sequence (FLIVI)-K-K_4, Lane 6: Linear sequence (FLIVIGSII)-K-K_4. (B) Cellular uptake of the branched peptide sequence bis(h_5)-K-K_4 partially labeled with Rhodamine B*

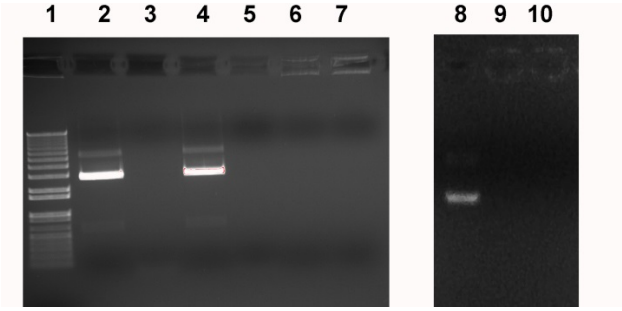

Figure A.3: *Agarose gel showing the results of bis(h_9:h_5)-K-K_4 peptiplex samples treated with DNase-1. Lane 1: 1kb dsDNA Ladder, Lane 2: plasmid (pEGFP-N3), lane 3: plasmid (pEGFP-N3) treated with DNase-1, lane 4: plasmid (pEGFP-N3) + $CaCl_2$ 1.0 mM, lane 5: plasmid (pEGFP-N3) + $CaCl_2$ 1mM treated with DNase-1, lane 6: bis(h_9:h_5)-K-K_4 peptiplex at N:P = 10.4, lane 7: bis(h_9:h_5)-K-K_4 peptiplex at N:P=10.4 treated with DNase-1, lane 8: plasmid (pEGFP-N3) lane 9: bis(h_9:h_5)-K-K_4 peptiplex at N:P = 65.5 and lane 10: bis(h_9:h_5)-K-K_4 peptiplex at N:P=65.5 treated with DNase-1. Lanes 7 and 10 show complete protection of pDNA. Lanes 3 and 5 show complete degradation of the plasmid.*

Appendix B

Supplementary Data for Chapter 3

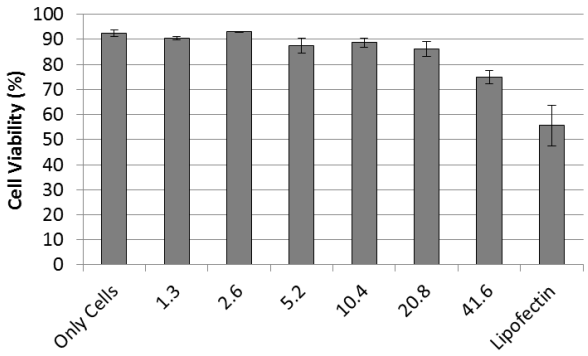

Figure B.1: *Cell viability after treatment with DNA/BAPC complexes at different N:P charge ratios as determined by PI analysis. Viability experiments were done using same conditions than transfection.*